UNIVERSITÀ DEGLI STUDI DELLA TUSCIA,VITERBO

DIPARTIMENTO DI ECOLOGIA E BIOLOGIA

Corso di Dottorato di Ricerca in

GENETICA E BIOLOGIA CELLULARE – XXVIII Ciclo.

MEAT AGING: THE 'OMICS' INTEGRATION TO THE ANALYSIS OF THE BIOCHEMICAL EVOLUTION DRIVING THE MUSCLE-TO-MEAT CONVERSION PROCESS.

BIO/11

Tesi di dottorato di:

Dott. Alessandro Lana

Coordinatore del corso

Prof. Giorgio Prantera

Tutore

Dott.ssa Anna Maria Timperio

INDEX

ABSTRACT

My PhD thesis is centered on the analysis of the 'muscle-to-meat' conversion process in the Piedmontese beef breed by an 'omic' approach. This process takes place when a farm animal is slaughtered and its muscles are left to a resting period, during which they develop the qualities of the final product, as to say, the eatable meat.

In my PhD thesis I have described the muscle conversion to meat throughout a 44 days – time course analysis, primarily relying on the variations of some key metabolites, and of the proteome by means of differential 1D and 2D gel electrophoresis coupled with MS protein identification. Moreover, I intertwined the classical, physical measurements for meat quality evaluation with the omic data.

After the rigor mortis (when muscle becomes meat and reaches its highest toughness), a proteolytic process takes place that promotes meat tenderization; the proteomic overview documents changes in sarcoplasmic and myofibrillar proteins. My results show the rapid impairing of creatine/phosphocreatine system, as well as of the aerobic production of ATP. Glycolysis becomes the only source of ATP for the meat cells; the increasing oxidative stress is the cause of the metabolic changes (meat cells try to counteract it), such as the increase of pentose phosphate pathway intermediates as to gain reducing power in the form of NADPH (necessary for the recovery of reduced glutathione). The statistical processing of physical and metabolomic measurements along the time points indicated the possibility to use some metabolites as markers for meat tenderness (in particular, serine, arginine and glutamate).

In the second part of my thesis, a more in-depth omic analysis showed that meat cells likely execute the apoptotic mechanisms when the oxidative stress inevitably becomes overwhelming. The proteomic results gave clues of apoptosis in the time course trend of annexin A2, Phosphatidylethanolamine Binding Protein, DJ1 protein, Heat Shock Protein B6, Adenylate Kinase, crystalline αB, and 31 kDa actin fragment; the metabolomic results gave clues of apoptosis looking at the general metabolic behavior and at particular key metabolites (such as nitrotyrosine and taurine); the phosphoproteomic results gave clues of apoptosis in cryαB, HSPB6, myosin 2, synaptopodin 2 and in the phosphorylation of some metabolic enzymes.

ABSTRACT (IN ITALIANO)

La mia tesi di dottorato è focalizzata sull'analisi, tramite approccio omico, del processo di conversione del muscolo in carne nella razza bovina Piemontese. Questo processo ha inizio nel momento della macellazione dell'animale da allevamento, quando i suoi muscoli vengono lasciati ad un periodo di riposo durante il quale essi sviluppano le qualità del prodotto finale, cioè la carne commestibile.

Nella mia tesi ho descritto la conversione del muscolo a carne attraverso un'analisi temporale del periodo di frollatura (44 giorni), principalmente considerando la variazione del proteoma, attraverso gel 1D e 2D con identificazione in MS, e di alcuni metaboliti chiave. Inoltre, ho integrato i dati omici con le classiche misure fisiche adottate nella valutazione della qualità della carne.

Dopo il rigor mortis (momento in cui il muscolo diviene carne e raggiunge la sua massima durezza), ha inizio un processo proteolico che promuove l'intenerimento della carne; la panoramica proteomica testimonia cambiamenti nelle proteine miofibrillari e sarcoplasmatiche. I miei dati mostrano il rapido degrado del sistema creatina/fosfocreatina, così come della produzione aerobica di ATP. La glicolisi diviene l'unica fonte di ATP per le cellule della carne; lo stress ossidativo in costante aumento, che le cellule della carne tentano di contrastare, è la causa di stravolgimenti metabolici quali l'aumento degli intermedi della via dei pentosofosfati allo scopo di ottenere potere riducente sotto forma di NADPH (necessario al recupero di glutatione ridotto). L'elaborazione statistica dei dati fisici e metabolomici raccolti lungo alcuni punti temporali suggeriscono la possibilità di utilizzare alcuni metaboliti come marker per la tenerezza della carne (serina, arginina e glutammato in particolare).

Nella seconda parte della tesi, un'analisi omica maggiormente approfondita mostra il probabile comportamento apoptotico delle cellule della carne nel momento in cui lo stress ossidativo diviene insostenibile. I risultati proteomici hanno fornito indizi al riguardo nel trend temporale di alcune proteine differenziali quali annessina A2, PEBP, DJ1, HSPB6, adenilato chinasi, crystalline αB, e frammento di 31 kDa dell'actina; la stessa metabolomica ha fornito indizi in questa direzione, sia nell'interpretazione del comportamento metabolico generale che di particolari metaboliti chiave (quali nitrotirosina e taurina); gli indizi forniti dalla fosfoproteomica si reggono sull'analisi temporale di cry αB, HSPB6, miosina 2, sinaptopodina 2 e di alcuni enzimi metabolici chiave.

A GENERAL INTRODUCTION

The omnivorous diet is at the base of the human nutrition. Meat likely began quite early to play an important part during the human evolution, as it has been suggested by Leonard et al. (2002), because the development of our sophisticated brains that need a large proportion of the whole body's energy intake could be permitted only by the exploitation of energy-rich foods like meat. After the period of the progresses in hunting techniques, the domestication of animals and the animal husbandry guarantee a more reliable source of meat, at the same time reducing the number of animal species from which it was obtained; nowadays, the utilized sources of meat are turkeys, geese, ducks, ostrich, farmed fish, goats, sheep, pigs, horses, rabbits, bovines, with various new species taken into account.

However, the most important meat-producing species are poultry, sheep, pigs and cattles, the first one giving the 'white meat' while the remaining giving the 'red meat'. Sheep are the most important in the Near East, pigs in Far East, and beef plays the role of the main character in North and South America, Africa and Europe (Warriss, 2010). Beside the classical division into red and white meat, also 'processed' meats have to be grouped in a specific class, including cured and smoked meats, ham, bacon, sausages, hamburgers, salami and tinned meat. For the purpose of my thesis, the mention of red meat from here on will refer only to red meat which is unprocessed. As evidenced by Linseisen et al. (2002), the EPIC (European Prospective Investigation into Cancer and Nutrition) investigation reports the daily red, white and processed meat consumption data for the principal European countries (Table 1). It is

TABLE 1. MEAT CONSUMPTION (g/day) IN 7 EUROPEAN COUNTRIES.						
	RED MEAT		WHITE MEAT		PROCESSED MEAT	
	MEN	WOMEN	MEN	WOMEN	MEN	WOMEN
GREECE	45.3	25.5	23.5	15.8	10	5.8
SPAIN	74	37.8	43.6	31.8	52.8	29.6
GERMANY	52.2	28.6	19.2	14.8	83.2	40.9
ITALY	57.8	40.8	48.8	25.7	33.5	19.6
DENMARK	69.6	44.1	19.6	18.9	51.9	25.3
NETHERLANDS	63.8	41.1	19.4	13..9	72.4	37.9
UK	40	24.6	29.7	25.4	38.4	22.3

evident that red meat is the most important in terms of consumption in all the considered nations (except for Germany), so the economic impact is strong, and the growing interest is so explained.

1.1 AN INTRODUCTION TO MEAT STRUCTURE

Meat is defined by the Codex Alimentarius (2005) as "All parts of an animal that are intended for, or have been judged as safe and suitable for, human consumption"; a more intuitive definition for meat is 'the flesh of an animal used as food'. When speaking of meat, everyone is surely leaded to associate it to 'muscle'; it is a simple, but also simplistic, association, because there exist a number of striking differences between muscle and meat. However, muscle is the starting point of meat production. The muscular tissue is one of the highest examples of structural organization found in the animal body which can perform a wide range of mechanical functions. Muscle cells are necessary for locomotion, for the movement of limbs and other gross movements, but also coordination and balance maintenance are among their tasks; the association of muscle movement and metabolism permits other different functions like the support to the blood circulation and the body temperature maintenance. Living muscle cells are able to undergo striking intracellular changes, a characteristic that heavily influences their response after the death of the organism. Their organization, structure

and metabolism are intertwined aspects that ensure the maintenance of muscle integrity both during contraction and during the moments following death (the early postmortem period), the latter being pivotal in the frame of meat transformation.

-*1.1.1 Composition of mammalian muscle.* (Table 2). Water is the major constituent of muscle (US Department of Agriculture, 2008), about 75%, but in postmortem muscle this percentage is variable into the range of 65-80%; it is the principal component of the extracellular fluid into the muscle and of the sarcoplasmic fluid, functioning as thermoregulator, as medium for muscular metabolic processes and as intramuscular/extramuscular transporter. The protein component is the second biggest one (16-22%), whose principal task is the contractile process; the myofibrillar proteins, insoluble at low ionic strength, are divided into contractile proteins (directly involved in movement) and regulatory proteins (involved in the regulation of the interactions between the contractile proteins). Another group is constituted by the sarcoplasmic proteins (soluble at low ionic strength), which are signaling proteins and important enzymes intervening into the cellular metabolism/remodeling. The muscular lipid content is variable (1-13%), depending on age, nutritional level, muscle type; however, it shows an inverse proportion with water (Callow, 1948). Some lipid is contained into the muscle cells, but the greatest percentage is located between the muscle bundles. Carbohydrates make up a relatively small percentage of muscular tissue (0.5-1.5%), but they are extremely important in the context of the normal and postmortem metabolism; the quantitatively and qualitatively most important muscular carbohydrate is glycogen. The picture is completed by the presence of non-protein nitrogenous compounds, such as nucleotides, free amino acids, and creatine metabolites.

TABLE 2. COMPOSITION OF MAMMALIAN MUSCLE.

COMPONENT	% OF MUSCLE WEIGHT
WATER	65-80%
PROTEINS	16-22%
LIPIDS	1-13%
CARBOHYDRATES	0.5-1.5%
NON PROTEIN NITROGENOUS SUBSTANCES	1-2%
OTHER NON PROTEIN SUBSTANCES	0.5-1%

-1.1.2 Basic muscle structure: from whole muscle to individual fibers. (Figure 1). The arrangement of muscle tissue, where the myofibers and the connective tissue are intertwined, is one of the most organized. Muscle fibers are multinucleated and postmitotic, and each nucleus is the responsible for the control of the protein synthesis necessary for that specific region (nuclear domain; Hikida, 2011) of the myofibril. A whole muscle is surrounded by the epimysium, a layer of connective tissue; the perimysium surrounds the bundles of fibers within the muscle, while the sarcolemma (cell membrane) surrounds any single muscle fiber.

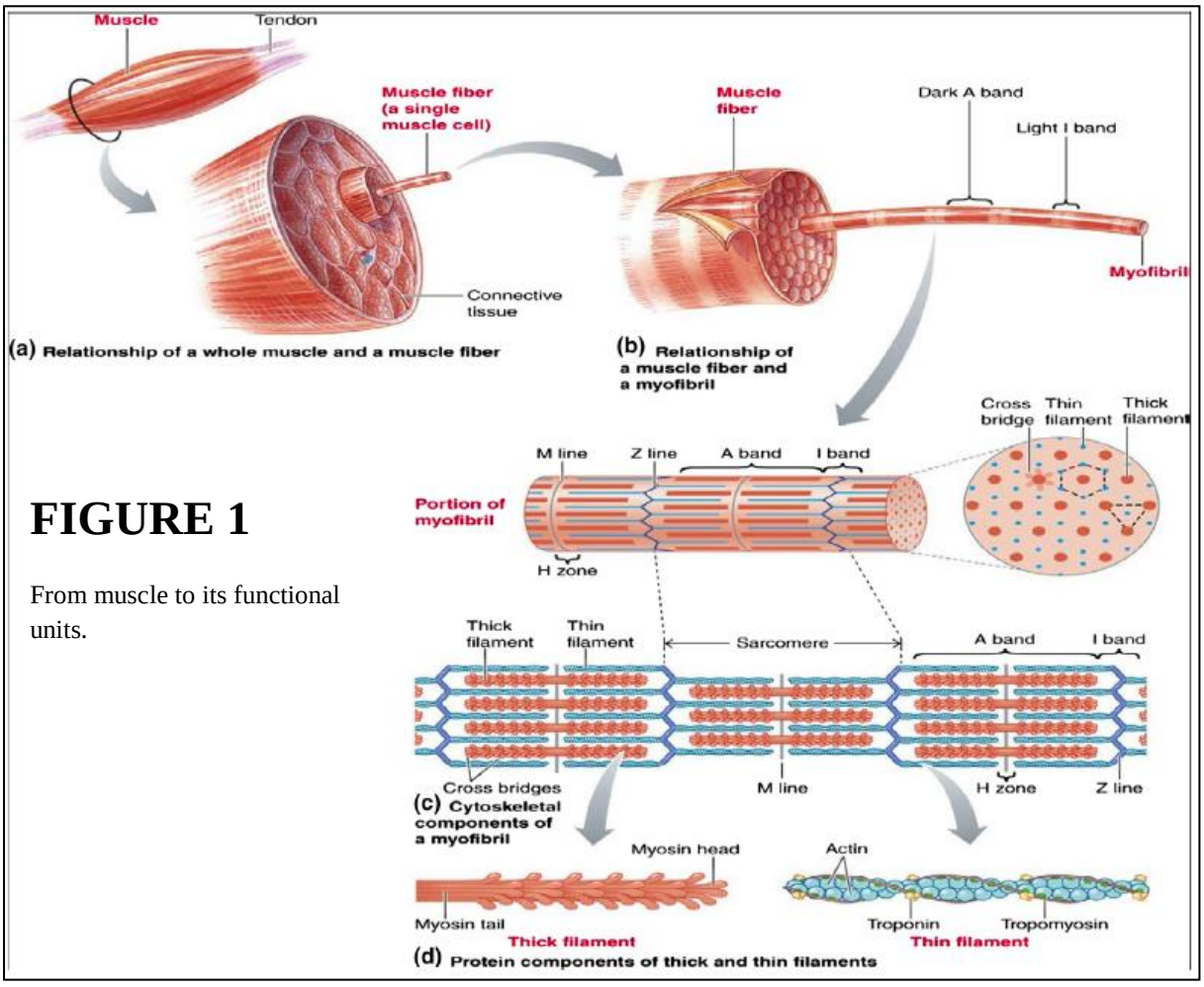

FIGURE 1

From muscle to its functional units.

Many proteins physically associate the sarcolemma with the internal myofilament structure, in particular with actin and myosin.

Skeletal muscles are highly heterogeneous, because of the functional relationship with their specific task. The diversity is not simply at the gross level, but even in the size and the

number of the cells; for example, we have hundreds of muscle cells forming the tensor tympani, whereas over a million forming the gastrocnemius (Feinstein et al., 1955). The number of cells has a strong influence on the functionality of the living muscle, but it is also of extreme importance for meat quality.

-*1.1.3 Muscle proteins*. (Figure 2). Each muscle fiber is made of thousands of myofibrils and contains billions of myofilaments, whose highly ordered pattern of assembly forms sarcomeres (the basic contractile units), containing more than 65 proteins (Fraterman et al., 2007). The striated appearance of the muscular cells is the result of the particular sarcomeric structure: protein dense A-bands and less dense I-bands alternate within the myofibril. In the middle of the I-bands, there are dark lines called Z-bands; the sarcomere is the structure put between two consecutive Z-lines, so it is constituted by Z-line/half I-band/A-band/half I-band/Z-line. In a relaxed muscle cell, the length of the sarcomere is approximately 2.2 µm, and the number of these repeated units determines the length of the myofibril (Wickiewicz et al., 1983). Proteinacious filaments, known as intermediate filaments, connect the myofibril with the Z-

FIGURE 2. A schematic view of the sarcomeric unit. MyoHC = myosin heavy chain; MyoLC = myosin light chain; TNN = troponin.

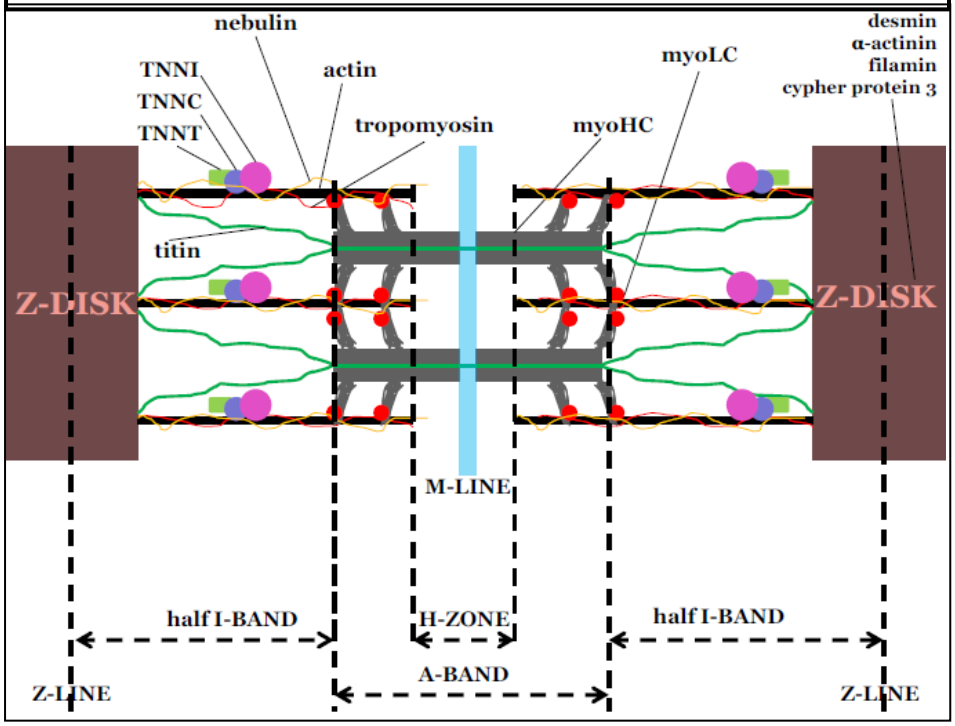

line, while other protein structures, costameres, attach the sarcolemma to the outermost myofibrils (Robson et al., 2004). Myofibrils are formed by many myofilaments, divided into two principal types classified as thick and thin; a third one is primarily composed by the titin protein (Ma et al., 2006). The I-bands are made up by thin filaments, while the A-bands are characterized by the overlap of thin and thick filaments, principally constituted by myosin and actin, respectively, and together they form approximately the 70-80% of the total protein content of a single fiber. Myosin is the main molecular motor and up to eleven sarcomeric myosin genes have been described in mammals. Other fundamental proteins, involved into the activation process of the myofilament sliding and force generation, are troponin T, I, C and tropomyosin. Titin is a large elastic protein that attaches to the Z-disk and to myosin to give stability and the correct alignment to the thick filament. Nebulin, on the other hand, is integrated with other proteins in the thin filaments (Ottenheim & Granzier, 2010). Titin and nebulin are principally involved into the maintenance of the integrity of the sarcomere, influencing passive tension and stiffness of any single cell. The principal proteins that form the Z-disk are α-actinin, filamin, cypher protein 3 and desmin.

-1.1.4 Muscle fiber organelles. The muscular functions are strictly dependent on the organelles network, where we can find the transverse tubular system (T tubule), the sarcoplasmic reticulum and the mitochondria; the exact amount of these elements varies with the fiber type. The T tubule system is of fundamental importance for the conduction of the action potential from the exterior to the interior of the muscle cell, ensuring that the excitation spread uniformly throughout the fiber (Jayashinghe & Launikonis, 2013).

The sarcoplasmic reticulum is responsible for the management of the intracellular concentration of calcium (storage, release and reuptake after activation). The terminal cisternae of the sarcoplasmic reticulum are in close contact with the T tubule system and contain calcium ions; each T tubule is flanked on both sides by two cisternae, forming a

structure called triad. Two proteins are of particular importance in maintaining calcium homeostasis: Ca^{2+}-ATPase (SERCA), responsible for the calcium reuptake into the cistern after muscle activation, and calsequestrin, which binds calcium loosely within the sarcoplasmic reticulum.

The mitochondria network is highly spatially organized in all the three dimensions throughout the cell; it supplies the cell with the energy necessary for muscle actions when oxygen is made available to the fiber (Dahl et al., 2014); the spatial disposition of the mitochondria, located closer to the sarcolemma, is organized in such a way that the diffusion distance for oxygen transported by capillaries is reduced; it is particularly useful during aerobic exercise, which increases the demand for oxygen. Another population of mitochondria is located in the intermyofibrillar space. A muscle used to heavy exertions has a greatest number of mitochondria with respect to a sedentary one, because of the mitochondrial biogenesis process, regulated by the peroxisome proliferator-activated receptor γ coactivator 1α (Yan et al., 2012).

1.2 UNDERSTANDING THE MUSCLE PHYSIOLOGY BEHIND THE CONVERSION INTO MEAT.

-1.2.1 Physiology of muscle activation. The generation of muscular force is the result of the so-called excitation-contraction coupling, which relies in the coordination of two processes: the transmission of the nerve impulse to the triad, with the consequent release of calcium from the cisternae of the sarcolasmic reticulum, and the formation of the actin/myosin cross-bridges. When the action potential arrives to the muscle fiber membrane, the T tubule system conduces it to the interior of the muscle cell; in the triad, the close proximity of the T tubule and the terminal cisternae permits to a voltage sensor subunit of the dihydropiridine receptors

on the T tubule to open and to allow an inward current of calcium (Rebbeck et al., 2014) that in turn triggers the opening of the ryanodine receptors in the terminal cisternae, leading to a massive release of calcium into the sarcoplasm. At this point, Ca^{2+} is picked up by troponin C, able to induce a conformational change in troponin I that leads to its dislocation from the thin

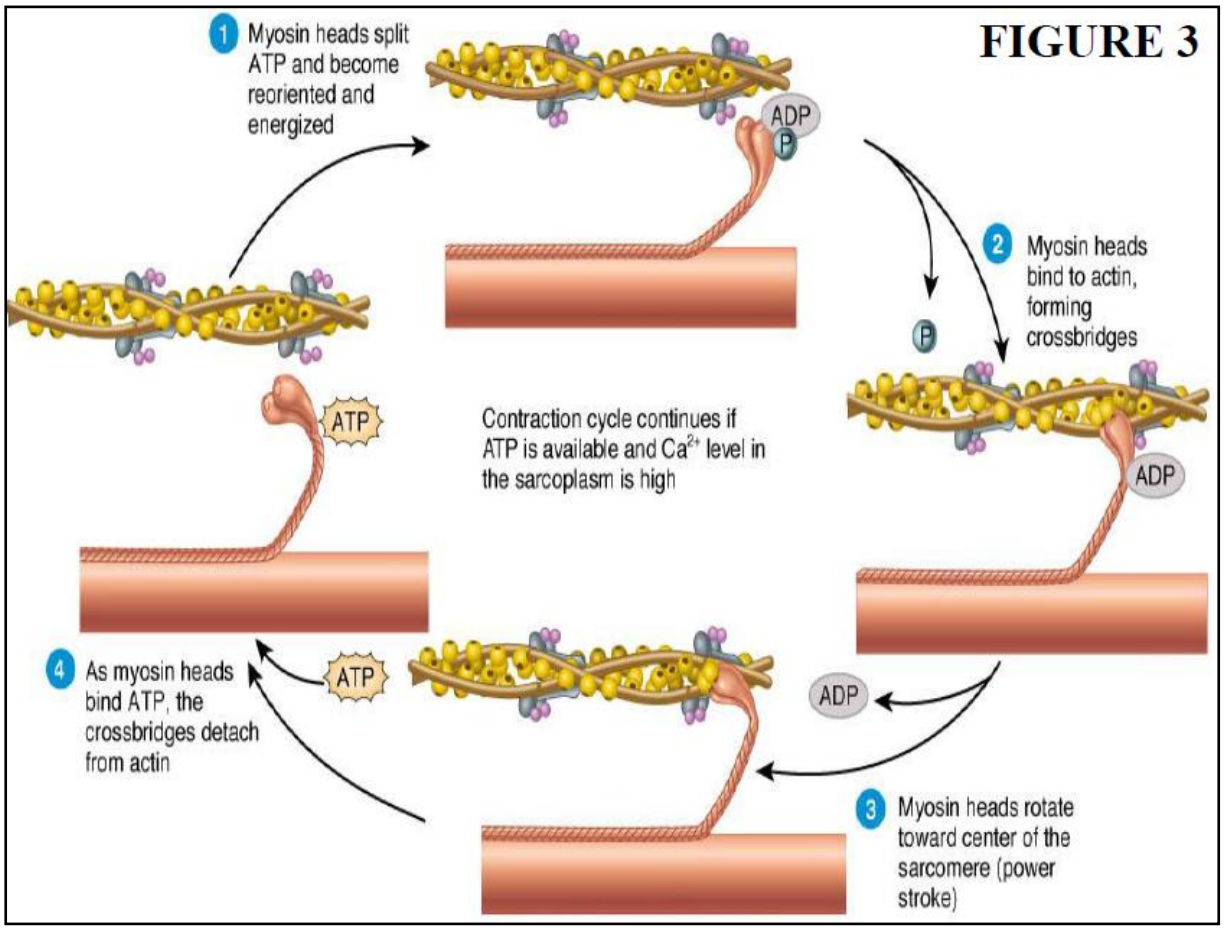

filaments (I as 'inhibitory', definition due to its inhibitory action against the formation of the actomyosin complex without nervous stimulus); if no action potential arrives, the tropomyosin complex sterically obstructs the myosin binding sites on actin, but after Ca^{2+} reception by troponin C, troponin T (the Tropomyosin-binding element of the heterotrimeric troponin complex) transmits the conformational change to the tropomyosin complex, making actin able to bind myosin. The actomyosin complex is able to dissociate only in the presence of ATP, because of the conformational change induced by ATP binding on a specific site of the myosin globular head; this domain has an ATPase activity, able to hydrolyze ATP into

ADP and inorganic phosphate. The released energy is conserved into the myosin structure, where ADP and Pi are initially maintained. The so-called 'power stroke' (figure 3) begins at the release of Pi from myosin crossbridge, event that allows the tension unloading by means of the mechanical movement of myosin, which pushes back the linked actin filament: the result is the sliding of thin and thick filament, the shortening of sarcomeres and contraction. At this step ADP is bound to the myosin head, and this conformational status allows only a weak binding to the actin filament; when ADP is released, the binding becomes really strong and essentially irreversible without another incoming ATP molecule. This is the explanation for the onset of rigor mortis, which is the starting point of the muscle-to-meat conversion.

-1.2.2 Muscle metabolism. (Figure 4). In an actively exercising animal, up to the 90% of the oxygen consumption of the whole body is accounted by the muscular tissue; the muscle's metabolic rate can increase of as much as 200% from the resting state (Hargreaves & Thompson, 1999). Obviously, central to the existence of the muscle cell is the production of ATP, and the muscular activity is dependent on ample ATP supplies within the muscle, so it has developed several ways to produce ATP. Blood is the principal source of nutrients; it transports circulating lipids and, first of all, glucose, but muscle cells can employ energy precursors reserves such as glycogen, lipids and

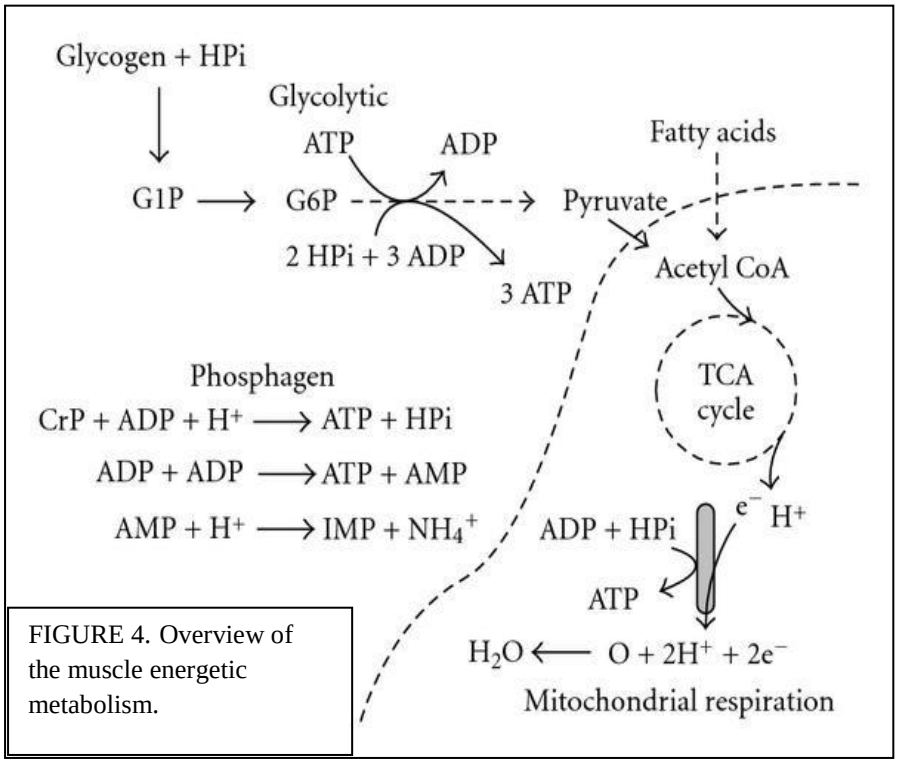

FIGURE 4. Overview of the muscle energetic metabolism.

phosphagens (ATP, phosphocreatine); the choice between the exploitation of the internal or circulating resources is dependent on the activity the muscle is carrying on: when the muscular task is not intense, it preferentially consumes the energy sources picked up from the blood stream, or the lipids contained in its cells (by means of a completely aerobic metabolism). When the muscular activity is of higher intensities, the ATP is very rapidly consumed, and the cells make use of the intracellular reserves of phosphagens and glycogen, which are burnt very rapidly, leading to fatigue. The ATP concentration within the muscle is critical; the relaxation of the fibers can occur when this value is approximately above the 30% of the resting stores, also because the removal of calcium from the sarcoplasm is an ATP-dependent mechanism (Hargreaves & Thompson, 1999).

-*1.2.2a Glycogen and glucose: glycogenolysis and glycolysis*. Glucose and glycogen are the preferred substrates for muscular energy production, and they can be utilized in an aerobic (oxidative phosphorylation) or anaerobic way (anaerobic glycolysis); lipids are molecules with a very high level of energetic density, but it is curious to underline that despite they are very efficient with respect to the amount of ATP that can be produced per unit of substrate, their rate of ATP synthesis is much slower compared to the ATP production rate of glycogen (about the half, 1.5mmol/kg/sec for free fatty acids versus 3mmol/kg/sec for the aerobic use of glycogen versus 5mmol/kg/sec for the anaerobic use of glycogen) (Joanisse, 2004). Over time, during muscular activity, the muscle glycogen stores diminishes and, as a consequence, the reliance on it diminishes, while the glucose import into myofibers increases; however, if the activity is heavy, little or no exogenous glucose is used for ATP production, and the reliance on glycogen proportionally increases with the increase of the effort (due to the shift toward the anaerobic catabolism). Glycogen is synthesized in the muscle at rest; diet has a heavy influence on the content of whole-body glycogen storage. Glycogen breakdown (figure 4) is under hormonal control, with the cAMP-dependent activation of phosphorylase kinase

by epinephrine, and it is further stimulated by the release of Ca^{2+} from the sarcoplasmic reticulum during contraction (Allen & Westerblad, 2001). The breakdown of glycogen directly involves two enzymes: glycogen phosphorylase (GP) and glycogen debranching enzyme; the rate of this process is limited by the availability of HPO_4^{2-}, that is not present at pH 5, due to the H_2PO_4 pK_a (7.2). The glycogen phosphorylase is in an inactive form during the muscular resting period, while it is activated by epinephrine, a stimulus that wakes up a signaling cascade involving calcium, cAMP, cAMP-activated protein kinase and phosphorylase kinase; glucose 6 phosphate and ATP exert an inhibitory effect on GP. HPO_4^{2-} or AMP bind to an effector site of GP, increasing the acceptance of glycogen at the active site. It is worth noting the amplification of the signal in this pathway: the relative concentrations of the three successive enzymes of the cascade (cAMP-dependent protein kinase, phosphorylase kinase and GP) occur as molar ratios of 1:10:240, including adrenalin at a ratio of $1x10^{-4}$, and a single molecule of epinephrine bound to a specific receptor on a muscle fiber results in 400'000 glucose-1P units cleaved by the GP per second (Lodish, 2000).

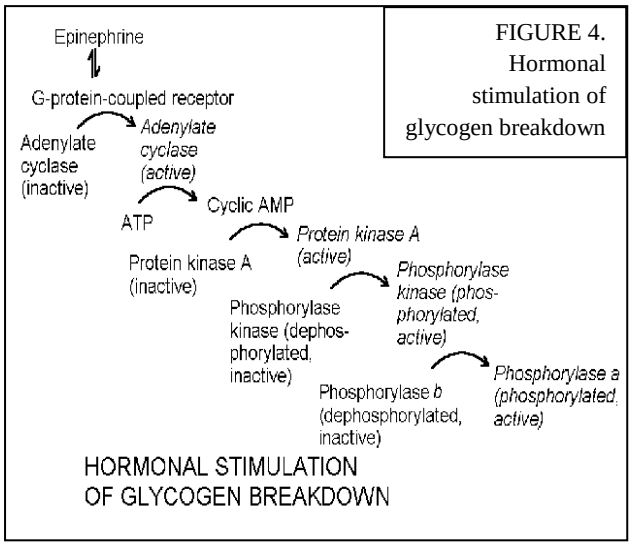

FIGURE 4. Hormonal stimulation of glycogen breakdown

The generation of ATP in skeletal muscle with an adequate oxygen supply is dependent on fatty acid β-oxidation, on the pyruvate dehydrogenase complex reactions, on the Krebs cycle, on the electron transport chain and on the oxidative phosphorylation. Acetyl-CoA is the central molecule of the aerobic behavior, able to undergo the Krebs cycle reactions and to give reducing equivalents of NADH and $FADH_2$; these molecules are then used by the electron transport chain to drive the proton gradient across the inner mitochondrial membrane,

leading to the recharge of ATP from ADP; oxygen is the final electron acceptor. The volume density of the mitochondria within the cell, the capacity for oxygen transport and storage within the myofiber (dependent on the intracellular levels of myoglobin) determine the capacity for oxidative phosphorylation; the controlling elements of the mitochondrial respiration vary with the state of the myofiber, as well as with its composition. However, major contributors are the concentrations of free ADP, P_i, the NADH/NAD^+ ratio, calcium levels and oxygen availability; the relative contribution of all these factors show a different importance under different conditions.

The carbon units of glucose encounter a key step at the level of pyruvate: it can be completely broken down in an oxidative way entering the mitochondria by means of the pyruvate dehydrogenase complex, giving CO_2 and H_2O as endproducts and yielding 36 mol of ATP per mole of glucose. By contrast, if the catabolic choice of the muscle cell is anaerobic (like it is in postmortem muscle), pyruvate does not enter the mitochondria, and it is converted into lactate, yielding only 2 mol of ATP per mol of glucose. So, there is an evident gap between the ratio of ATP moles aerobically produced per mole of substrate and the ratio of ATP moles anaerobically produced, but, reminding the higher speed of ATP production in a time interval, it is not correct to judge the anaerobic metabolism as less convenient: the particular activity, the availability of nutrients and oxygen and so on (in other words, the context), are the deciding factors for the aerobic or the anaerobic behavior in the living muscle, while the only choice for the postmortem muscle is to enter the anaerobic metabolism when oxygen reservoirs are exhausted.

The role of the anaerobic production of lactate is important to understand in the contexts of both living and dead muscles, because many reactions occurring in the postmortem muscles resemble the physiologic reactions of a living muscle subjected to a strong anaerobiosis. The

complete oxidative consumption of glucose is impaired, because the pyruvate production occurs at rates that exceed the mitochondrial take-up of pyruvate. The reaction

° pyruvate + NADH + H^+ → lactate + NAD^+ ,

catalyzed by the lactate dehydrogenase (LDH), is pivotal for the prevention of the reduction in the rate of glycolytic ATP regeneration: it permits to remove pyruvate (figure 5), to sustain a high-rate glycolysis, and to regenerate cytosolic NAD^+ (Robergs et al., 2004). The latter is the substrate for the glycolytic oxidation/reduction reactions, and the cytosolic [NAD^+] must be maintained at high levels to avoid the drastic slowdown of the glycolysis. An ulterior advantage of the lactate production is the retardation of muscular acidosis: the LDH employs two electrons and one proton from NADH, and a second H^+ from the environment, so it has a metabolic proton buffering function.

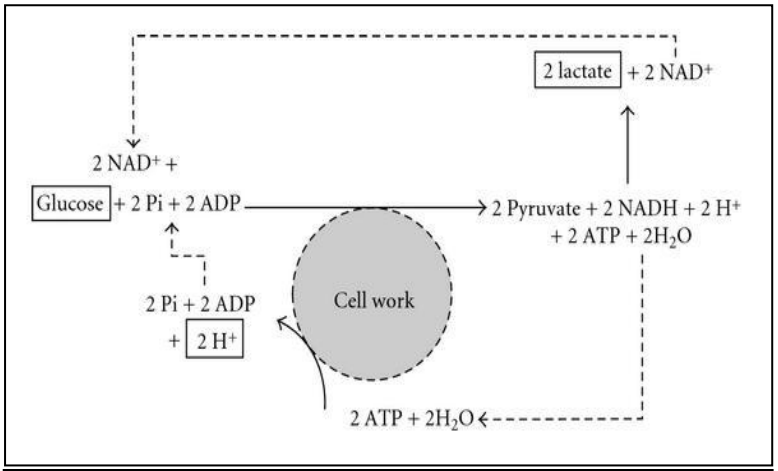

FIGURE 5. Lactic acid fermentation reaction.

-1.2.2b The phosphagen system. Muscle contraction depends on the free energy released from the breakdown of ATP. Despite the strong need for ATP, the ATP store within the muscle cells are not so large (approximately 8 mmol/kg wet weight of muscle), and, as I have briefly explained, they have to produce it by means of the catabolism of energetic molecules (fatty acids, glycogen); here it is important to stress that muscle cells rely on a sensitive control system to rapidly increase ATP production when it is needed, and that they are unique in this frame as they can vary their metabolic rate to a greater extent than the cells of other tissues

(Glaister, 2005). Indeed, muscular tissue is able to buffer even a 1000-fold increase in ATP demand, maintaining the stability of the ATP concentration (the decrease does not exceed 2 mmol/kg wet weight of muscle during these conditions) (Spriet, 1992). The levels of ATP and associated molecules, such as ADP, AMP and P_i, are an essential requirement for muscle cell function. The fluctuations of their concentration are the sensors for muscular energetic situation; an ATP reduction leads to the rapid development of fatigue in vital muscles, and to rigor mortis in dead muscles (Vollestad & Sejersted, 1988). Muscular cells are able to respond to a sudden increase in ATP demand, and beside the two major systems for ATP resynthesis (glycolysis and mitochondrial respiration), there is a third system in muscle cells, called 'Phosphagen system'.

Three principal enzymes are involved into this system, participating to three different but intertwined reactions:

°Creatine kinase: Creatine phosphate + ADP + $H^+ \rightarrow$ ATP + creatine

°Adenylate kinase: ADP + ADP $\rightarrow$ ATP + AMP

°AMP deaminase: AMP + $H^+ \rightarrow$ IMP + NH_4^+

The first and the second reaction both produce ATP, but the creatine kinase reaction has by far the greatest capacity for ATP regeneration. In the living muscle, creatine phosphate shows a relatively high concentration with respect to ATP (up to 100 mmol/kg dry muscle weight, depending on the fiber type, against the 25 mmol/kg for ATP; Joanisse, 2004), but a relatively low concentration with respect to glycogen (500 mmol/kg). The creatine kinase reaction is reversible, so it can be adapted to the ATP request: when it is strong, the phosphate group is transferred from pCr to ADP, and when it is weak, pCr supplies can be readily restored. In a living muscle, the creatine kinase reaction shows also the advantage of consuming a proton, thus reducing the muscle cell acidosis associated with anaerobic glycolysis. The principal role

of pCr in skeletal muscle is that of an energy buffer operating when the ATP demand overcomes the ATP production by the mitochondrial respiration. The so-called 'creatine/pCr shuttle' acts as a cellular energy transport system (based on the existence of different cytosolic and mitochondrial creatine kinase isoforms [figure 6]) that gives to Cr and pCr the roles of energy transporters: Cr becomes pCr in the mitochondria, and after its diffusion in the cytosol, it releases the phosphate group for the recharge of ADP into ATP, employed in the contraction process (Wallimann et al, 1992). So the Cr/pCr system is a low threshold ADP sensor that functions to maintain [ATP]/[ADP] ratios in subcellular locations where creatine kinase is functionally coupled to ATP-consuming and ATP-producing pathways; when Cr reacts with ATP in the mitochondria, the increase in local [ADP] stimulates the mitochondrial respiration (Greenhaff, 2001). In the physiological postmortem conditions, however, the pCr system is not a major contributor to metabolism, because of the rapid depletion of pCr supplies.

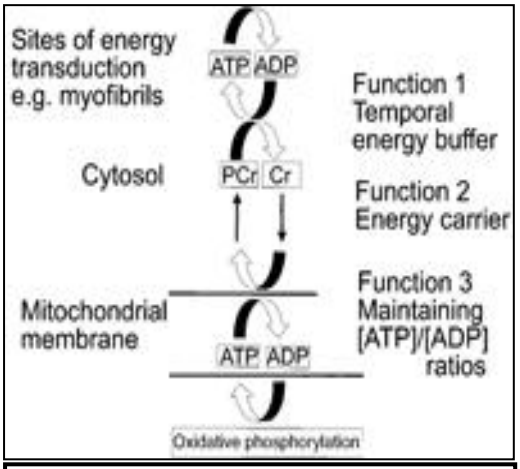

FIGURE 6. The Cr/pCr shuttle.

An important feature of the adenylate kinase reaction is the production of AMP. It is a strong allosteric activator for the glycogen phosphorylase, starting point of the glycogenolysis, as well as a strong activator for the phosphofructokinase, a key enzyme for the glycolytic destiny of the glucose 6P molecules.

The AMP deaminase reaction does not regenerate ATP. However, it is correct to insert it into the phosphagen system, because the AMP conversion into IMP is necessary for the maintenance of the phosphate transfer potential within the muscle (Atkinson, 1977). If the [ADP] and [AMP] are kept at a low level, even a small reduction in [ATP] is sufficient to release the quantity of free energy necessary to fuel the muscular contraction.

This brief excursus about the muscular metabolism has to be kept in mind to understand the striking changes that characterize the physiology of the muscle during its conversion into meat.

In the following section, I will introduce the reader to the importance of the 'omics' technologies in the field of meat science.

1.3 MEAT SCIENCE AND THE OMICS TECHNOLOGIES.

Meat science, a branch of farm animal science, is a leading field of research with a strong economic importance; the target is the production of a high-quality meat to attract the largest number of consumers. Meat quality is an ensemble of many features; the end-consumers judge the different meat products in particular on the basis of flavor, juiciness and tenderness (Bendixen et al., 2011). The 'classical', standard methods for the characterization of meat products mainly consisted in physical measurements such as Warner-Bratzler shear force (an assay for meat resistance to cut, as to 'measure' tenderness), Minolta values (for meat color) and pH. In order to understand the molecular basis of meat development, many biochemical researches have been conducted over the last decades (Paredi et al., 2012; Huff-Lonergan et al., 2010). Gradually, the biochemical investigations integrated the physical measurements, beginning with the spectrophotometric determination of myofibrillary fragmentation indexes that measured the increasing concentrations of peptides and amino acids released by the proteolytic processes in the postmortem muscle (Olson et al., 1976). The last two decades have seen the strong technological growth of the field of 'omics' sciences; genomics,

transcriptomics, proteomics and metabolomics have been engaged in meat science, and the scientific community is directing many efforts in an attempt to join the different techniques in an organic fashion.

-*1.3.1 Proteomics.* The first example of omics application to meat science was the genomic investigation of genome associations with meat-quality parameters; gradually, the interest shifted towards the use of mRNA quantitative assays like PCR or microarrays as to appreciate the changes of the genomic expression (Xu et al., 2013). The natural integration with the proteomic technology has been rapidly reached, and big strides have been achieved towards the completion of the biological understanding underlying muscle-to-meat conversion (D'Alessandro & Zolla, 2013; Hollung et al., 2007). Beside the improvements of the proteomic methodologies like protein isolation and fractionation, bioinformatic tools have begun to give a strong contribution, relying on the consolidation and expansion of databases covering animal-genome sequences.

-*1.3.1a 2D Gel electrophoresis.* The separation of the proteome components of a biological sample by means of gel-based techniques have been firmly established over the last thirty years. Muscles are made of proteins, so the association between meat science and gel electrophoresis has been easily reached. 2D gels are probably the most employed in meat characterization. Depending on the project and hypothesis of a particular meat experiment, different strategies for extraction and pre-fractionation of muscle proteins before 2D-separation could be considered. Some muscle proteins are part of large protein aggregates, like the myofibrillar proteins, some are localized in membranes and others are cytosolic enzymes. With the help of pre-fractionation of the proteins based on solubilization and extraction procedures, the enrichment of soluble sarcoplasmic or myofibrillar proteins can be achieved. These proteins will have very different chemical properties which can be used to isolate the proteins in different fractions (Righetti et al., 2005). Several issues should be

considered before developing a sample preparation strategy. It is advisable to keep sample preparation as simple as possible to avoid protein losses. However, if only a subset of the proteins in the tissue or cells is of interest, pre-fractionation can be employed during sample preparation.

The approach of the proteomic experiments is the opposite with respect to the approach of the traditional, physical experiments: the latter are based on few measurements and variables over many animals, while the former are based on many measurements and variables over a limited number of animals, due to the heavy work-load. In this context, the statistical methodologies play a pivotal role in the validation of the results, and multivariate analysis such as principal component (PCA) are becoming an integral part of proteomic (and in general, omic) experiment (Jacobsen et al., 2007).

Beside the classical 2D-gels, recent technical improvements like the adoption of fluorophores for sample labeling, have permitted the simultaneous analysis of multiple samples in the same gel, a compromise that can abate technical variability issues and increase the sensitivity of the assay (0.25 ng for DIGE) (Jia et al., 2009)

-1.3.1b Two-dimensional HPLC. This technique employs an online combination of ion-exchange and reversed-phase strategies to separate peptide samples; the online elution into a mass spectrometer allows the direct peptide-based identification and their absolute or relative quantification. 2D-HPLC has the potential for a successful application in the field of meat qualities investigation, but it has not hitherto found a systematic use for these purposes; it could be complementary to electrophoresis analysis of more hydrophobic or very high molecular weight proteins, given the technical difficulties of electrophoresis with these species.

-1.3.1c Quantitative approaches with mass spectrometry. The MS-based techniques for the quantification of targeted proteins may be inserted into meat science as validation strategies for potential protein biomarkers of a particular meat quality. The AQUA (Absolute QUAntification of proteins) strategy allows the determination of absolute proteins against synthetic standards. The emPAI (Exponentially Modified Protein Abundance Index) is the logarithmic correlation between protein abundance and the relative intensity of the arbitrary ion count given by the MS analyzer (Cifuentes, 2010). Alternative approaches are ICAT (Isotope Coded Affinity Tag), iTRAQ (Isobaric Tag for Relative and Absolute Quantitation) and SILAC (Stable-Isotope Labeling by Amino acids in cell Culture), which employ isotopic labeling; they have been built as to avoid some inherent quantitative limits of the label-free strategies, coming from the wide range of physicochemical properties that can influence the MS signal for a specific peptide. The stable-isotope-labeled peptide used during the isotopic labeling experiments shows the same chemistry of the non-labeled counterpart, so they have the same reactions to the experiment steps, but their ratio (that provides the quantitative information about the relative abundance of a specific protein) can be calculated since they remain distinguishable in terms of molecular weight (Cifuentes, 2010).

The advantages of these gel-free based approaches are the higher reproducibility, accuracy and swiftness, with the drawbacks of the costs of MS equipments and the need for strong expertise and training either for data acquisition and processing.

-1.3.1d Post-translational modifications. Meat researchers have begun to demonstrate a clear interest for PTM in the field of meat quality investigations, due to the strong influence that a PTM can exert on the final role of a protein. Sumoylation, ubiquitination, glycosylation and phosphorylation showed the greatest importance in meat science (D'Alessandro & Zolla, 2013). Their detection requires preparative techniques such as the 2D-HPLC, with the serial combination of strong cation-exchange or reversed phase columns (Edelmann, 2011), or the

selective enrichment of specific peptides characterized by a particular PTM, for example the glycopeptides captured by lectin columns or the phosphopeptides enriched with Immobilized Metal Affinity Chromatography (IMAC) or TiO_2 microcolumns. The Electron Transfer Dissociation mass spectrometry (ETD) is adequate for PTM detection, overcoming the limits of the CID MS analysis that causes the loss, and so the undetectability, of the side chains of the modified peptides (Mikesh et al., 2006).

In the field of meat science, phosphorylation surely deserves a particular mention; during the muscle-to-meat conversion process, ATP reservoirs are completely exhausted, and given that ATP is the token used for the phosphorylation of proteins, it is easy to hypothesize that the normal phosphorylation pattern of the muscle fibers is impaired, reflecting the changes in tissue structure and in its physiologic metabolism; many glycolytic enzymes are subjected to the modulation by means of phosphorylation, and it has been shown for many metabolic key enzymes involved in the anaerobic metabolism of aging meat (D'Alessandro et al., 2012). The recent MS advances in the identification and quantification of phosphopeptides may be a useful tool for the assessment of methodologies applied to meat production chain for the improvements of meat tenderness, as it has been shown a probable connection between low-voltage electrical stimulation of carcasses, postmortem glycolytic rates and phosphorylation levels in pig meat (Huang et al, 2011).

-1.3.2 Redox proteomics and oxidative modifications. The metabolic impairment suffered by the slaughtered muscle cells leads to an extended redox modification of muscle proteins which heavily influences the organoleptic properties of the meat (D'Alessandro & Zolla, 2013). Once again, ETD mass spectrometry can perform the investigation on protein sulfonation, oxidation or nytrosylation (Mikesh et al., 2006), as well as the analysis of ROS-induced protein fragmentation; however, these interesting topics have been hitherto underinvestigated.

-1.3.3 Metabolomics. Mass spectrometry has unparalleled specificity and sensitivity, high resolution and wide dynamic range, and the potential to enable comprehensive qualitative and quantitative measurements of large-scale small-molecular metabolites in complex biological samples; for this reason, MS has emerged as the foremost technology in metabolomics studies, and as a relatively new mean to investigate food at its metabolome level; food analysis regarding the quality and the safety of the food has become a topic of enormous interest to consumers. Thanks to the potential of MS-based metabolomics, meat industry has paid increasing attention to comprehensive determination of the complex meat composition in raw materials, semi-manufactured and final products involved in authenticity, functionality, quality and safety issues (Herrero et al., 2012). Meat science is always in search for new means and technologies to employ for the improvement of final meat products qualities; given the complexity of the biological mechanisms underlying the develop of meat characteristics, MS-based metabolomics can represent a new, leading approach to the analysis of the muscle-to-meat conversion process. Beside the more commonly used omic techniques, metabolomics could furnish another point of view; the integrated pictures of proteome, genome, transcriptome, phosphoproteome and metabolome could help to delve into the physiology of the postmortem muscle. Muscle-to-meat conversion starts soon after animal slaughter; the bleeding promotes deoxygenation, anoxia and the loss of nutrients supply. The metabolism suffers a sort of revolution, because of the switch to the anaerobiosis. It is clear that in this context, the analysis of the metabolome could be extraordinarily informative, especially when performed by means of MS; until a few years ago, pH monitoring and spectrophotometric approaches constituted the strategy of choice, limited by the small number of metabolites roughly detected at the quantitative level. The technological improvements of MS, and the bioinformatic advancements (with the increasing completeness and accuracy of metabolite-spectra databases), allow the elaboration of raw mass spectra for feature detection, peak

alignment, tentative identification, isotopic distribution and relative quantification, so exponentially enlarging the range of the detected metabolites as to follow a bigger part of the entire metabolome. MS-based metabolomic have been successfully applied to investigate several biological issues in meat science (D'Alessandro & Zolla, 2013; Bowker et al., 2000).

-1.3.4 Omics strategies: their integration in systems biology. The comprehension of the biochemistry and molecular mechanisms leading to the develop of meat qualities cannot be complete if we simply collect the bits of information from separate omics disciplines. Meat scientists are beginning to integrate all the collected pieces of the puzzle, in order to propose a complete, unified overview of the molecular phenomena underpinning meat production events. Muscle-to-meat conversion process involves pH, metabolism, glycolytic enzymes, PTMs, proteases, fragmentation of the muscular structure, ROS; these aspects are all integrated in a single concept where each piece interacts to some extent with at least some of the others. A systems-biology approach is opposed to a reductionist approach; it permits to find out specific characteristics appreciable only as emerging properties of the general system and not of the distinct parts. Applied to meat science, it could represent a step toward the building of a definitive model for meat qualities development, which is a multifactorial process, affected by the characteristics of the living animal (species, breed, gender, age [D'Alessandro et al., 2011]), rearing environment (Kwasiborski et al., 2008), feeding regimen, modalities of transportation to the abattoir and slaughter (Yamane et al., 2006), postmortem treatments (Li et al., 2012), bleeding, hanging, deboning procedures and cooling rate (Bertram et al., 2001). Clearly, a unique model for meat formation is utopian. However, models that could be valid for specific species (more often, specific breeds) appear to be more reliable: centuries of selection of livestock for breeding have narrowed the genetic diversity of the animals, while other variables could be constantly checked during laboratory experiments.

The conversion of muscle into meat as a whole and the postmortem development of the eating quality are far from being understood. Improvement of our knowledge about the underlying mechanisms is particularly faced to the large biological variability of meat qualities and to the non-identification of their major determinants. Research tools to investigate the *in toto* biochemical mechanism, such as the integrated omics device, can play a major role in farm animal and meat science. Given the intricate scenario of this process, my PhD thesis wanted to be an attempt to establish a few milestones as to delve into the events leading from muscle to meat, exploiting some of the discussed potentialities of omics technologies.

REFERENCES

Allen DG, Westerblad H (2001). Role of phosphate and calcium stores in muscle fatigue. Journal of Physiology 536:657-665.

Atkinson DE (1977). Cellular Energy Metabolism and Its Regulation, Academic Press, New York, NY, USA, 1st edition.

Bendixen E, Danielsen M, Hollung K, Gianazza E, Miller I (2011). Farm animal proteomics – a review. J. Proteomics 74(3):282–293.

Bertram HC, Donstrup S, Karlsson AH, Andersen HJ, Stodkilde-Jorgensen H (2001). Postmortem energy metabolism and pH development in porcine M. longissimus dorsi as affected by by two different cooling regimes. A (31)P-NMR spectroscopic study. Magnetic Resonance Imaging 19(7):993-1000.

Bowker BC, Grant AL, Forrest JC, Gerrard DE. Muscle metabolism and PSE pork (2000). Journal of Animal Science 79:1-8.

Callow, EH (1948). Comparative studies of meat. II. Changes in the carcass during growth and fattening and their relation to the chemical composition of the fatty and muscular tissues. Journal of Agricultural Science 38:174.

Cifuentes A (2010). Food science, foodomics and capillary electromigration methods, Electrophoresis 31(13):2091.

Codex Alimentarius (2005). Code of hygiene practices for meat. CAC/RCP 58-2005.

D'Alessandro A, Marrocco C, Zolla V, D'Andrea M, Zolla L (2011). Meat quality of the longissimus lumborum muscle of Casertana and Large White pigs: metabolomics and proteomics intertwined. Journal of Proteomics 75(2):610-627.

D'Alessandro A, Rinalducci S, Marrocco C, Zolla V, Napolitano F, Zolla L, Love me tender: an Omics window on the bovine meat tenderness network. Journal of Proteomics 75(14):4360–4380.

D'Alessandro A, Zolla L (2013). Meat science: From proteomics to integrated omics towards system biology. Journal of Proteomics 78:558-577.

Dahl R, Larsen S, Dohlmann TL, Qvortrup K, Helge JW, Dela F, Prats C (2015). Three-dimensional reconstruction of the human skeletal muscle mitochondrial network as a tool to assess mitochondrial content and structural organization. Acta Physiol (Oxf) 213(1):145-155.

Edelmann MJ (2011). Strong cation-exchange chromatography in analysis of posttranslational modifications: innovations and perspectives. Journal of Biomedicine and Biotechnology 2011:936508.

Feinstein B, Lindegard B, Nyman E, Wohlfart G (1955). Morphologic studies of motor units in normal human muscles. Acta Anatomica 23:127-142.

Fraterman S, Zeiger U, Khurana TS, Wilm M, Rubinstein NA (2007). Quantitative proteomic profiling of sarcomere associated proteins in limb and extraocular muscle allotypes. Molecular Cell Proteomics, 6:728-737.

Glaister M (2005). Multiple sprint work: physiological responses, mechanisms of fatigue and the influence of aerobic fitness. Sports Medicine 35(9):757–777.

Greenhaff PL (2001). The creatine-phosphocreatine system: there's more than one song in its repertoire. Journal of Physiology 537(3):657.

Hargreaves M, Thompson M (eds) (1999). Biochemistry of Exercise, 10. Champaign, III: Human kinetics.

Herrero M, Simo V, Garcia-Canas V, Ibanez E, Cifuentes A (2012). Foodomics: MS-based strategies in modern food science and nutrition. Mass Spectrometry Reviews 31:49-69.

Hikida RS (2011). Aging changes in satellite cells and their functions. Current Aging Science 4:279-297.

Hollung K, Veiseth E, Jia X, Faegerstad EM, Hildrum KI (2007). Application of proteomics to understand the molecular mechanisms behind meat quality. Meat Science 77(1):97-104.

Huang H, Larsen MR, Karlsson AH, Pomponio L, Costa LN, Lametsch R (2011). Gel-based phosphoproteomics analysis of sarcoplasmic proteins in postmortem porcine muscle with pH decline rate and time differences. Proteomics 11(20):4063–4076.

Huff Lonergan E, Zhang W, Lonergan SM (2010). Biochemistry of postmortem muscle – lessons on mechanisms of meat tenderization. Meat Science 86(1):184-195.

Jacobsen S, Grove H, Jensen KN, Sørensen HA, Jessen F, Hollung K *et al* (2007). Multivariate analysis of two-dimensional gel electrophoresis protein patterns - Practical approaches. Electrophoresis 28:1289‑1299.

Jayashinhe ID, Launikonis BS (2013). Three-dimensional reconstruction and analysis of the tubular system if vertebrate skeletal muscle. Journal of Cell Science 126:4048-4058.

Jia X, Veiseth-Kent E, Grove H, Kuziora P, Aass L, Hildrum KI, Hollung K (2009). Peroxiredoxin-6 – a potential protein marker for meat tenderness in bovine longissimus thoracis muscle. Journal of Animal Science 87(7):2391– 2399.

Joanisse DR (2004). Skeletal muscle metabolism and plasticity. In Functional Metabolism, Regulation and Adaptation, Storey KB (ed), 295-318. Hoboken NJ: Wiley-Liss.

Kwasiborski A, Sayd T, Chambon C, Santè-Lhoutellier V, Rocha D, Terlouw C (2008). Pig longissimus lumborum proteome: Part I. Effects of genetic background, rearing environment and gender. Meat Science 80(4):968-981.

Leonard WR, Robertson ML, Snodgrass JJ, Kuzawa CW (2002). Metabolic correlates of hominid brain evolution. Comparative Biochemistry and Physiology Part A 136, 5-15.

Li CB, Li J, Zhou GH, Lametsch R, Ertbjerg P, Bruggeman DA, Huang HG, Karlsson AH, Hviid M, Lundstrom K (2012). Electrical stimulation affects metabolic enzyme phosphorylation, protease activation, and meat tenderization in beef. Journal of Animal Science 90(5):1638-1649.

Linseisen J, Kesse E, Slimani N, Bueno-de Mesquito HB, Ocke MC, Skeie G, et al (2002). Meat consumption in the European Prospective Investigation into Cancer and Nutrition (EPIC) cohorts: Results from 24-hour dietary recalls Public Health Nutrition, 5(6B)1243‑1258.

Lodish H (2000). Molecular Cell Biology, 4th Edition; Section 20.6, Second Messengers.

Ma K, Forbes JG, Gutierrez-Cruz G, Wang K (2006). Titin as a glant scaffold for integrating stress and src homology domain 3-mediated signaling pathways – the clustering of novel overlap ligand motifs in the elastic pevk segment. Journal of Biological Chemistry 281:27539-27556.

Mikesh LM; Ueberheid B, Chi A, Coon JJ, Syka JEP, Shabanowitz J, Hunt DF (2006). The utility of ETD mass spectrometry in proteomic analysis. Biochimica et Biophysica Acta 1764(12):1811-1822.

Olson DG, Parrish Jr FC, Stromer MH (1976). Myofibril fragmentation and shear force resistance of three bovine muscles during postmortem storage. Journal of Food Science 41:1036-1041.

Ottenheim CAC, Granzier H (2010). Lifiting the nebula: novel insights into skeletal muscle contractility. Physiology 25:304-310.

Paredi G, Raboni S, Bendixen E, de Almeida AM, Mozzarelli A (2012). ‘’Muscle to meat’’ molecular events and technological transformations: the proteomics insight, Journal of Proteomics 75(14):4275–4289.

Rebbeck RT, Karunasekara Y, Board PG, Beard NA, Casarotto MG, Dulhunty AF (2014). Skeletal muscle excitation–contraction coupling: who are the dancing partners? Int J Biochem Cell Biol 48:28–38.

Righetti PG, Castagna A, Antonioli P, Boschetti E (2005). Prefractionation techniques in proteome analysis: the mining tools of the third millennium. Electrophoresis 26:297‑319.

Robergs RA, Ghiasvand F, Parker D (2004). Biochemistry of exercise-induced metabolic acidosis. American Journal of Physiology 287(3):502–516.

Robson RM, Huiatt TW, Bellin RM (2004). Muscle intermediate filament proteins. Methods of Cell Biology 78:519-553.

Spriet LL (1992). Anaerobic metabolism in human skeletal muscle during short-term, intense activity. Canadian Journal of Physiology and Pharmacology 70(1):157–165.

US Department of Agriculture, ARS (2008). USDA national nutrient database for standard reference, release 21, Nurient Data Laboratory Home Page. http://www.ars.usda.gov/Services/docs.htm?docid=8964.

Vollestad NK, Sejersted OM (1988). Biochemical correlates of fatigue. A brief review. European Journal of Applied Physiology and Occupational Physiology,57(3):336–347.

Walliman T, Wyss M, Brdiczka D, Nicolay K, Eppenberger HM (1992). Intracellular compartmentation, structure and function of creatine kinase isoenzymes in tissues with high and fluctuating energy demands: the 'phosphocreatine circuit' for cellular energy homeostasis. Biochem J 281(1):21–40.

Warriss PD. Meat science: an introductory text (2010). Cabi Series, Modular Texts. Cabi Ed., 234 pages.

Wickiewicz TL, Roy RR, Powell PL, Edgerton V (1983). Muscle architecture of the lower limb. Clinical Orthopedics and Related Research 179:277.

Xu H, Xu Y, Liang X, Wang Y, Jin F, Liu D, Ma Y, Yuan H, Song X, Zeng W (2013). Porcine skeletal muscle differentially expressed gene ATP5B: molecular characterization, expression patterns, and association analysis with meat quality traits, Mammalian Genome 24(3-4):142-150.

Yamane H, Kanouchi H, Arimizu G, Obi T, Oka T (2006). Increases in pig major acute-phase protein in wasting pigs brought to the abattoir. Journal of Veterinary Medical Science 68(5):511-513.

Yan Z, Lira VA, Greene NP (2012). Exercise training-induced regulation of mitochondrial quality. Exercise and Sport Science Reviews 40:159-164.

PART 2

PROLONGED MEAT AGING: THE METABOLOMIC INVESTIGATION COMPLETES THE PHYSICAL CHARACTERIZATION.

2.1 INTRODUCTION

My research on muscle-to-meat conversion process has been conducted on a particular bovine meat, the Piedmontese. The Piedmontese is a typical breed of cattle from the region of Piedmont, in north-west Italy. The breed originated when migrating Zebu (Bos indicus) cattle crossed with the autochthonous Aurochs, approximately 25 thousand years ago (Piedmontese – Origins of Breed. Breeds of Livestock, 2014). However, processes of natural selection and domestication, especially from the late nineteenth century, resulted in the selection of characteristic postpartum hypertrophic muscle growth (‘‘double muscling’’), a peculiarity that stems from the inherited inactivation of the myostatin gene and favors muscle growth in this breed (Wheeler et al., 2001). Piedmontese has been historically considered a triple feature/ attribute/characteristic (meat, milk and work). In 1976 the Piedmontese breed became a specialized variety for meat. The individuals reach the average slaughter weight (males 550–650 kg, females 400–450 kg) in about 14–18 months. The Piedmontese breed is mainly known for its superior yields of lean and tender meat. In comparison to other breeds, the double-muscled Piedmontese meat is characterized by higher water and protein contents. Normally the intramuscular fat content is about 1% or lower. Consequently, the triacylglycerol content is greatly reduced, resulting in lower fat deposition, with a positive

increase of the polyunsaturated/saturated fatty acid ratio (Brugiapaglia et al., 2014). The meat of the hypertrophied Piedmontese animals is also very tender, because of a large reduction in muscle collagen and a lower proportion of stable non-reducible cross-links (Destefanis & Barge, 1993; Destefanis & Brugiapaglia, 1993). As a result, the Piedmontese is amongst the most important Italian autochthonous beef breed, and it contributes for 37% to the beef production and for about 50% to the gross sealable product in Piedmont, with approximately 300,000 heads of cattle (Destefanis, Barge et al., 1993; Destefanis, Brugiapaglia et al., 1993). Tenderness is a key factor influencing consumers' repurchase intention, and biochemical models have been proposed over the years to describe the main events driving muscle to meat conversion and meat tenderization processes (Ouali et al., 2006; D'Alessandro & Zolla, 2013a). Overall, the complexity of the process of muscle to meat conversion process can be summarized in three main steps, with (i) a short pre-rigor phase during which muscle still remains excitable; (ii) the rigor phase, during which high energy phosphate compounds (ATP, phosphocreatine) and glycogen are exhausted, while tissue reaches its maximum toughness; and (iii) the post-rigor tenderizing phase, largely depending on ageing duration and temperature, muscle types, individual animals and animal species (Becila et al., 2010). During phase three, tenderization is driven by the activity of proteases (calpains, cathepsins, proteasomes, caspases, serinpeptidases and metalloproteases) on skeletal muscle (Ouali et al., 2006; D'Alessandro & Zolla, 2013a). Other than proteolysis, non-enzymatic aspects such as temperature, pH, calcium concentration, sarcomere length, and connective tissue/collagen content of the muscles can all affect meat quality, as these variables have an impact on proteolytic activity in the muscle (Ouali et al., 2006; D'Alessandro & Zolla, 2013a). Lepetit & Culioli (1992) defined tenderness of meat as 'the ease, perceived by the consumer, with which meat structure is disorganized during mastication'; there is not a strict definition in physical terms, but it depends directly on the mechanical properties of the meat. The most used among

all the standard parameters is the Warner-Bratzler shear force (Lepetit & Culioli, 1992), measured in the homonymous test; until the last decades, it was empirically employed to evaluate the effect of different treatments on tenderness values (i.e. feeding, breed, etc.). Despite their practical usefulness, Warner-Bratzler shear force test and other similar techniques were not able to give an accurate description of the biological mechanisms, and the first part of my PhD research has exploited the synergy between the classical meat techniques and the proteomics and metabolomics potentialities.

All the biochemical factors that influence tenderness can be summarized in three groups: background toughness, postmortem toughness and postmortem (and post-rigor) tenderization. The first one is defined as 'the resistance to shearing of the unshortened muscle' (Marsh & Leet, 1966), and this is principally due to the muscular connective tissue component, in particular to the organization of the perimysium (that shows a general correlation with the tenderness of muscles in chicken and beef [Strandine et al., 1949]). This typology of toughness is not dependent on postmortem events, while the toughening and the tenderization phases are related to the actual muscle-to-meat conversion process; the postmortem toughening, as previously explained, depends on the sarcomere shortening of the rigor mortis onset: from this moment on, muscle can be defined as meat (despite a 'young' meat). Here I want to underline that the toughening mechanism shows a lower degree of variability (in carcasses under similar processing conditions) with respect to the tenderization phase, which on the contrary is characterized by a large variation in both rate and extent, very often resulting in the inconsistency of meat tenderness found at the consumer level (Koohmaraie & Geesink, 2006).

Juiciness is strictly correlated to water-holding capacity of meat. WHC is defined as the ability to retain water even though external pressures (for example, heating or gravity) are

applied to it. The mechanism by which water is lost from meat is influenced by both the pH of the tissue and by the amount of space in the muscle cell; for example, an acidic pH causes the denaturation of some muscle proteins leading to reduction in their water holding capacity. This happens because the myofibrillar components expel the fluid into the extracellular space which increases in volume (Warriss, 2000). When such meat is cut the fluid is released resulting in the exudates. A large amount of exudates reflects poor water holding capacity (as found in the so-called Pale Soft Exudative meats).

Meat color mostly depends on myoglobin in the sarcoplasm of muscular fibers. This protein is an unstable chemical compound and when the oxygen availability is high, it changes to oxymyoglobin giving meat with a bright red color. On the contrary, if the oxygen tension is low, an oxidation reaction happens and metmyoglobin of brown color is formed. Currently, food color is measured in terms of CIE L*, a*, b* values, hue angle and chroma. The L* a* b*, or CIELab, color space is an international standard for color measurement: L* is the lightness component, which ranges from 0 to 100 (from black to white) and the parameters a* (redness) (from green if negative to red if positive) and b* (yellowness) (from blue if negative to yellow if positive) are two chromatic components which range from –120 to + 120 (Yam & Papadakis, 2004).

While the molecular mechanisms underlying muscle to meat conversion and meat tenderization have yet to be fully disclosed, precious insights have been gained during the last few years upon the introduction of omics technologies in the field of farm animal proteomics (D'Alessandro & Zolla, 2012; Ibáñez et al., 2013; for a more detailed discussion, refer to the first part of the thesis) and, in particular, in meat science (D'Alessandro & Zolla, 2013b), and their integration with standard physical assays to investigate meat quality parameters (for example, on pig and bovine meat quality [D'Alessandro, Gevi & Zolla, 2011; D'Alessandro,

Marrocco et al., 2011; D'Alessandro et al., 2012]). Biochemical evidence accumulated so far has provided a scientific rationale supporting the beneficial effects on meat tenderness of prolonged aging for a limited time span (from 7 to 15 days, on average), while no significant improvements are gained by further extending such period. The rationale behind such conclusion is that a series of factors end up negatively affecting protease activities in the long term, including pH lowering, altered cation homeostasis, oxidative stress and proteolytic cleavage mediated by cross-interactions (Ouali et al., 2006; D'Alessandro & Zolla, 2013a). Nevertheless, recent empirical evidence in Piedmont farms has suggested the possibility to obtain highly marketable tender meat from cull cows simply by extending the ageing period up to more than forty days. While the producers insisted on the effectiveness of their approach, firmly supported by consumers' appraisal of their products, no scientific experimental evidence has been produced to underpin their statements. Therefore, we hereby investigated whether the prolonged ageing (up to 44 days at 1°C) of Piedmontese cull cow meat was actually correlated to improved palatability (mostly affected tenderness, juiciness) and desirability (color), as gleaned by standard biomechanical assays (Warner Bratzler Shear force measurement – Wbs; water holding capacity – WHC; Minolta values).

Physiological/mechanical assays were then supported by 'Omic' analyses, as to delve into the biochemical events driving muscle to meat conversion in Piedmontese Longissimus thoracis in a time course-wise fashion. Particularly, the effects of long ageing were studied in the Longissimus thoracis muscle (by monitoring 5 different time points, including day 0, 1, 10, 17 and 44 from the moment of slaughter) examining the main biochemical changes by means of mass spectrometry-based metabolomics and proteomics. In order to correlate and integrate 'omics' reading of biochemical changes regarding prolonged-stored meat with standard meat quality assays, we performed principal component analyses (PCA) and Pearson's correlations between omics and physiological/mechanical results.

2.2 MATERIALS AND METHODS.

Animals. Ten Piedmontese cull cows between 4 and 13 years old, were raised in farms belonging to Consorzio La Granda (CN, Italy), located in Piedmont, a north-west region in Italy. All the animals were slaughtered in an industrial slaughterhouse, the carcasses were stored in a chilling room at 2° C. Average slaughter weight of the carcasses was 389.99 ± 6.18 kg. Carcasses were transported to a meat processing plant on post-slaughter day 1. Longissimus thoracis (LT) muscle (that is, the thoracic region of Longissimus dorsi) was removed and stored in a cooler at 1°C (steady or dynamic) and a relative humidity of 78%. At 0, 1, 10, 17 and 44 days of ageing, a 10 cm section was removed from the LT muscle and used for all subsequent analyses.

- *2.2.1 Classical standard analyses.* Classical standard analyses on meat samples include the measurement of microbial safety, together with physical and chemical meat parameters, in order to assess meat safety and quality.

- *2.2.1a Microbiological analysis.* The hygienic status of meat samples were assessed through the Total Bacteria Counts (TBC), the Enterobacteriaceae counts analysis and the standardized methods ISO 4833 (2004) and AFNOR NF V08-054 (1999). For the assessment of fecal contamination, Escherichia coli and Listeria monocytogenes levels were also measured according to ISO 16649-2:2001 and ISO 11290-1:1996/Amd 1:2004 (2004) procedures, respectively. Colonies with a typical L. monocytogenes appearance were identified using a species-specific PCR, according to D'Agostino et al. (2004).

- *2.2.1b Chemical and physical analysis.* The evaluation of meat quality at d0 and d1 was assessed carrying out the following analysis:

– *pH measurements* at 1–3 h after slaughter and 24 h after slaughter, made by a Crison pH-metre with an Ingold Spear electrode and automatic temperature compensator.

– *Sarcomere length* according to the diffraction method by Cross, West and Dutson (1981). The diffraction patterns from muscle samples compressed between glass microscope slides were obtained using a helium–neon laser (632.8 nm) as the light source.

– *Heme iron content* (µg/g muscle) according to Hudzik (1990).

– *Water, protein and ether extraction contents* (AOAC, 1970). The Kjeldhal method has been applied to achieve the determination of nitrogen using a Buchi System apparatus (Buchi Labortechnik, Flawil, Switzerland); crude protein was calculated by multiplying N x 6.25. A Buchi extraction system has been used for the determination of lipids content, according to the Soxhlet method.

– *Lightness (L), redness (a) and yellowness (b)* on meat samples at d1, d10, d17 and d44. A Minolta CR-331C Chroma Meter (Minolta Camera Co., Japan) (Petracci et al., 2004) has been used in the CIELAB space (CIE, 1978) calibrated on the D65 illuminant. The measures were carried out after 1 h of blooming on a 3 cm thick steak. Chroma and hue were calculated from a and b values according to expressions: $C = (a^2 + b^2)^{1/2}$ and hue: $h = \tan^{-1} (b/a)$.

– *Grau and Hamm* (1953). 300 mg of meat were put on the centre of a filter paper contained between two plates of Plexiglass; a constant pressure was applied for 5 min, and the areas of the meat film layer (M) and of the total surface area (T) were calculated. The M/T ratio was then calculated. At the end of each period of ageing, the aged samples were frozen at -25°C.

After a 12 h of slow thawing period at 4°C, the following analyses were carried out:

– *Thawing loss* on a 3 cm thick steak was calculated as the % of weight loss before and after thawing.

– *Cooking loss* was measured as the percentage of weight reduction of the cooked sample (3 cm thick steak, vacuum sealed in a polyethylene bag and heated in a water bath to an internal temperature of 70°C) compared with the raw sample (Barton-Gade et al., 1994).

– *Warner Bratzler shear force (Wbs)* (N) on samples of 1x1x3 cm (height x width x length), cut parallel to muscle fibers and obtained from the steaks used for the determination of cooking losses. The Wbs values were obtained through the use of an Instron Universal Testing machine (Model 5543, Instron Corp., Minnesota, USA) (Peachey et al., 2002) equipped with a triangular Warner Bratzler blade and crosshead speed set at 200 mm/min (AMSA, American Meat Science Association).

– *Hardness* as the force required to drive a 10x10 mm square compression cell on a sample of raw meat. The cell was equipped with two lateral walls to limit free strain of the sample to a direction parallel to the myofibers (Lepetit & Culioli, 1994). Meat samples 1x1x3 cm were compressed at 200 mm/min perpendicular to the fiber axis to 20% (H20%) and 80% (H80%) of their original height.

- *2.2.2 Omics analysis.*

- *2.2.2a 1D SDS–PAGE LC–MS/MS.* Samples of LT from 10 Piedmontese cows were collected at day 0, 1, 10, 17 and 44 after slaughter. Sample preparation and solubilization were performed by slight modification of the SWISS-2D PAGE sample preparation procedure (Hoogland et al., 2004). Frozen samples (approximately 6 mg per sample) were crushed in a mortar containing liquid nitrogen. After grinding, the samples were resuspended in an extraction buffer containing 7 M urea, 2 M thiourea, 2% (w/v) CHAPS, 40 mM Tris, 0.1 mM

ethylenediaminetetraacetic acid (EDTA) (pH 8.5), 2% (v/v) protease inhibitor cocktail (Sigma–Aldrich, Basel, Switzerland), 2 mM phenylmethanesulfonylfluoride (PMSF) and 1 mM dithiothreitol (DTT). After incubation with agitation at 4°C for 60 min, samples were centrifuged at 17,000g for 20 min at 4°C and the supernatant collected. The protein concentration of each group was determined using 2D Quant kit (GE Healthcare Life Sciences, UK) according to the manufacturer's instructions. 1D SDS–PAGE were performed according to the Laemmli (1970) method, as previously reported (Hwang, 2004). Gels were digitalized using a Chemi-Doc imaging system (Bio-Rad Hercules, CA, USA). The densitometric image analysis was conducted by Image Lab software. Bands which were significantly different between groups (time course analysis) were excised and trypsin digested (Shevchenko et al., 1996) and underwent subsequent identification by nano-HPLC–MS/MS. The nano-HPLC system consisted of a split-free nano-flow liquid chromatography system (EASY-nLC II, Proxeon, Odense, Denmark) coupled to a 3D-ion trap (AmaZon ETD, Bruker Daltoniks, Germany) equipped with an online ESI nano-sprayer (the spray capillary was a fused silica capillary, 0.090 mm o.d., 0.020 mm i.d.) (D'Alessandro, Gevi, et al., 2011; D'Alessandro, Marrocco, et al., 2011). For all experiments, a sample volume of 15 µl of tryptic digest was loaded by the autosampler onto a homemade 2 cm fused silica precolumn (100 µm I.D.; 375 µm O.D.; Reprosil C18- AQ, 5 µm, Dr. Maisch GmbH, Ammerbuch-Entringen). Sequential elution of peptides was accomplished using a flow rate of 300 nL/ min and a linear gradient from Solution A (2% acetonitrile; 0.1% formic acid) to 50% of Solution B (98% acetonitrile; 0.1% formic acid) in 40 min over the precolumn, in-line with a homemade 15 cm resolving column (75 µm I.D.; 375 µm O.D.; Reprosil C18- AQ, 3 µm, Dr. Maisch GmbH, Ammerbuch-Entringen, Germany). The acquisition parameters for the instrument were as follows: dry gas temperature, 220°C; dry gas, 4.0 L/min; nebulizer gas, 10 psi; electrospray voltage, 4000 V; high-voltage end-plate offset, 200 V; capillary exit, 140 V;

trap drive: 63.2; funnel 1 in, 100 V, out 35 V and funnel 2 in, 12 V out 10 V; ICC target, 200,000; maximum accumulation time, 50 ms. The sample was measured with the ‘‘Enhanced Resolution Mode’’ at 8100 m/z per second (which allows monoisotopic resolution up to four charge stages), polarity positive, scan range from m/z 300 to 1500, 5 spectra averaged, and rolling average of 1. The ‘‘Smart Decomposition’’ was set to ‘‘auto’’. Acquired ETD/CID spectra were processed in DataAnalysis 4.0, and deconvoluted spectra were further analysed with BioTools 3.2 software and submitted to Mascot search program (in-house version 2.2, Matrix Science, London, UK). The following parameters were adopted for database searches: NCBInr database (release date 22/10/2011; 15.670.865 sequences; 5.387.755.057 residues); taxonomy = Mammalia; peptide mass tolerance of ±0.3 Da; fragment mass tolerance of ±0.3 for CID ions; enzyme specificity trypsin with 2 missed cleavages considered; fixed modifications: carbamidomethyl (C); variable modifications: oxidation (M).

- *2.2.2b Metabolomics*. Metabolomic analysis has been performed as previously reported, with minor modifications (D’Alessandro, Gevi, et al., 2011; D’Alessandro et al., 2012). Metabolites from each Piedmontese individual were extracted from 50 mg of meat at 0, 1, 10, 17, 44 days from slaughtering. Samples were crushed in a mortar containing liquid nitrogen and extracted in 1 ml of ice cold methanol : acetonitrile : water (50 : 30 : 20). Samples were vortexed for 30 min at max speed at 4°C and then centrifuged at 16,000 g for 15 min at 4°C. Supernatants were thus collected for subsequent metabolomics analysis, while insoluble debris was discarded. Samples were thus loaded onto a rapid resolution HPLC system (LC Packings, DIONEX, Sunnyvale, CA, USA) as to perform chromatographic separation of hydrophilic metabolites. The system featured a binary pump and vacuum degasser, well-plate autosampler with a six-port micro-switching valve, a thermostated column compartment. A Phenomenex Luna 3 µm HILIC 200A (Torrance, CA, USA) (150 x 2.0 mm), protected by a

guard column HILIC 4 x 2.0 mm ID (Phenomenex) was used to perform metabolite separation over a phase B to phase A gradient lasting 35 min.

In details, we set the following LC parameters: injection volume, 20 µL; column temperature, 25°C; flow rate of 0.2 mL/min. The LC solvent gradient and timetable were identical during the whole period of the analyses. A 0–100% linear gradient of solvent B (100% acetonitrile + 10 mM ammonium acetate) to A (double distilled 18 mΩ water + 10 mM ammonium acetate) was employed over a 35 min gradient, divided into a 5 min hold in 95% B, a linear gradient to 95% A lasting 20 min, followed by a 95% A hold of 5 min, returning to 95% B in 1 min and a 5 min post-gradient solvent 95% B hold. Metabolomics analyses were performed through direct elution onto an electrospray hybrid quadrupole time-of flight mass spectrometer MicroTOF-Q (Bruker-Daltoniks, Bremen, Germany) equipped with an ESI-ion source. Instrument calibration was performed externally every day with a sodium formate solution consisting of 10 mM sodium hydroxide in 50% isopropanol : water, 0.1% formic acid. External mass scale calibration was performed twice a day through direct automated injection of the calibration solution by a 6-port divert-valve. Mass spectrometer runs were exported into mzXML files and analyzed through the software MAVEN (Clasquin, Melamud, & Rabinowitz, 2012) for correct metabolite assignment, on the basis of absolute intact mass (within a 10 ppm window) against the KEGG database (Kanehisa & Goto, 2000), and expected retention times on the basis of metabolite chemical properties.

- *2.2.2c Statistics.* Data elaboration was performed with Excel 2007 (Microsoft), XLStat 2013.6.3 (Addinsoft SARL) and GraphPad Prism 5.0 (GraphPad Software Inc). Pearson's correlations coefficients and principal component analyses were performed via the XLStat suite on the mean results for each independent assay on each distinct animal. Results were

plotted as in D'Alessandro et al. (2012). In correlation tables, absolute values close to 0 indicate low correlation, while |values| ≈ 1 indicate high correlation.

2.3 RESULTS AND DISCUSSION.

The hypothesis concerning the potential beneficial effects of prolonged ageing on meat quality (especially in terms of tenderness), as reported by the producers and underpinned by consumers' appraisal, was tested by performing analysis for physical (Warner Bratzler shear force, myofibrillar degradation, sarcomere length, water holding capacity, Minolta values) and microbiological parameters during a carcass ageing period of 44 days at 1°C.

- *2.3.1 Microbiological results.* Meat is one of the most perishable food; microbial growth during chilling storage mainly determines meat deterioration or spoilage. Although various microbial groups contribute to meat spoilage, traditionally TBC and *Enterobacteriaceae* were counted to determine the shelf-life of food chilled products. Initial microbial load, temperature and other conditions of storage concur to bacterial proliferation. Extended ageing

TABLE 3 – MICROBIOLOGICAL RESULTS (log CFU/gr).

	DAY 1	DAY 10	DAY 17	DAY 44
TOTAL BACTERIAL COUNT	1.9	3.7	3.9	6.2
TOTAL ENTEROBACTERIACEAE COUNT	0	0	0	2.7

period at 1°C might bring concerns about the preserved safety of Piedmontese meat, therefore, in order to test Piedmontese meat for microbial contamination, the traditional Total Bacterial Counts and Total Enterobacteriaceae Counts have been carried out. In this study the median value of the TBC was comprised between 1.9log and 6.2log CFU/gr (Table 3). During the first days of aging (d1-d10) there was an increase of 2 log (arriving at 3 log CFU/gr); it remains constant from d10 to d17; ending up to 6 log UFC/gr at d44. Considering Total

Enterobacteriaceae Count the median value was always 0 CFU/gr at d1, d10, d17 and reached up to 2.7log CFU/gr at d44. The low increase of *Enterobacteriaceae* could be ascribed to the correct application of the Good Handling Practice (GHP) and the Good Manufacturing Practice (GMP), in particular regarding the cold chain. The meat during the aging period was stored at controlled temperature and humidity (1°C, 78% humidity). Only during the deboning phase this parameter has been risen. The absence of *L. monocytogenes* and *E.coli* in all the samples throughout the whole duration of the aging period confirms the safety of these products. Results are reported in table 3.

- *2.3.2 Physical results.* Results for physical parameters are reported in Tables 4-6. In terms of color, meat was not negatively affected by the prolonged ageing (Table 4). The

TABLE 4 – CHEMICAL AND PHYSICAL ANALYSIS					
	MEAN	SD	RSD (%)	MIN	MAX
pH (30h)	5.47	0.04	0.73	5.41	5.56
SARCOMERE LENGTH (µm)	1.83	0.14	7.61	1.59	2.17
Fe (µg/g)	16.36	2.58	15.77	11.98	20.31
WATER (%)	73.91	0.83	1.12	72.27	75.08
PROTEIN (%)	22.11	0.73	3.30	20.61	23.19
ETHER EXTRACT (%)	2.84	1.16	40.85	1.27	5.44
ASH (%)	1.05	0.03	2.86	0.99	1.09

overall WHC, as expected (D'Alessandro et al., 2012; Huff-Lonergan & Lonergan, 2005), underwent through a progressive decrease with ageing (Table 4). The results of Wbs measurements indicated that it was significantly lower ($P < 0.01$) at d10 (39.45 N) in comparison with d1 (67.61 N) and at d44 (29.08 N) in comparison with d10 (table 5). The decrease was about 42% between d1 and d10 and 26% between d10 and d44. These measurements indicated the improved tenderness of Piedmontese meat when subjected to ageing extension up to 44 days, thus justifying consumers' appraisal for the resulting product.

According to Lepetit and Culioli (1992), compression at 20% can be related to myofiber strength, which changes during aging, and compression at 80% to connective tissue (table 5). Regarding 80% compression, the absence of significant differences due to ageing was not unexpected because there is no evidence supporting influences of ageing on the mechanical strength of connective tissue, so these data do not contrast the prolonged ageing procedure.

TABLE 5 - PHYSICAL PARAMETERS MEASUREMENTS DURING MEAT AGING PERIOD.

	DAY 1	DAY 10	DAY 17	DAY 44
WARNER BRATZLER (N)	67.61	39.45*	34.66**	29.08**
GRAU & HAMM (M/T RATIO)	0.44	0.49	0.53*	0.61**
THAWING LOSS (%)	5.09	3.94*	3.30*	1.40**
COOKING LOSS (%)	24.60	18.99*	20.80*	19.32*
HARDNESS 20% (N)	16.30	13.01*	13.56*	13.40*
HARDNESS 80% (N)	29.98	28.32	32.39	30.11
LIGHTNESS	37.81	37.9	38.22	37.73
REDNESS	15.77	15.85	16.91	17.85
YELLOWNESS	13.06	13.22	14.07	14.13
CHROMA	39.68	39.48	39.83	38.4
HUE	20.5	20.67	22.03	22.78

The first * indicates the statistical significance ($p < 0.05$) of the difference between the measured value of day N and day 1. The second *, where present, indicates the statistical significance ($p < 0.05$) of the difference between the measured value of day N and the previous time point.

Data regarding 20% compression showed a decrease in resistance to 20% compression force in raw meat between samples analyzed on day 1 and 10 of aging, but no significant changes were found between samples analyzed on day 10, 17 and 44, apparently indicating a myofibrillar degradation steady-state from day 10, but the following proteomics and metabolomics data give a deeper glance into biomolecular changes driving meat ageing up to 44 days, granting compelling evidences about an ongoing myofibrillar fragmentation (and so about the consequent improved tenderness).

Lean muscle, as I discussed in the first part of this thesis, contains approximately 65-80 % of water, (hereby 73.91 + 0.83 - Table 4). Water in the muscle is mostly entrapped in structures of the cell, that include the intra- and extramyofibrillar spaces. Tenderization events result in

key changes in the intracellular architecture of the cell and thus intuitively influence the ability of muscle cells to retain water. Concordantly, water bath losses and thawing losses decreased proportionally to the hanging period, in a statistically significant fashion ($p<0.05$ – Table 5).

Prolonged aging did not significantly affect color-related parameters, including Minolta values (L* a* b*), hue and chroma (table 5).

- *2.3.3 Proteomic results. Prolonged ageing affected proteome stability starting from day 10 onwards, suggesting alterations to structural protein integrity and metabolic deregulation.*

One of the key events driving muscle to meat conversion and tenderization processes is related to the progressive alteration of the muscle protein stability. These alterations tend to influence both meat tenderness and its capacity to retain water moisture, thus affecting meat juiciness (D'Alessandro & Zolla, 2013). During the last decade, proteomics technologies have been extensively applied to investigate the influence of post mortem events on muscle proteins, as it has been extensively discussed in the 'general introduction' section of my thesis. Amongst proteomics technologies exploited in this research endeavor, gel electrophoresis has provided significant insights (Hwang, 2004). In this view, 1DE and 2DE gel electrophoresis have become mainstream approaches to the muscle proteome. 2DE allows to separate thousands of protein spots on the basis of protein molecular weights and isoelectric points while 1DE only enables separation of approximately 50 bands in a 15 cm gel, but in this first part of my work I used the 1DE as to give a quick glance to the proteome evolution along the time-course analysis of the Piedmontese longissimus lumborum meat maturation. Furthermore, as it has been recently reported in the literature, the proteomic community is reconsidering the potentialities of the 1DE technique (Cottingham, 2010); the

1DE approach surely offers a simpler and faster method with respect to the 2DE, which clearly demonstrates a higher resolving power than 1DE, but also some intrinsic difficulties when applied to resolve high molecular weight and more hydrophobic proteins (which is often the case when dealing with structural components of muscle fibers, such as myosin heavy chains). While the first part of this thesis has been primarily dedicated to the metabolomic side and its interconnections with the physical measurements, the second part is principally focused on a deeper proteomic analysis, carried out with 2DE gels.

Application of 1DE, coupled to statistical analyses of digitized images, trypsin digestion of statistically significant ($p < 0.05$, fold change > 1.5) differential bands and nanoLC–MS/MS-based identification yielded the individuation of six bands decreasing while four increasing thereon from post mortem day 10 up to day 44 (Fig. 7, Table 6). Differential proteins were identified either as structural proteins (α-actinin 3, tropomyosin α-1, troponin T and I, profilin-1) or metabolic enzymes (glycogen phosphorylase, 6-phosphofructokinase, fructose-bisphosphate aldolase A, glyceraldehyde-3-phosphate dehydrogenase, triosephosphate isomerase, L-lactate dehydrogenase A, creatine kinase M-type, AMP deaminase 1), together with residual hemoglobin and small HSP (α-crystallin B chain, HSP-β5) (Table 6). These results are consistent with proteomics literature about muscle to meat conversion events (D'Alessandro & Zolla, 2013a, 2013b), documenting changes in the sarcoplasmic proteins, myofibrillar proteins (such as partial dissociation of actomyosin, cleavage of disulphide linkages, depolymerization of F-actin filaments, cleavage of myosin filaments, disorganization of Z-bands and troponin–tropomyosin complex) and sarcolemma. For a schematic localization of the discussed structural proteins, you can refer to figure 2 of the 'general introduction' section. In particular, progressive decrease of structural proteins (especially from post slaughter day 10 – Table 6) is consistent with the expected protease-mediated degradation of myofibrils (also confirmed by decreasing

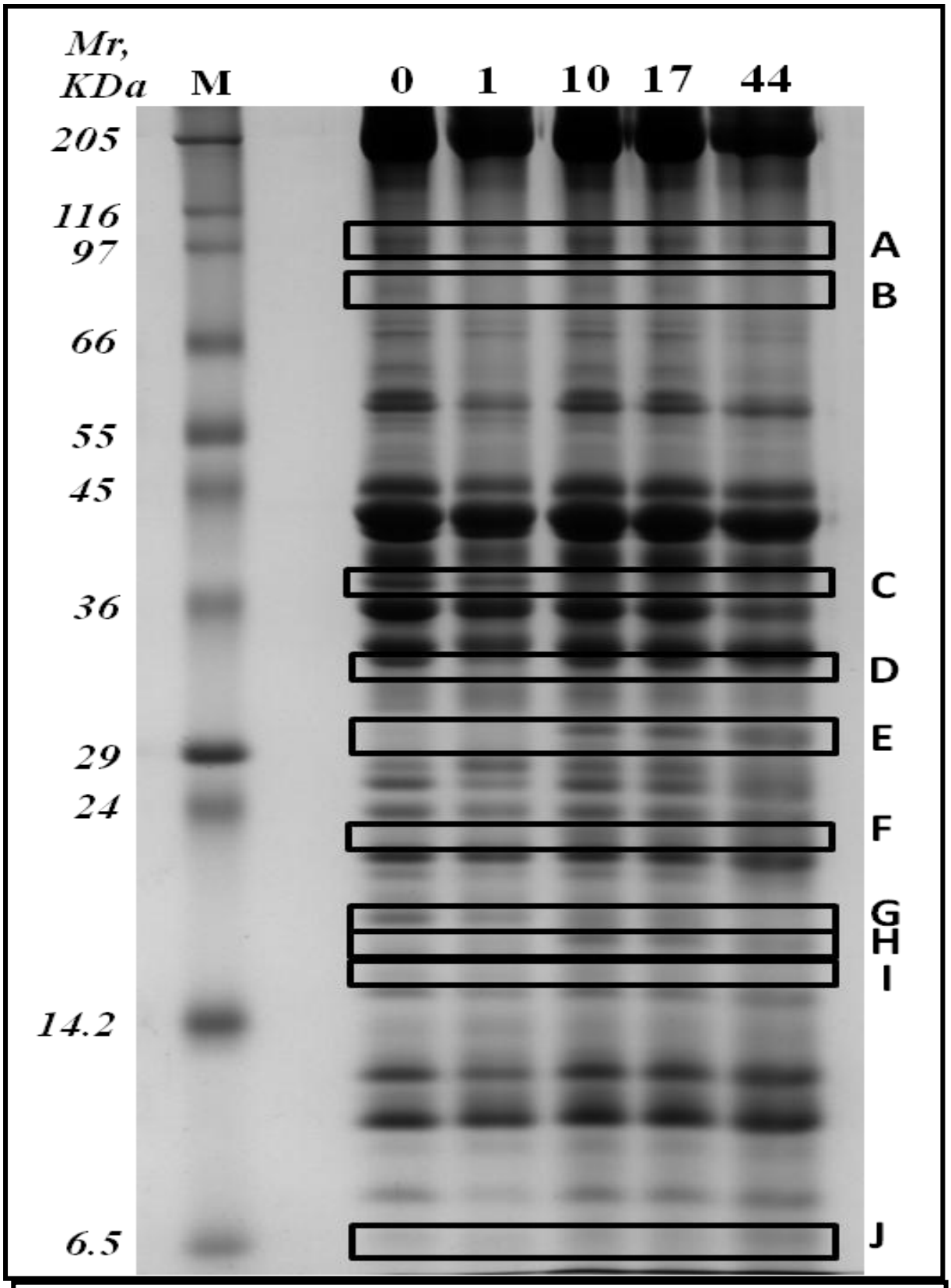

FIGURE 7 - 1DE gel of protein extracts from the *longissimus dorsi* of meat from formerly dairy Piedmontese cows at post slaughter day 0, 1, 10, 17 and 44. Statistically differential bands (*p<0.05 ANOVA)* are highlighted and indicated with letters from A to J; the identified proteins are reported in **TABLE 6**. Molecular weights ladder is presented on the left side of the gel.

Wbs). This is consistent with previous proteomics reports on the Maremmana beef breed (D'Alessandro et al., 2012), where significant correlations were observed between Wbs and structural protein degradation. This holds relevant pitfalls not only in relation to tenderness, but also in terms of WHC, since failure to degrade myofibrils post mortem after the rigor phase would result in cell shrinkage and thus reduced intra-myofibrillar space, leading to subsequent drip loss (Huff-Lonergan et al., 2005). Correlations between HSPs and bovine meat tenderness is now held as a consolidated fact (D'Alessandro et al., 2012; Guillemin et al., 2011), owing to their likely involvement in protease activity preservation, protein protection from proteolysis (D'Alessandro & Zolla, 2013b) and mediation of apoptotic cascades (Beere, 2005). This was hereby further confirmed by the alteration of α-crystallin levels in Piedmontese meat during the ageing period (Table 6). Traces of accumulating hemoglobin (as gleaned through proteomics approaches – Table 6) in tenderizing bovine meat have already been reported in the past in relation to accumulation of oxidative stress triggered by heminic iron-mediated reactions (D'Alessandro et al., 2012). The main outcome of the rapid proteomics overview gained via 1DE is that post mortem events yield the progressive increase in target key metabolic enzymes involved in glycogen mobilization/ energy metabolism regulation (glycogen phosphorylase and AMP deaminase 1), glycolysis (6-phosphofructokinase, fructose-bisphosphate aldolase A, glyceraldehyde-3-phosphate dehydrogenase, triosephosphate isomerase, L-lactate dehydrogenase A), creatine/phosphocreatine shuttle (creatine kinase M-type). Metabolic alteration in post mortem muscles is not an unexpected finding (D'Alessandro, Gevi, et al., 2011; D'Alessandro, Marrocco, et al., 2011; D'Alessandro et al., 2012), since depletion of energy rich compounds is a hallmark of the pre-rigor to rigor stage, and impaired glycolysis ensues as pH declines below a certain threshold resulting in negative inhibitory feedback on

TABLE 6 – Differential gel bands ($p < 0.05$ ANOVA) from 1DE.

The trends of the proteins under the same gel band have been confirmed by the relative abundances of their peptides as identified by nanoHPLC/tandem mass spectrometry.

Gel band	MW,Da	no of peptides identified	Mascot score	NCBI accession no.	Protein ID (Bos Taurus)	TREND
A	97702	102	1984	gi|57163939	glycogen phosphorylase, muscle form	↓
	103713	26	708	gi|115495613	alpha-actinin-3	
B	86095	58	1292	gi|115497288	6-phosphofructokinase, muscle type	↓
	87202	32	623	gi|154152079	AMP deaminase 1	
C	39925	56	1122	gi|156120479	fructose-bisphosphate aldolase A	↓
D	36916	88	1250	gi|27806559	L-lactate dehydrogenase A chain	↓
	32732	57	1245	gi|61888866	tropomyosin alpha-1 chain	
E	32105	61	683	gi|21038992	troponin T fast skeletal muscle type	↑
F	26901	28	745	gi|61888856	triosephosphate isomerase	↑
	43190	33	608	gi|60097925	creatine kinase M-type	
G	23707	62	636	gi|148744237	TNNI2 protein	↓
H	21561	33	458	gi|300797481	troponin I, fast skeletal muscle	↑
	20024	11	228	gi|27805849	alpha-crystallin B chain (Heat shock protein beta-5)	
I	20024	33	492	gi|27805849	alpha-crystallin B chain (Heat shock protein beta-5)	↓
	21561	22	330	gi|300797481	troponin I, fast skeletal muscle	
J	16001	17	539	gi|27819608	hemoglobin subunit beta	↑
	36073	18	260	gi|77404273	glyceraldehyde-3-phosphate dehydrogenase	
	15213	7	243	gi|62751593	profilin-1	

glycolytic enzymes activity (Ouali et al., 2006; D'Alessandro & Zolla, 2013a). Of note, we observed a time-dependent decrease in the levels of glycogen phosphorylase and AMP deaminase 1, two rate-limiting enzymes of the glycolytic process as they mediate glycogen conversion to glucose 1-phosphate and AMP conversion to IMP. Indeed, depletion of AMP impairs the possibility to restore ADP reservoirs and thus hampers progression of glycolysis (Scopes, 1974). Similarly, Van Laack et al. (2001) indicated that in pork muscle, glycogen phosphorylase activity explains 28% of the differences in pHu, while a higher amount of AMP-deaminase was associated with a 10% higher pHu in beef muscle.

It is also worthwhile to stress that band J, increasing during the ageing period from post mortem day 10 onwards, was identified as glyceraldehyde 3 phosphate dehydrogenase, a 36 kDa protein, even if the band mapped at an approximate apparent MW of 6.5 kDa (based upon the MW ladder markers – figure 7). This is suggestive of the likely storage-dependent fragmentation of this key glycolytic enzyme in the LT of Piedmontese cows.

- *2.3.4 Metabolomics highlighted an attempt to counteract the energetic shortening and the increasing oxidative stress.* Little is known about actual changes to the metabolome after slaughter. Metabolic changes in the post mortem muscle (D'Alessandro & Zolla, 2013b) might underpin the peculiarities related to the beneficial effects of prolonged ageing of carcasses of Piedmontese cattles on tenderization. The recent availability of analytical platforms based upon HPLC–MS instrumentation and bioinformatics tools for chromatogram analyses has paved the way for the introduction of metabolomics platforms in the field of meat science, as I have discussed in the general introduction section. In this view, in this first part of my research I decided to complement physical analyses with mass spectrometry-based metabolomics assays, and to correlate results through statistical

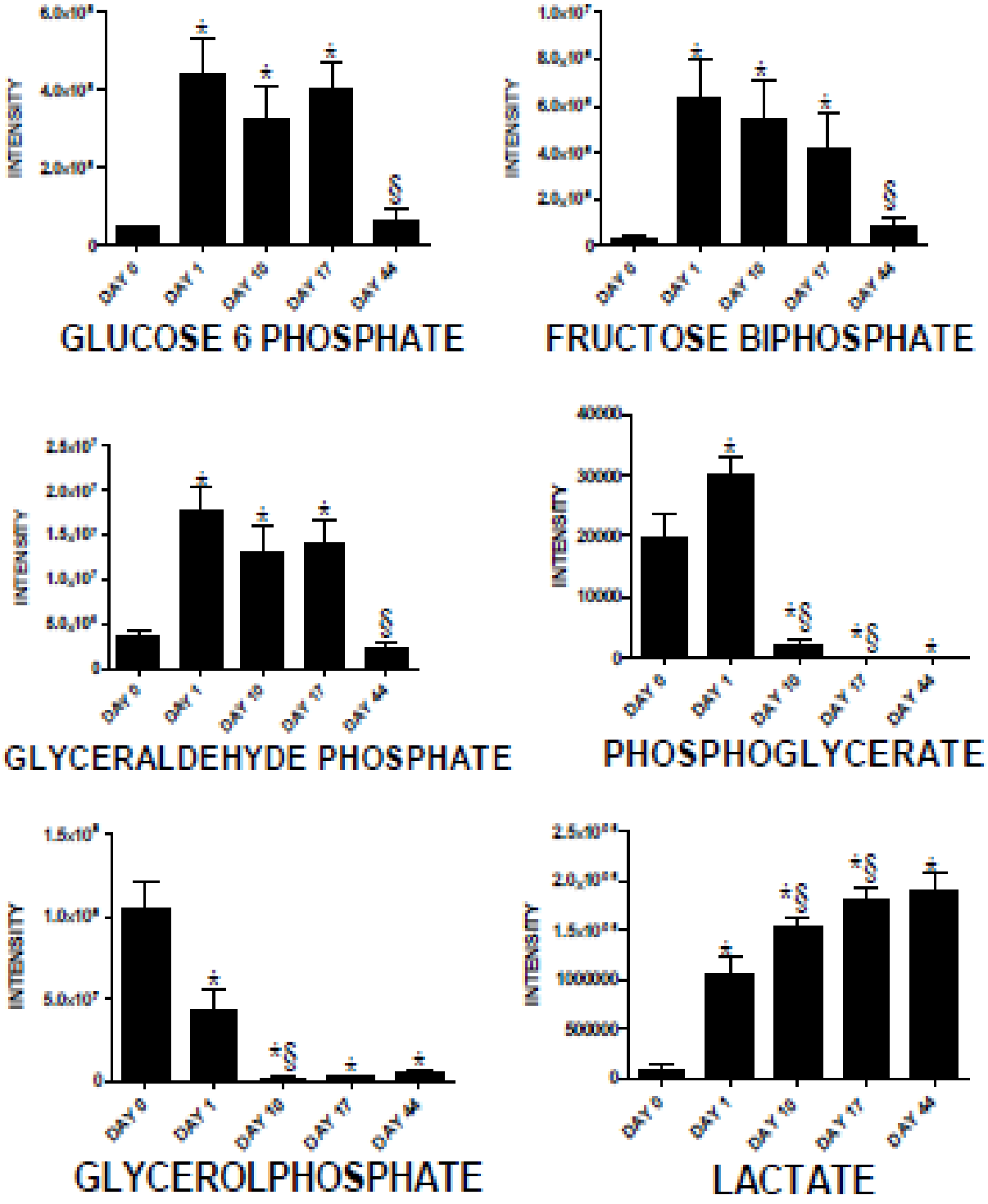

Figure 8 – Relative quantification (arbitrary ion counts) of the indicated glycolytic metabolites along the time-course analysis of the *Piedmontese longissimus lumborum* muscle.

*indicates a statistically significant difference ($p < 0.05$) existing between the relative quantification at day N and day 0.

§ indicates a statistically significant difference ($p < 0.05$) existing between the relative quantification at day N and the previous time point.

interpretations. Metabolomics analyses were performed to monitor the levels of metabolites involved in energy metabolism, redox metabolism and Krebs cycle, serine metabolism and amino acids levels (Figures 8-16). Analyses were performed throughout the whole duration of the ageing period, at post slaughter day 0, 1, 10, 17 and 44. In living animals, skeletal muscles are amongst major oxygen consuming tissues, since muscle mitochondria show a higher respiration rate than those in liver, kidney and brain (Rolfe, Hulbert, & Brand, 1994). However, sudden blood flow arrest and exsanguination after slaughter promote anoxia, drastically impairing energy production via oxidative metabolism in muscle cells, especially in terms of ATP production in the mitochondria (Sierra & Oliván, 2013). As a result, anaerobic glycolysis ensues, resulting in glycogen mobilization and glucose consumption to produce ATP, while anaerobic fermentation of pyruvate results in the progressive accumulation of lactate. However, ongoing glycolysis in the muscle results in pH lowering (Figure 9) which in turn plays an inhibitory feedback on glycolytic enzymatic activity (Ohlendieck, 2010). This results in the progressive inhibition of glycolytic fluxes in the long term and pH reaching a lower threshold followed by a progressive stabilization. In the present model, we observed a time-dependent accumulation of lactate, reaching a climax between day 17 and 44 after slaughter (Figure 8). This is suggestive of ongoing glycolysis during the first 17 days

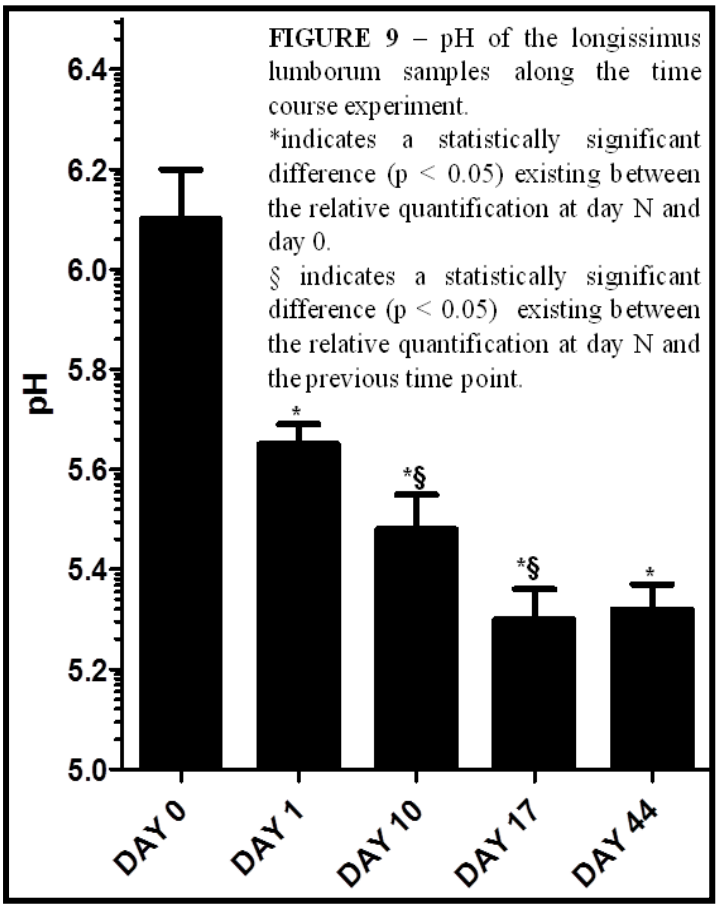

FIGURE 9 – pH of the longissimus lumborum samples along the time course experiment.
*indicates a statistically significant difference ($p < 0.05$) existing between the relative quantification at day N and day 0.
§ indicates a statistically significant difference ($p < 0.05$) existing between the relative quantification at day N and the previous time point.

of storage, resulting in the intermediate accumulation of early glycolytic metabolites during the first two post-slaughter weeks (glucose 6-phosphate, fructose bisphosphate, glyceraldehyde phosphate – figure 8). Decreased levels of these metabolites by day 44, together with the plateau reached by lactate levels, are indicative of the likely consumption of glycolytic precursors, such as through the exhaustion/impaired mobilization of glycogen (in agreement with the observed decrease in the levels of glycogen phosphorylase – Table 6) or the reduced activity of glycolytic enzymes acting on triose phosphates (downstream to glyceraldehyde 3-phosphate and upstream to phosphoglycerate – Figure 8) soon after post mortem day 10; the pH trend follows the lactate trend. In this view, it is worthwhile to recall the observed increased fragmentation of glyceraldehyde 3-phosphate dehydrogenase since ageing day 10, as gleaned via 1DE (Table 6).

Progressive depletion of glycerol phosphate (Figure 8) might indicate a blockade in anabolic reactions, such as those involved in triglyceride biosynthesis via the generation of glycerol backbones.

While glycolysis represents the main source to sustain the muscle under anaerobiosis in the long term, the phosphocreatine shuttle sustains cell energy demands in the short term, as it relies on the accumulation of energy tokens in the form of phosphocreatine (refer to the 'general introduction' section for a more detailed description). Metabolomics results revealed that while creatine levels were apparently stable up until post-slaughter day 17, day 44 corresponded to an evident drop in the levels of this metabolite (figure 10). Conversely, phosphocreatine underwent a strong decrease from day 0 to day 1, then a drop near to the total absence from day 10, and maintained its steady state up to the end of the aging period (figure 10). This result follows the expectations, as the phosphocreatine shuttle plays its role during the very first moments of the anaerobic conditions (as it is in the living muscle during, for

example, an intense activity), and, as explained in the first part of the thesis, it has to be reloaded by the oxidative phosphorylation that needs oxygen; the phosphocreatine levels at day 1 (low, but not near to zero) recalls the presence of residual oxygen in the muscular tissue (due to the Heme groups) which permits a weak reload of the phosphocreatine shuttle, no more possible when the aerobic activity is totally depleted (as it obviously is from day 10 onward). The Cr/pCr shuttle impairment is also underlined by the gel band F and the relative

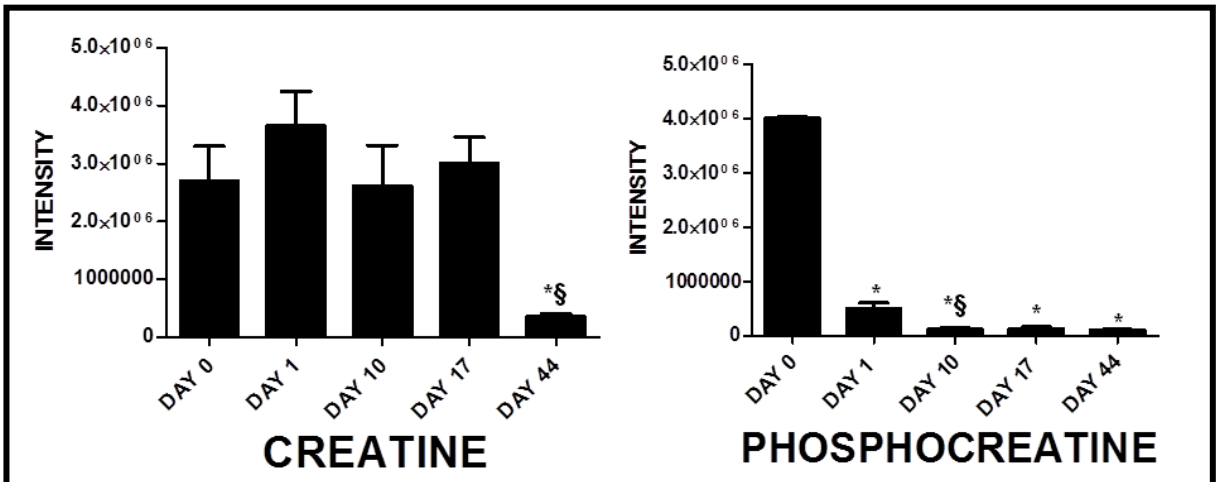

FIGURE 10 – Relative quantification of creatine and phosphocreatine in a time-course fashion
*indicates a statistically significant difference ($p < 0.05$) existing between the relative quantification at day N and day 0.
§ indicates a statistically significant difference ($p < 0.05$) existing between the relative quantification at day N and the previous time point.

identification (creatine kinase M-type; figure 7, table 6); the observed MW is approximately 26 kDa, so I inferred that it is a fragmented species of the enzyme (whose MW is about 40 kDa), showing an upward trend that witnesses the deregulation of the shuttle.

Muscle responses to anoxia also imply mitochondrial uncoupling, as the lack of oxygen results in the mitochondria-dependent promotion of reactive oxygen species (ROS) accumulation, including superoxide anion and hydrogen peroxide. This is consistent with the role of mitochondria as mediator of a wide range of other cellular processes, including signal transduction, cell cycle regulation, oxidative stress, thermogenesis and cell death (Sierra & Oliván, 2013). In previous studies my research group reported increases in the levels of

antioxidant enzymes, such as superoxide dismutase (SOD), and highlighted a correlation between oxidative stress (in the form of oxidized glutathione – GSSG), SOD levels and Chianina Longissimus dorsi tenderness (D'Alessandro et al., 2012). ROS generation was individuated in two main causes: (i) residual myoglobin/ hemoglobin (D'Alessandro et al., 2012) (hereby hemoglobin fragments accumulated from day 10 onwards in band J – figure 7, and table 6); and (ii) impaired mitochondrial respiration. The rationale underpinning this hypothesis is that inhibition or disorders of mitochondrial respiration promotes ROS production. This is consistent with recent reinterpretation of post mortem events in the light of the role of hypoxia/anoxia on mitochondrial activity (Sierra & Oliván, 2013), in analogy to the role of these organelles in other models of prolonged exercise, starvation, hypoxia or ischaemia/reperfusion (I/R) injury (Solaini et al., 2010). ROS accumulation in the muscle might promote proteolysis on one hand, while impairing meat color (D'Alessandro & Zolla, 2013b) by promoting carbonylation and other non-enzymatic oxidative modifications on the other (Rowe et al., 2004); however, curiously meat color resulted not affected, neither after the prolongation of the aging period up to 44 days (table 5). This evidence supports the quality of 44 days-aged Piedmontese meat in the frame of consumers' purchase intentions.

In the present study, even if no significant alteration in terms of meat color was observed, reduced glutathione levels remained stable up until storage day 17 and decreased by day 44 (Figure 11). Conversely, GSSG accumulated significantly soon after one day from slaughter, even if its levels did not further increase throughout storage duration (Figure 11). As to indirectly estimate GSH biosynthesis, the levels of glutamate and its precursor glutamine were monitored throughout the ageing period, the former accumulating constantly until day 44, while the latter only spiked at day 10 and remained constant for the rest of the storage period (Figure 11). Glutamate accumulation in stored meat might stem from advanced

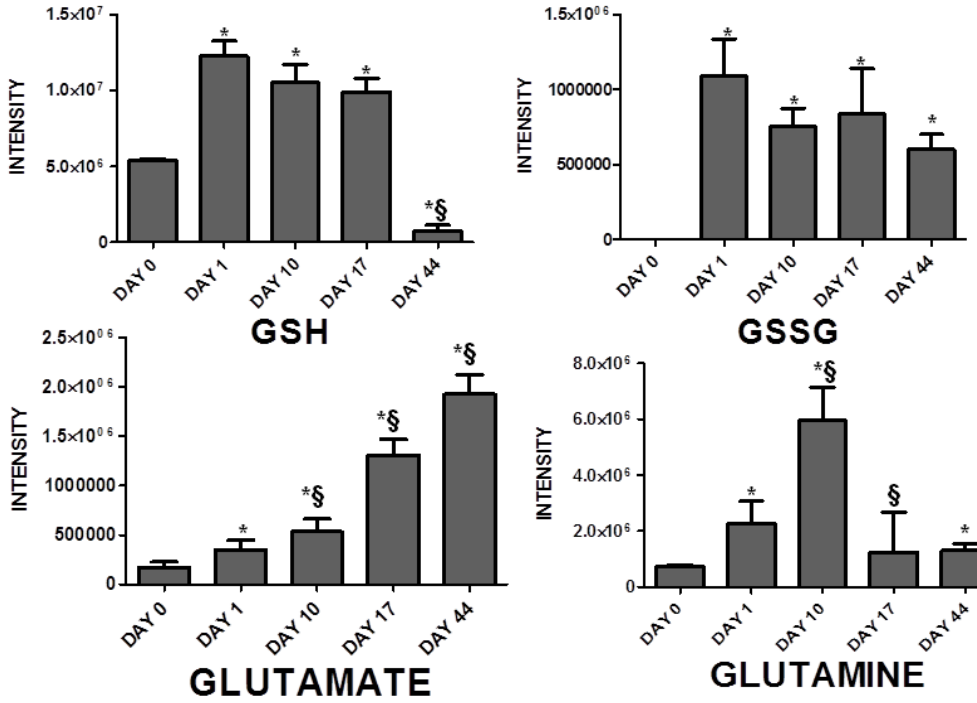

FIGURE 11 – Relative quantification of metabolites of the glutathione metabolism (time course trend).
*indicates a statistically significant difference ($p < 0.05$) existing between the relative quantification at day N and day 0.
§ indicates a statistically significant difference ($p < 0.05$) existing between the relative quantification at day N and the previous time point.

proteolysis, which would release aminoacids, and glutamine carboxylation. At the same time, glutamate might hold beneficial effects in terms of meat quality, since it has been indicated as a positive contributor to meat palatability as a mediator of the umami taste (Bellisle, 1999). The glutamine trend is quite puzzling, but its effective behavior is probably affected by the high biological variability (that is evident from the large standard deviation bars, figure 11): despite the spike at day 10 and the low level at day 17, I can hypothesize that the true trend would resemble the GSH trend (that is, an increase at day 1, 10, 17 as to follow the parallel GSH increase).

Maintenance of GSH levels up until storage day 17 might be achieved by the observed simultaneous up-regulation of the pentose phosphate pathway (PPP) (especially phosphogluconolactone – Figure 12), a metabolic pathway devoted to the generation of pentose phosphate compounds (e.g. ribose phosphate – Figure 12), as to fuel nucleoside

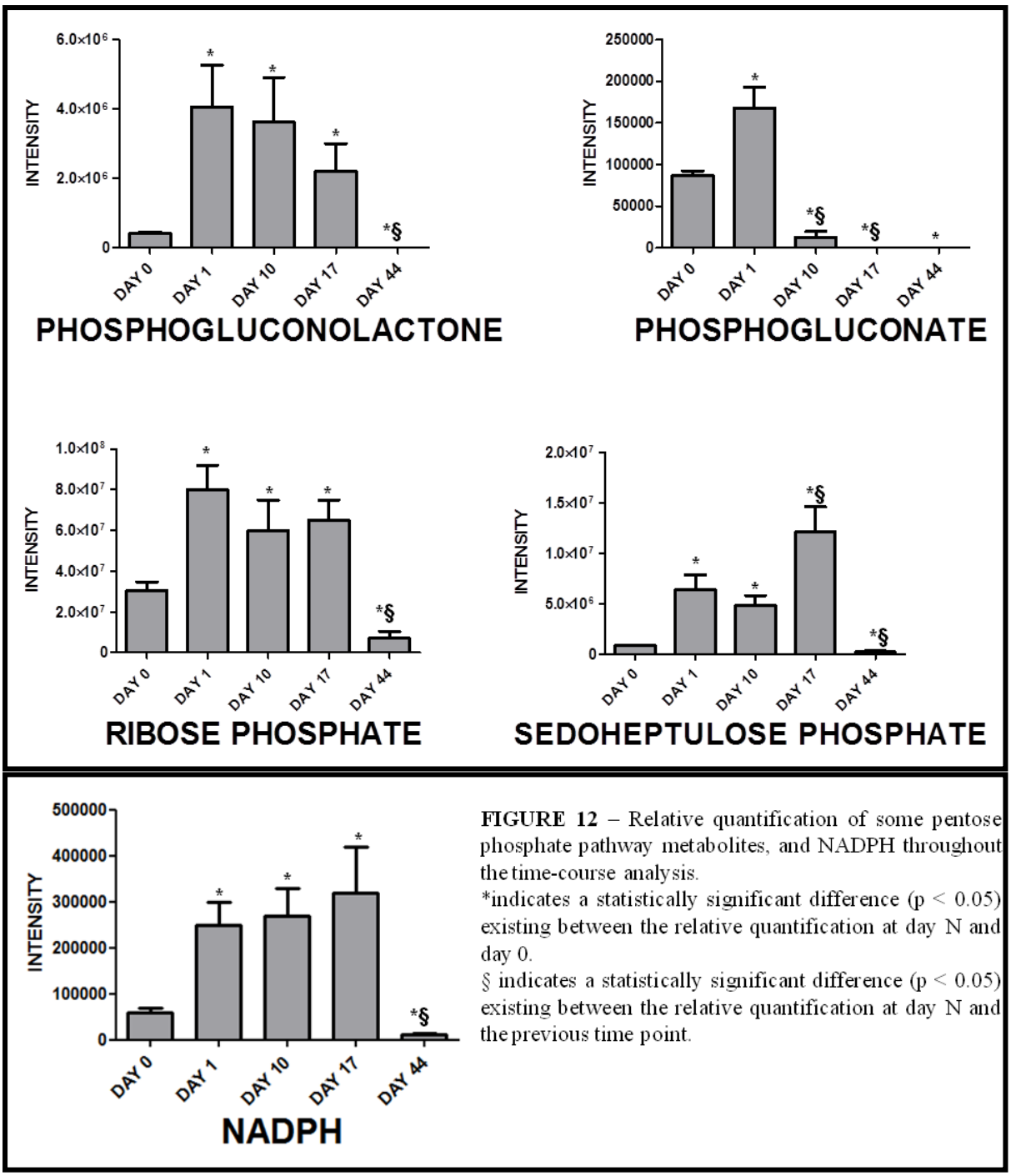

FIGURE 12 – Relative quantification of some pentose phosphate pathway metabolites, and NADPH throughout the time-course analysis.
*indicates a statistically significant difference ($p < 0.05$) existing between the relative quantification at day N and day 0.
§ indicates a statistically significant difference ($p < 0.05$) existing between the relative quantification at day N and the previous time point.

biosynthetic reactions, and the generation of NADPH, a key coenzyme promoting GSSG reduction back to GSH in glutathione homeostasis. NADPH levels throughout the time course experiment follow the GSH trend (figure 12); the reloading potential permits to GSSG to be reduced to GSH during the intermediate days, whereas the further aging extension up to 44 days impairs any possibility to counteract the increasing oxidative stress.

While most of NADPH is metabolically generated via the PPP, other enzymatic reactions might contribute to its generation, such as reactions involving the malic enzyme, whose function is to produce pyruvate, CO_2 and NADPH from malate. Consistently, malate was

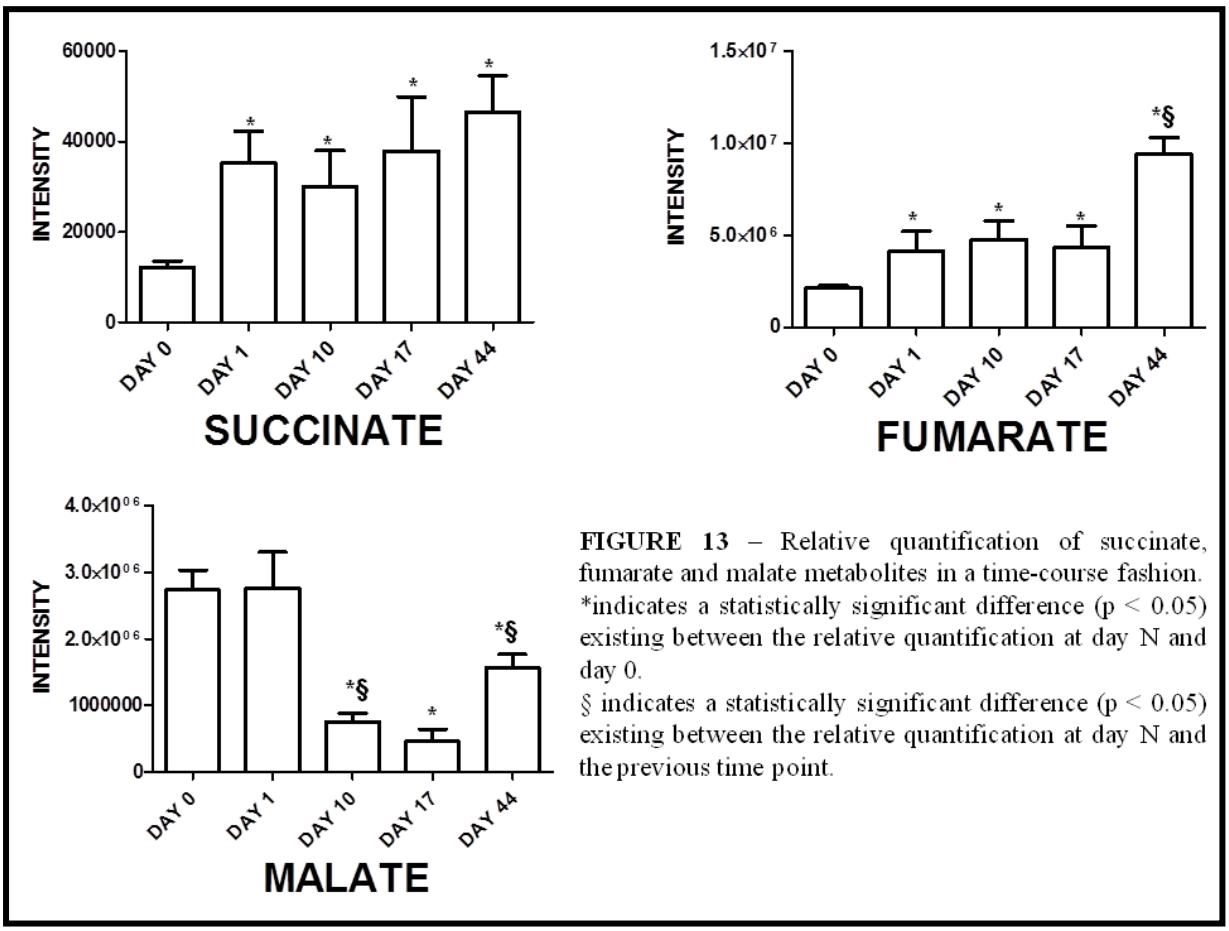

FIGURE 13 – Relative quantification of succinate, fumarate and malate metabolites in a time-course fashion. *indicates a statistically significant difference ($p < 0.05$) existing between the relative quantification at day N and day 0.
§ indicates a statistically significant difference ($p < 0.05$) existing between the relative quantification at day N and the previous time point.

progressively consumed during the first 17 days after slaughter (Figure 13). Accumulation of Krebs cycle intermediates fumarate and succinate is also a symptom of uncoupled mitochondrial metabolism (as expected in the anoxic environment of post mortem muscle).

However, this metabolic behavior is apparently restrained by storage day 44, probably because the accumulation of lactate inhibits the ulterior reduction of pyruvate to lactate, so hampering the oxidation of malate to give pyruvate driven by malic enzyme. It is worth noting that hypoxic environment might promote glycolytic metabolism through accumulation of Krebs cycle ‘‘oncometabolites’’ succinate and fumarate, which trigger succinylation of

prolyl hydroxylase, the enzyme responsible for the degradation of Hypoxia Inducible Factor (HIF) 1-alpha. In turn, HIF1α promotes glycolytic metabolism and depresses shuttling of late glycolytic byproducts to the Krebs cycle, by mediating the expression of pyruvate dehydrogenase kinase. (Boulahbel et al., 2009; Kim et al., 2006).

Recently, biochemical events driving muscle to meat conversion and meat tenderization have been associated to mitochondrial-dependent (intrinsic) apoptosis (Ouali et al., 2006) or autophagy (Sierra & Oliván, 2013). While apoptosis promotes cell death cascades, autophagic responses imply a finely tuned process that is either committed to rescue the cell from stress or to promote cell sacrifice in the worst case scenario. Cell rescue passes through a process in which eukaryotic cells self-digest part of their cytosolic components to the end of degrading proteins and organelles in order to survive starvation, while maintaining cell homeostasis through the elimination of oxidatively-damaged, aberrant macromolecules and organelles (Sierra & Oliván, 2013). Autophagic responses are mediated by amino acid sensing via mammalian target of rapamycin (mTOR) and AMPK activity (Kim, Kundu et al., 2011). Notably, precocious activation of AMPK in pigs is associated with the so-called pale soft exudative (PSE) phenotype, which is responsible for poor pig meat quality (poor WHC, pale color, flat taste) (Shen et al., 2006). Up-regulation of serine metabolism is relevant in that it provides the substrate for glycine and cysteine biosynthesis, via one carbon metabolism and either cysteine or cystathionine synthetase activity, respectively. It is probably worthwhile to recall that, since cysteine and glycine are precursors to GSH, boosting their biosynthesis ends up promoting anti-oxidant potential of the cell as to cope with oxidative stress. As a result, metabolomics analyses outlined a progressive accumulation of serine and its precursor phosphoserine, together with increases in the levels of cystathionine (cysteine precursor

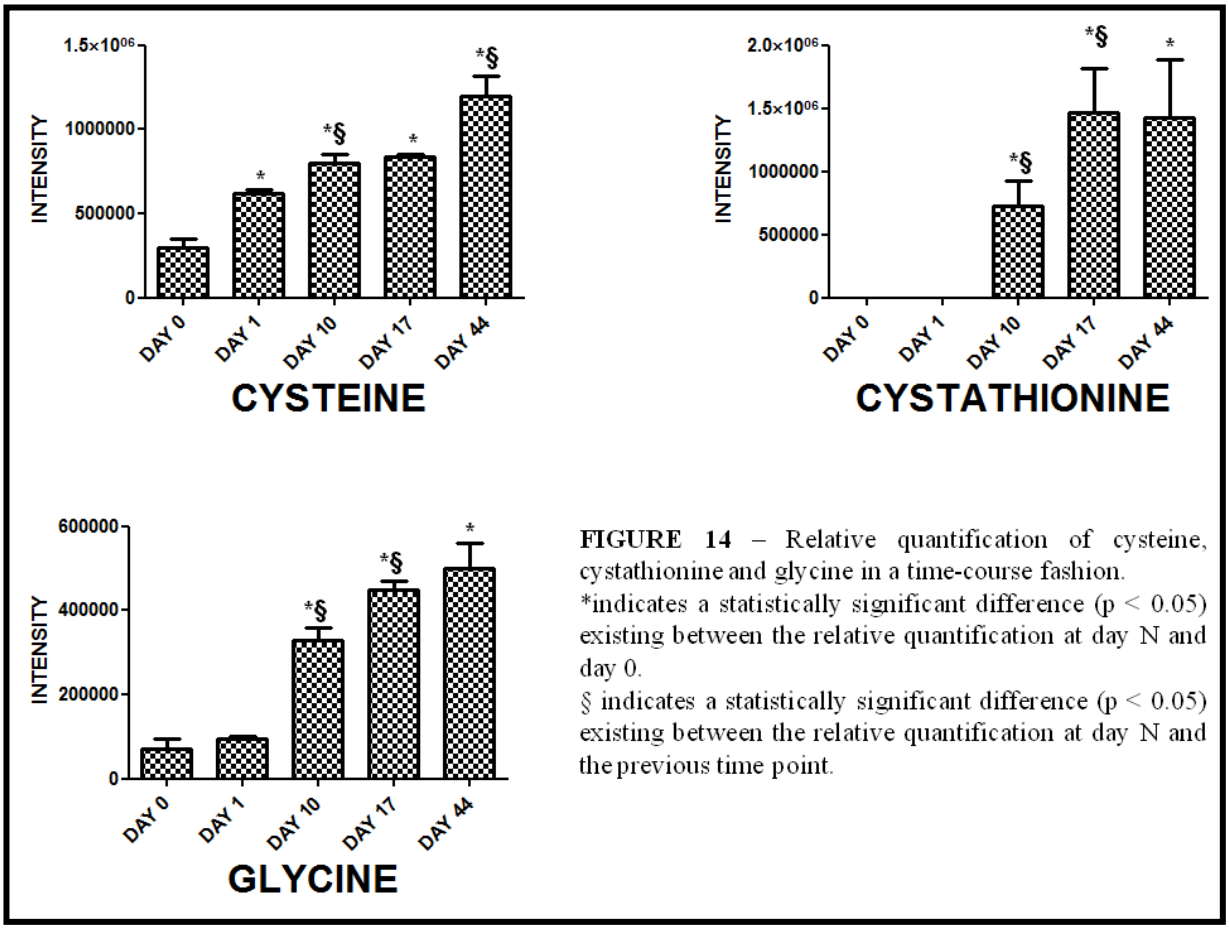

FIGURE 14 – Relative quantification of cysteine, cystathionine and glycine in a time-course fashion.
*indicates a statistically significant difference ($p < 0.05$) existing between the relative quantification at day N and day 0.
§ indicates a statistically significant difference ($p < 0.05$) existing between the relative quantification at day N and the previous time point.

deriving from enzyme-mediated reaction of serine with homocysteine), cysteine and glycine (Figure 14). Furthermore, reminding that a serine biosynthetic pathway has its starting point from the glycolytic phosphoglycerate, the increase of phosphoserine and serine could be seen as a way to avoid the phosphoglycerate accumulation, favoring the glycolytic flux. It is in my opinion noteworthy that the level of phosphoglycerate drops down from day 10 (figure 8), when the accumulation of lactate begins to hamper the glycolysis: there could be the activation of the serine biosynthesis as to contrast this event. The 'switch' to the serine biosynthetic pathway also promotes the net formation of ATP from biphosphoglycerate to phosphoglycerate, in an attempt to restore the energetic reservoirs of meat cells. Consistently with this hypothesis, the levels of phosphoserine begin to increase from day 10; my supposition is that, in the frame of the 'serine switch' hypothesis, phosphoserine level is much more indicative than serine level, because the latter is heavily influenced by the ongoing

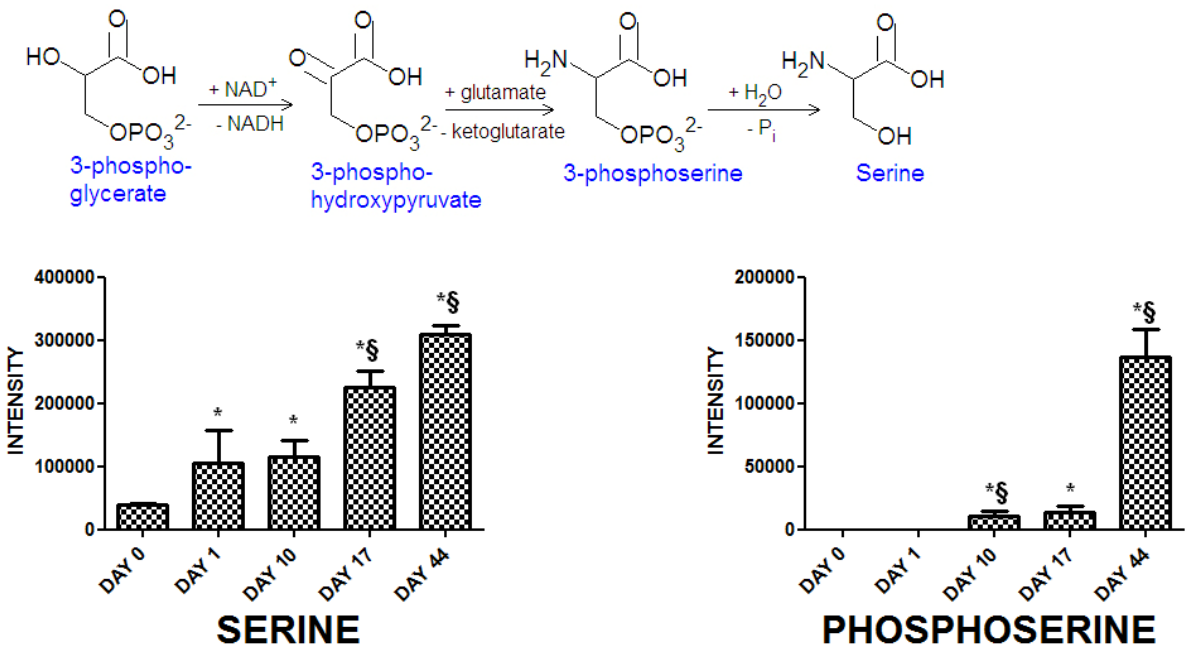

FIGURE 15 – Relative quantification of serine and phosphoserine throughout the time-course analysis; above, the serine biosynthetic pathway starting from the glycolytic 3-phosphoglycerate is represented.
*indicates a statistically significant difference ($p < 0.05$) existing between the relative quantification at day N and day 0.
§ indicates a statistically significant difference ($p < 0.05$) existing between the relative quantification at day N and the previous time point.

proteolysis (that results in a constant increase of serine level, not directly correlated to the present hypothesis). However, serine shows a statistically significant increase from day 10 to day 17 (figure 15).

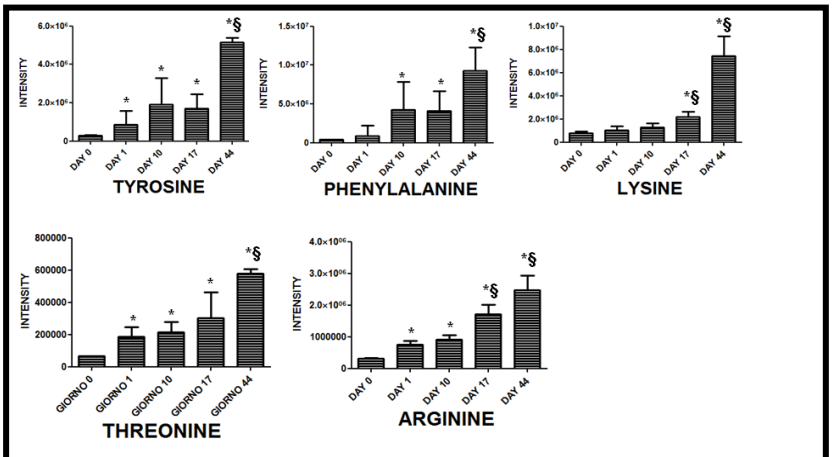

FIGURE 16 – Relative quantification of some exemplificative amino acids throughout the time-course analysis, as to certify the proteolytic process.
*indicates a statistically significant difference ($p < 0.05$) existing between the relative quantification at day N and day 0.
§ indicates a statistically significant difference ($p < 0.05$) existing between the relative quantification at day N and the previous time point.

Protein degradation as a byproduct of protease activity resulted in myofibrillar degradation. Myofibrillar degradation results in the accumulation of protein fragments of variable length, which are utterly degraded into free amino acids. Our results are in line with this hypothesis, as it is

evident from the figure 16: I have reported the time course trends of five exemplificative amino acids (tyrosine, phenylalanine, lysine, threonine and arginine) that show a progressive accumulation to reach the highest levels at day 44. Glutamate (figure 11), cysteine, glycine (figure 14) and serine (figure 15) have already been discussed. The remaining amino acids (data not showed) resemble this trend. The higher levels of free amino acids at day 44 certify once again the increase in the degree of tenderness reached by the Piedmontese meat subjected to prolonged aging.

- *2.3.5 Statistical analyses: principal component analysis suggested that serine, arginine and glutamate might serve as good predictors of ultimate meat tenderness and juiciness*. In order to provide an additional statistical support to the reported data, I performed Pearson's correlation analysis and principal component analysis of physical and metabolomics results, in agreement with previous work from my research group (D'Alessandro et al., 2012).

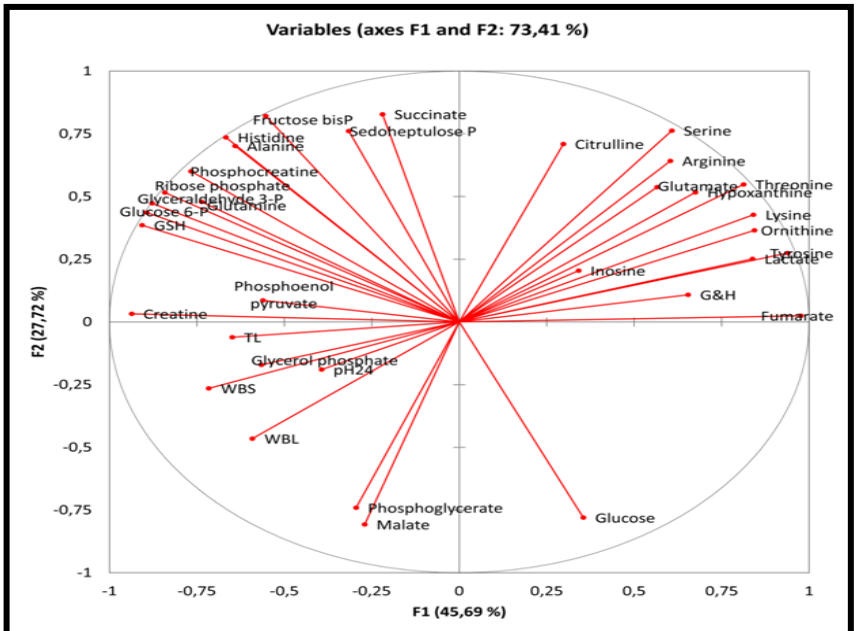

SUPPLEMENTARY FIGURE 1 – Group clustering on Cartesian plots (PCA) for metabolites and physical parameters.

Layouts are reported in Table 7 (in grey are highlighted the results from Pearson's correlations showing absolute values higher than 0.70), while principal component coordinates are summarized in Supplementary Table 1. Finally, results are graphed in

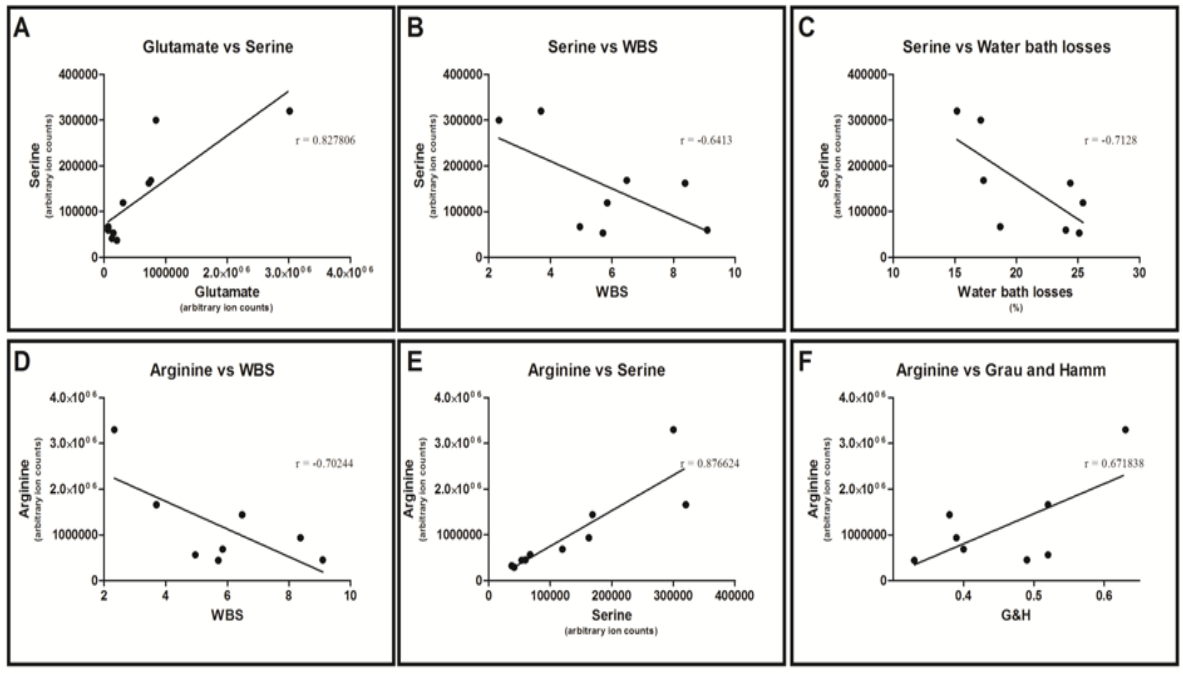

SUPPLEMENTARY FIGURE 2 – Plotting of at least 10 different single measurements and interpolation for Warner Bratzler shear force (Wbs), water bath losses and water holding capacity (Grau and Hamm method) in relation to the level of three metabolites (serine, arginine and glutamate) at post slaughter day 0, 1, 10, 17 and 44 in the *longissimus dorsi* of meat from formerly dairy Piedmontese cows. Interpolation curves are continuous and linear correlation coefficients (r) are reported in the right portion of the graph.

Supplementary figure 1 as to highlight group clustering on Cartesian plots for metabolites and physical parameters, including tenderness (Wbs), juiciness (WHC determined through Grau and Hamm, thawing loss and water bath loss) and ultimate pH. At a first glance, it is evident that metabolites in the first quarter (positive:positive quadrant of PC1 and PC2) are characterized by high positive correlation with Grau and Hamm values, while they are strongly negatively correlated to all the other physical parameters (supplementary figure 1). While Table 7 also highlights the interconnectedness of metabolic pathways (though this is not a novel finding), it also suggests the likely correlation of metabolite levels and the predictability of physical parameters, such as in the case of serine

Table 7- Pearson correlation of metabolites and physical variables; in grey are highlighted the results from Pearson's correlations showing absolute values higher than 0.70.

VARIABLES	Glutamate	Serine	arginine	pH24	WBS	WBL	G&H	TL	Glucose	G6P	F1,6P	GA3P	PG	PEP	Lactate	succinate	fumarate	malate	RiboseP	Sed7P	GSH	glutamine	alanine	inosine	hypoxanthine	ornithine	citrulline	histidine	lysine	threonine	tyrosine	creatine	glycerolP	phosphocreatine
glutamate	1																																	
serine	0,825	1																																
arginine	0,435	0,852	1																															
pH24	-0,288	-0,323	-0,345	1																														
WBS	-0,443	-0,641	-0,702	-0,003	1																													
WBL	-0,646	-0,713	-0,658	0,602	0,660	1																												
G&H	0,300	0,559	0,672	-0,468	-0,584	-0,615	1																											
TL	-0,297	-0,338	-0,464	0,705	0,479	0,784	-0,412	1																										
Glucose	-0,294	-0,478	-0,343	0,067	-0,089	0,215	-0,158	-0,312	1																									
G6P	-0,299	-0,221	-0,250	0,282	0,469	0,303	-0,528	0,531	-0,634	1																								
F1,6P	0,109	0,285	0,188	0,105	0,181	0,020	-0,294	0,379	-0,816	0,855	1																							
GA3P	-0,257	-0,186	-0,233	0,238	0,499	0,301	-0,539	0,524	-0,653	0,996	0,879	1																						
PG	-0,531	-0,657	-0,560	0,036	0,457	0,342	0,125	0,232	0,183	-0,078	-0,485	-0,117	1																					
PEP	-0,197	-0,157	-0,230	0,868	0,067	0,460	-0,279	0,817	-0,396	0,545	0,406	0,504	0,115	1																				
Lactate	0,351	0,662	0,830	-0,240	-0,718	-0,424	0,568	-0,491	0,175	-0,632	-0,225	-0,612	-0,529	-0,390	1																			
succinate	0,281	0,546	0,537	-0,158	-0,043	-0,388	0,158	0,002	-0,894	0,533	0,747	0,553	-0,324	0,215	0,024	1																		
fumarate	0,634	0,618	0,535	-0,375	-0,619	-0,496	0,562	-0,544	0,339	-0,873	-0,502	-0,844	-0,348	-0,551	0,808	-0,256	1																	
malate	-0,371	-0,729	-0,801	-0,033	0,606	0,402	-0,151	0,191	0,378	-0,138	-0,540	-0,154	0,875	-0,069	-0,635	-0,553	-0,250	1																
RiboseP	-0,233	-0,142	-0,175	0,271	0,478	0,314	-0,588	0,504	-0,635	0,976	0,896	0,986	-0,215	0,495	-0,529	0,586	-0,802	-0,245	1															
Sed7P																																		
GSH																																		
glutamine																																		
alanine																																		
inosine																																		
hypoxanthine																																		
ornithine																																		
citrulline																																		
histidine																																		
lysine																																		
threonine																																		
tyrosine																																		
creatine																																		
glycerolP																																		
phosphocreatine																																		

Phosphocreatine	glycerolP	Creatine	Tyrosine	Threonine	Lysine	Histidine	Citrulline	Ornithine	Hypox	Inosin	Alanine	Glutamine	GSH	sedoheptulose
-0,123	-0,310	-0,543	0,667	0,812	0,867	0,045	0,848	0,891	0,570	-0,136	0,022	-0,266	-0,335	0,252
-0,034	-0,323	-0,592	0,799	0,939	0,902	0,166	0,767	0,851	0,735	0,216	0,200	-0,172	-0,288	0,347
-0,076	-0,369	-0,544	0,772	0,826	0,723	0,050	0,383	0,639	0,704	0,518	0,136	-0,136	-0,301	0,194
0,043	0,772	0,188	-0,252	-0,298	-0,377	0,176	-0,227	-0,381	-0,232	-0,108	0,218	-0,059	0,180	-0,360
0,415	0,236	0,649	-0,799	-0,727	-0,718	0,310	-0,206	-0,711	-0,548	-0,263	0,220	0,385	0,575	0,187
0,064	0,524	0,366	-0,607	-0,684	-0,762	0,117	-0,348	-0,790	-0,375	0,037	0,031	0,055	0,309	-0,181
-0,445	-0,177	-0,644	0,628	0,549	0,680	-0,387	0,115	0,623	0,203	0,000	-0,212	-0,478	-0,588	-0,104
0,292	0,813	0,343	-0,520	-0,471	-0,486	0,465	0,024	-0,538	-0,388	-0,286	0,448	0,139	0,447	0,092
-0,713	-0,318	-0,285	0,109	-0,163	-0,161	-0,817	-0,473	-0,085	0,042	0,265	-0,897	-0,490	-0,574	-0,669
0,948	0,417	0,862	-0,722	-0,499	-0,577	0,910	0,018	-0,604	-0,379	-0,201	0,867	0,895	0,981	0,624
0,894	0,176	0,512	-0,287	-0,001	-0,131	0,983	0,457	-0,193	0,100	0,041	0,913	0,788	0,810	0,829
0,960	0,373	0,845	-0,703	-0,466	-0,552	0,931	0,078	-0,582	-0,330	-0,173	0,873	0,900	0,985	0,667
-0,206	0,461	0,235	-0,503	-0,653	-0,444	-0,365	-0,663	-0,422	-0,855	-0,586	-0,209	-0,215	-0,044	-0,471
0,337	0,925	0,332	-0,355	-0,296	-0,315	0,481	-0,076	-0,351	-0,383	-0,353	0,584	0,151	0,417	-0,057
-0,524	-0,501	-0,817	0,905	0,816	0,692	-0,368	0,273	0,629	0,844	0,727	-0,355	-0,504	-0,665	-0,149
0,702	0,119	0,261	0,034	0,299	0,219	0,737	0,340	0,152	0,112	-0,026	0,849	0,497	0,516	0,540
-0,757	-0,569	-0,954	0,924	0,820	0,840	-0,613	0,433	0,841	0,730	0,342	-0,635	-0,743	-0,885	-0,240
-0,249	0,248	0,236	-0,539	-0,670	-0,457	-0,413	-0,479	-0,387	-0,757	-0,609	-0,387	-0,207	-0,065	-0,391
0,957	0,340	0,812	-0,640	-0,397	-0,528	0,945	0,100	-0,563	-0,226	-0,060	0,880	0,882	0,972	0,640
0,719	-0,248	0,342	-0,180	0,080	0,030	0,765	0,615	-0,012	0,210	0,051	0,606	0,730	0,613	**1**
0,962	0,321	0,915	-0,771	-0,547	-0,631	0,876	-0,036	-0,648	-0,398	-0,174	0,819	0,926	**1**	
0,936	-0,002	0,847	-0,634	-0,416	-0,508	0,801	0,011	-0,513	-0,225	-0,019	0,704	**1**		
0,893	0,453	0,585	-0,372	-0,101	-0,181	0,946	0,244	-0,242	-0,167	-0,190	**1**			
0,425	0,347	-0,123	-0,241	0,174	0,201	0,087	0,041	0,015	0,729	**1**				
-0,142	-0,524	-0,299	0,408	0,349	0,084	-0,072	0,035	0,015	1					
-0,237	-0,616	-0,647	0,801	0,839	0,663	-0,042	0,629	1						
-0,428	-0,413	-0,784	0,887	0,917	0,988	-0,291	1							
0,134	-0,267	-0,367	0,461	0,664	0,647	1								
0,932	0,292	-0,810	0,913	-0,123	1									
-0,406	-0,384	-0,780	0,946	0,948										
-0,317	-0,439	0,946	1											
-0,588	-0,446	1												
0,814	1													
1														

Supplementary Table 1 - Coordinates of variables							
variables	**F1**	**F2**	**F3**	**F4**	**F5**	**F6**	**F7**
glutamate	0,566	0,537	0,198	-0,308	0,462	-0,176	-0,110
Serine	0,608	0,763	0,186	-0,108	0,014	0,045	-0,021
Arginine	0,603	0,642	0,025	0,091	-0,440	0,147	-0,010
pH24	-0,393	-0,190	0,687	0,513	0,022	-0,270	0,000
WBS	-0,716	-0,265	-0,248	-0,130	0,323	0,386	-0,292
WBL	-0,592	-0,465	0,181	0,477	0,229	0,345	-0,045
G&H	0,654	0,108	0,170	-0,417	-0,452	0,306	0,244
TL	-0,649	-0,061	0,594	0,212	0,256	0,316	0,109
Glucose	0,355	-0,780	-0,273	0,353	0,108	-0,232	0,031
G6P	-0,893	0,436	-0,017	0,023	-0,037	-0,052	0,085
F1,6P	-0,553	0,821	0,018	0,090	0,051	0,061	0,073
GA3P	-0,878	0,473	-0,048	0,025	0,015	-0,008	0,050
Phosphoglycerate	-0,295	-0,741	0,143	-0,488	-0,227	0,234	-0,015
PEP	-0,561	0,086	0,787	0,182	-0,080	-0,113	0,081
Lactate	0,838	0,251	-0,012	0,386	-0,233	0,175	-0,013
Succinate	-0,219	0,828	0,091	-0,238	-0,326	0,075	-0,300
Fumarate	0,976	0,025	0,016	0,039	0,195	0,079	-0,010
Malate	-0,270	-0,807	-0,043	-0,459	0,216	0,120	-0,041
riboseP	-0,842	0,516	-0,053	0,136	0,017	-0,017	-0,062
sedoheptulose P	-0,316	0,761	-0,331	-0,130	0,248	0,190	0,311
GSH	-0,907	0,386	-0,162	-0,004	-0,019	-0,040	-0,029
glutamine	-0,736	0,479	-0,427	-0,007	-0,081	-0,152	0,128
Alanine	-0,641	0,701	0,230	-0,091	-0,156	0,032	-0,106
Inosine	0,341	0,204	-0,388	0,774	-0,197	0,225	-0,060
Hypoxanthine	0,675	0,517	-0,137	0,466	0,190	0,064	-0,043
Ornithine	0,844	0,365	0,177	-0,283	0,142	-0,149	-0,028
Citrulline	0,298	0,709	0,128	-0,085	0,602	0,122	0,088
Histidine	-0,667	0,736	0,062	0,042	0,073	0,047	-0,021
Lysine	0,841	0,427	0,213	-0,238	0,085	-0,033	-0,014
Threonine	0,813	0,548	0,150	0,031	0,048	-0,018	-0,113
Tyrosine	0,939	0,274	0,164	0,112	-0,034	-0,003	-0,047
creatine	-0,936	0,032	-0,261	-0,086	-0,095	-0,189	-0,052
glycerolP	-0,566	-0,171	0,793	-0,032	-0,138	0,032	-0,034
phosphocreatine	-0,767	0,601	-0,174	-0,087	-0,055	-0,080	-0,064

and arginine with Wbs, Grau and Hamm or water bath losses (supplementary figure 2). However, it is worthwhile to note that some correlations might be affected by single outliers (e.g. supplementary figure 2F) or rather be biased by the relatively small subset of biological samples assayed in the present study. Of note, PCA and correlations were performed on metabolic and physical assays on the same animals at the same time points, thus strong correlations throughout the whole storage period are suggestive of the likely indirect predictability of physical values through the assessment of metabolites such as serine,

arginine and glutamate soon after slaughter. While these results are but preliminary, I believe that this research/applicative aspect will deserve further attention in the future.

2.4 CONCLUSIONS.

The Piedmontese breed of cattle is one of the most valuable in Italy, owing to the high carcass yield and good quality of its meat. In the first part of the thesis, Longissimus thoracis muscles from Piedmontese cull cows were assayed for physical, microbiological, proteomics (1D gel electrophoresis) and metabolomics parameters during a carcass ageing period of 44 days at 2°C. The rationale behind this study was to verify, through accurate and analytical strategies, if the extension of the ageing period up to 44 days could improve the commercial value of Piedmontese cull cows meats, actually considered less valuable. Routine practice and currently available biochemical knowledge encouraged further research, since no beneficial effects of extended ageing periods over two weeks after slaughter has been hitherto reported. However, physical analyses confirmed the empirical reports by the producer and consumers, while indicating a progressively increased tenderness and decreased water holding capacity of longer stored meat. Quality and safety of meat were confirmed by microbiological analyses. Proteomics and metabolomics confirmed a progressive decline in myofibrillar structural integrity and impaired energy metabolism. From a metabolomics standpoint, key metabolites such as glutamate, which is known to be related to the umami taste of the meat, were found to constantly accumulate until day 44. Statistical analyses conduced on physical and omics data showed the synergy between classical standard measurements and omics platforms in the disclosure of biochemical changes intervening in ageing meat, revealing that glutamate, together with serine and arginine, could serve as good predictors of ultimate meat quality parameters, even though further studies are mandatory.

2.5 CONCLUSIONS AS A STARTING POINT.

From the collected data, it emerged that energy metabolism undergoes a drastic change soon from day 1; all the following metabolic behaviors, in my opinion, have to be considered as an attempt to maintain an adequate energetic supply, at the same time fighting the oxidative stress caused by the progressive mitochondrial impairment.

In the frame of muscle-to-meat conversion process, the oxidative stress becomes a pivotal argument. Here I want to recall the accumulation of hemoglobin fragments especially from day 10 onward, which is an indirect clue for the increase of the oxidative stress into the aging meat. Skeletal muscles are among the major oxygen-consuming tissues, characterized by a high rate of mitochondrial respiration and a correspondently high risk of ROS production (Murphy, 2009). Nowadays, ROS are no longer seen only as harmful compounds (Barbieri & Sestili, 2011); beside their toxicity, many physiological signaling functions in muscle have been recognized: a transient, moderate increase can be the fuse for triggering a healthy process (as it is in living animals), whereas an excessive and uncontrolled production falls into irremediable cellular damages. During the process of muscle-to-meat conversion, ROS activity is inevitably persistent in time, and the progressive accumulation mobilizes all defensive responses that the muscular cell can produce; in the slaughtered muscle, the production of ROS progressively increases, while antioxidant capacities constantly decrease.

- *2.5.1 Sources of ROS in skeletal muscle.* Like any other kind of cell, the muscular cell is subjected to the 'Oxygen paradox' (Davies, 1995), with the oxygen being the two-face central molecule of higher eukaryotes aerobic metabolism: on the one hand, oxygen is the final acceptor of the electron transport chain; on the other hand, it shows a dangerous 'dark side', assisted by the innate imperfections of the mechanism of oxidative phosphorylation.

Mitochondria are considered the major sources of ROS production, because of the heavy use of O_2 in their metabolic activities (Brand, 2010) and of the intrinsic hallmarks of the oxidative phosphorylation, which is based on the oxygen as the final acceptor of electrons donated by reducing substrates: indeed, one electron at a time is used for O_2 reduction to H_2O, and between the first and the final step, the intermediate products are all ROS ($O_2 \rightarrow O_2^{-\cdot} \rightarrow H_2O_2 \rightarrow {}^{\cdot}OH \rightarrow H_2O$) (Grivennikova & Vinogradov, 2013); the superoxide anion O_2^- is the primary species and the precursor of the other reactive species (not only oxygen-derived but also nitrogen-derived; Radi, Cassina, & Hodara, 2002), produced by NADPH oxidase, cytochrome P450-dependent oxygenases and xanthine oxidase; its enzymatic dismutation by superoxide dismutase is the responsible for the formation of H_2O_2. H_2O_2 in turn is transformed to hydroxyl radical OH by the Fenton reaction because of the comodulation guaranteed by the presence of metal ions (Altun et al., 2007), especially iron ions contained into mitochondria and myoglobin molecules of muscles. Overall, at least ten mitochondrial enzymes contribute to ROS production (Marchi et al., 2012). Although mitochondria are generally accepted as the major source of ROS in muscular cells, in the last years a few evidences contradicted this hypothesis, opening the debate on the argument (Brown & Borutaite, 2012). The PLA2 (phospholipase A2), particularly the calcium-dependent isoform, has been proposed to turn on under stress conditions to trigger ROS production (Gong et al., 2006). Furthermore, it has been demonstrated that xanthine oxidase, under prolonged ischemic conditions (such as in the slaughtered muscle), is operative in both mitochondrial and cytoplasmic production of ROS (Kelley et al., 2010). The slaughtered muscle can undergo inflammation reaction; the infiltrated polymorphoneutrophils activate NADPH oxidases by means of ROS production (respiratory burst) and secrete cytokines within the muscle, which bind specific membrane receptors and activate cyclooxygenases- and xanthine oxidase-ROS producing enzymes; a positive feedback cycle takes place thanks to the

secretion of interleukins (IL-1, IL-6, IL-8) and TNF-α by injured endothelial cells into the muscle, so triggering a continuous ROS production (Ji, 2007). While this inflammation-triggered ROS formation is essential under physiologic conditions to the restoration of antiseptic environment and normal homeostasis, an uncontrolled stress status contributes to the decrease of antioxidant defensive mechanisms. Other important sources are NADPH oxidases within the sarcoplasmic reticulum and transverse tubules (Holmstrom & Finkel, 2014).

- *2.5.2 Oxidative stress effects.* Mitochondria, especially in muscle cells, are both the main source and the main target of ROS (Figure 17). ROS are particularly effective on mitochondrial DNA, because of its close proximity to the respiratory chain (it is attached to the inner mitochondrial membrane). Mitochondrial DNA is prone to oxidative damages due to the lack of introns and histones; both bases and sugars are susceptible of oxidation, resulting in strand breaks (Cadet & Wagner, 2013), and the situation is aggravated by the oxidizing action of ROS on polymerase γ (coincident with the drop in its activity and with the decrement of DNA-replicating and repairing abilities; Graziewicz et al., 2002). An immediate target of ROS attack is the respiratory chain itself, because of its metal ion content. The consequent dismantling results in a sort of 'positive feedback' for an increasing production of ROS and RNS species; the latter are reported to be the cause of Complex I inhibition through, for example, tyrosine nitration (Castro et al., 2011). Another victim of oxidation is the mitochondrial permeability transition pore (mPTP), particularly regarding its adenine nucleotide translocase (ANT) subunit, where critical thiolic oxidized residues induce the opening of mPTP (Mailloux et al., 2014), with the consequent imbalance of physiologic ion equilibrium and membrane swelling. At the membrane levels, ROS, and especially OH, oxidize unsaturated fatty acids of phospholipids; lipoperoxides cause the formation of reactive aldehydes and establish the lipid peroxidation cycle, which is self-amplifying. The increasing

amounts of lipid radicals give rise to an extreme mitochondrial membrane fluidity, which causes the loss of ionic selectivity and the imbalance of homeostatic ionic equilibrium; the high diffusibility of lipid radicals permits covalent modifications of mitochondrial membrane proteins and mtDNA (Sayre et al., 2006; Zhong & Yin, 2015). All these ROS effects affect

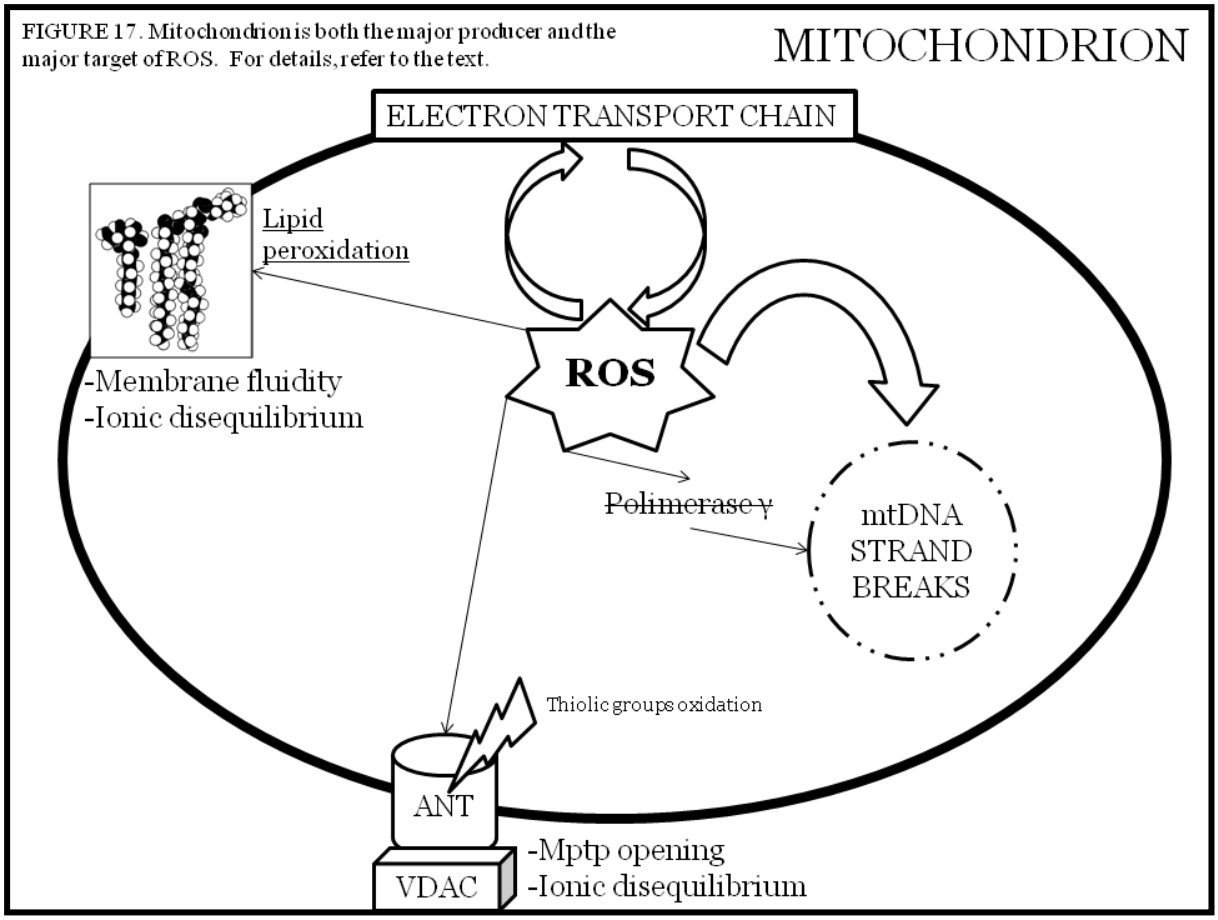

FIGURE 17. Mitochondrion is both the major producer and the major target of ROS. For details, refer to the text.

muscle cells with no escape, due to their progressively increasing amounts. The normal physiology is no longer recoverable: muscle cells need a valid alternative.

- *2.5.3 ROS can trigger both autophagy and apoptosis.* ROS are a central argument when considering the development of meat from a sacrificed animal; they are the consequences of the loss of the organism's systemic organization, no more able to drive oxygen and nutrients to its constituent parts. ROS generation is a beneficial event in physiological conditions, but it becomes a doom when the postmortem anoxic conditions are irreversible. The overwhelming oxidative stress little by little exasperates the defensive mechanisms of muscle cells, unable to

reload without the aerobic ATP formation. The result of the collapse of cellular resistance is a progressively mounting rate of physical damages suffered by cell structures, particularly at mitochondria (as explained). For the muscle cells it is now time to take a drastic decision; indeed, like any other cell, muscular cells own a 'B plan' that is selectable when it is not possible to block an exasperated oxidative stress. The B plan involves a crossroad that gives to the muscle cells the possibility to choose between two divergent directions. One option is the direct methodical apoptotic suicide, but just like a person who tries to heal a wound before thinking at suicide, a cell that is undergoing oxidative damages could reasonably try to repair its damaged parts, rescuing and/or substituting the malfunctioning macromolecules and organelles: in other words, it can start up autophagy. Autophagy is a biomolecular process which makes use of the endosomal/lysosomal pathway to self-digest aberrant macromolecules or entire damaged organelles after their engulfment into a double-membrane 'autophagosome' (Kraft & Martens, 2012), needy of lysosomal cathepsins to acquire hydrolytic activity (Repnik et al., 2012). The degradation reactions render monomeric units (simple sugars, amino acids, nucleotides and fatty acids) available for reutilization (Feng et al., 2014), particularly useful in starvation conditions, known to be strong activators of autophagic reactions (Chen et al., 2009). It is clear that the context of an anoxic muscle from a slaughtered animal could logically be considered a suitable crable for the establishment of autophagy as the very last resort against the oxidative damage; and it is not important that muscular cells are fatally directed to failure, because autophagy can turn from a rescue pathway to a death pathway, the so-called type 2 cell death. Compared to apoptosis, the autophagic death shows striking differences from both morphological and biomolecular standpoints, even reflected in distinct peculiar markers (Marino et al., 2014). The controversial role of autophagy raises many debates on its two-face nature: survival or death decisions are both possible, and the discriminant is a focal but still unclear point; a hypothesis

places the mitochondrial permeability transition (MPT) at the crossroad between salvage and execution, as mitochondrial permeabilization is observable in autophagy, apoptosis and necrosis: where limited, autophagic rescue can intervene, but where extensive, it can trigger controlled apoptotic or autophagic death or, in the worst case, necrosis (Rasola & Bernardi, 2011). Given that, the muscle-to-meat conversion process seems to fit the hallmarks for both autophagy and apoptosis because ROS are central in both mechanisms, and they are massively produced in aging meat. Mitochondria are the 'operative centers' where decisions about the cellular destiny are taken, also because of the direct effects exerted by ROS on them.

Meat cells are constrained to die. But what is the preferential way? To date, no evidence of necrosis has been collected, and the attention has been focused on apoptosis and autophagy. Due to ROS production, during the muscle-to-meat conversion process apoptosis and autophagy are both plausible reactions. Theoretically, autophagic behavior is a possible strategic framework available both as an extreme defensive mechanism and as a programmed cell death pathway. What for the short and the long period after slaughter? Do muscle cells adopt autophagy as the last chance to counteract the sudden deprivation of oxygen and nutrients? And if they do, what happens when this extreme attempt inevitably fails? Do the dying cells commit suicide through the conversion of the autophagic mechanism into the apoptotic one, or do they undertake type 2 programmed cell death? (Figure 18). With all these questions about the effective molecular mechanisms of muscle-to-meat conversion process, the second part of my research has been dedicated to the search for clues to gain understanding of apoptosis/autophagy duality, by means of the 'omics' witness.

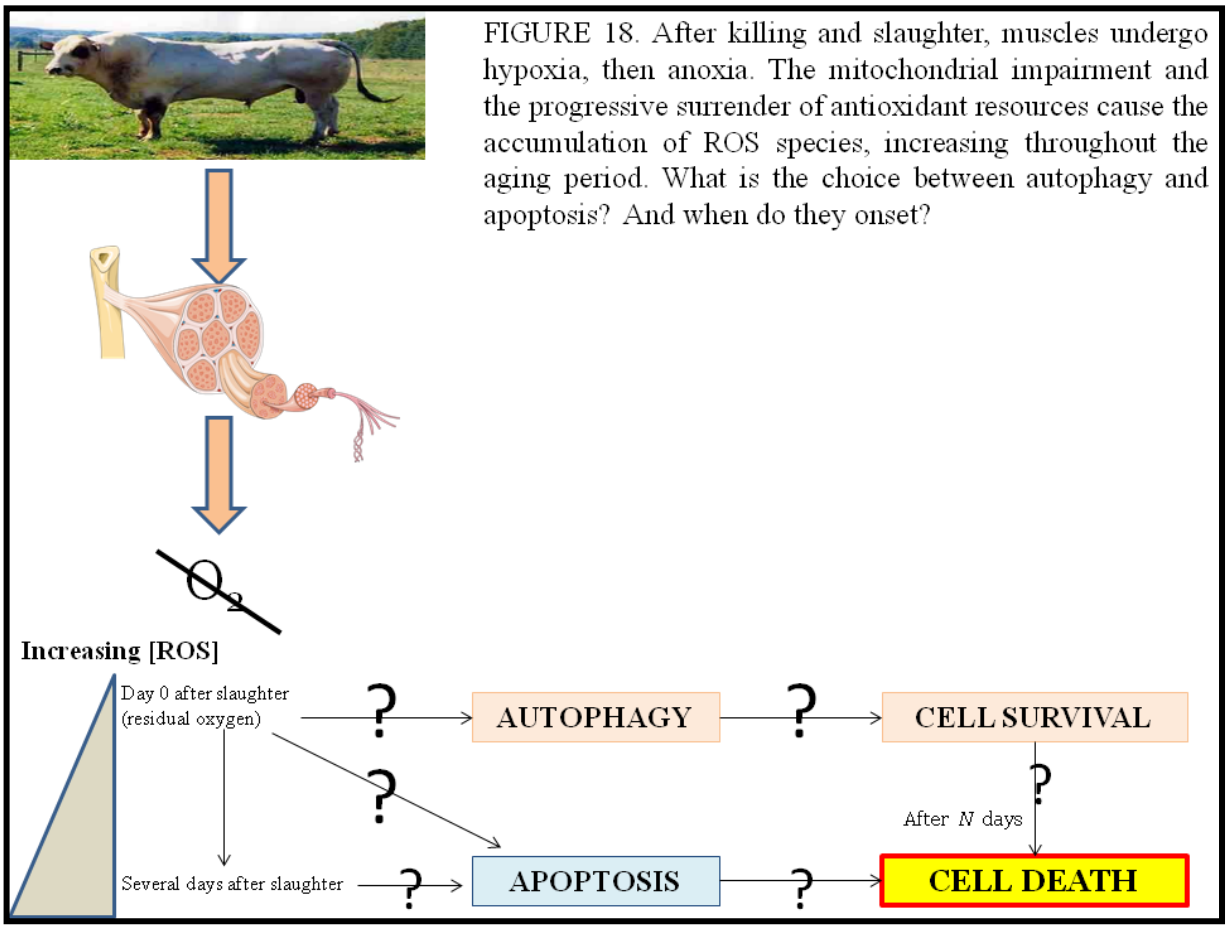

FIGURE 18. After killing and slaughter, muscles undergo hypoxia, then anoxia. The mitochondrial impairment and the progressive surrender of antioxidant resources cause the accumulation of ROS species, increasing throughout the aging period. What is the choice between autophagy and apoptosis? And when do they onset?

REFERENCES

Altun M, Edstrom E, Spooner E, Flores-Moralez A, Bergman E, Tollet-Egnell P et al. (2007). Iron load and redox stress in skeletal muscle of aged rats. Muscle and Nerve 36(2):223-233.

AOAC (1970). Official methods of analysis (11th ed.). Washington, DC, USA: Association of Official Analytical Chemistry.

Barbieri E, Sestili P (2011). Reactive oxygen species in skeletal muscle signaling. Journal of Signal Transduction 2012:Article ID 982794.

Barton-Gade PA, Demeyer D, Honikel KO, Joseph RL, Poulanne E, Severini M, Smulders FJM, Tomberg E (1994). Final version of reference methods for water holding capacity in meat and meat products. Procedures recommended by an OECD working group. Proceedings of 40th International Congress of Meat Science and Technology. The Hague, Netherlands, 28 August–2 September 1994. SV05.

Becila S, Herrera-Mendez Hernan C, Coulis G, Labas R, Astruc T et al. (2010). Postmortem muscle cells die through apoptosis. European Food Research Technology 231:485–493.

Beere HM (2005). Death versus survival: Functional interaction between the apoptotic and stress-inducible heat shock protein pathways. Journal of Clinical Investigation 115:2633–2639.

Bellisle F (1999). Glutamate and the UMAMI taste: Sensory, metabolic, nutritional and behavioural considerations. A review of the literature published in the last 10 years. Neuroscience Biobehavioral Reviews 23(3):423–438.

Boulahbel H, Durán RV, Gottlieb E (2009). Prolyl hydroxylases as regulators of cell metabolism. Biochemical Society Transactions 37(1):291–294.

Brand MD (2010). The sites and topology of mitochondrial superoxide production. Experimental Gerontology 45(7-8):466-472.

Brown GC, Borutaite V (2012). There is no evidence that mitochondria are the main source of reactive oxygen species in mammalian cells. Mitochondrion 12:1-4.

Brugiapaglia A, Lussiana C, Destefanis G (2014). Fatty acid profile and cholesterol content of beef at retail of Piemontese, Limousin and Friesian breeds. Meat Science 96(1):568–573.

Cadet J, Wagner JR (2013). DNA base damage by reactive oxygen species, oxidizing agents, and UV radiation. Cold Spring Harbor Perspective in Biology, 5(2).

Castro L, Demicheli V, Tortora V, Radi R. (2011). Mitochondrial protein tyrosine nitration. Free Radical Research 45(1):37-52.

Chen F (2012). JNK-induced apoptosis, compensatory growth, and cancer stem cells. Cancer Research 72(2):379-386.

Clasquin MF, Melamud E, Rabinowitz JD. (2012). LC–MS data processing with MAVEN: A metabolomic analysis and visualization engine. Current Protocol in Bioinformatics 37(14):1-23.

Cottingham K (2010). 1DE proves its worth... again. Journal of Proteome Research 9(4):1636.

Cross HR, West RL, Dutson TR (1981). Comparison of methods for measuring sarcomere length in beef semitendinosus muscle. Meat Science 5:261–266.

D'Agostino M, Wagner M, Vàzquez-Boland JA, Kuchta T, Kapriskova R, Roofar J et al. (2004). A validated PCR method to detect Listeria monocytogenes using raw milk as a food model-towards an International standard. Journal of Food Protection 67:1646–1655.

D'Alessandro A, Gevi F, Zolla L (2011a). A robust high resolution reversed-phase HPLC strategy to investigate various metabolic species in different biological models. Molecular Biosystems 7(4):1024–1032.

D'Alessandro A, Marrocco C, Zolla V, D'Andrea M, Zolla L (2011b). Meat quality of the longissimus lumborum muscle of Casertana and Large White pigs: Metabolomics and proteomics intertwined. Journal of Proteomics 75(2):610–627.

D'Alessandro A, Rinalducci S, Marrocco C, Zolla V, Napolitano F, Zolla L (2012). Love me tender: An omics window on the bovine meat tenderness network. Journal of Proteomics 75(14):4360–4380.

D'Alessandro A, Zolla L (2012). We are what we eat: Food safety and proteomics. Journal of Proteome Research 11(1):26–36.

D'Alessandro A, Zolla L (2013a). Meat science: From proteomics to integrated omics towards system biology. Journal of Proteomics 78:558–577.

D'Alessandro A, Zolla L (2013b). Foodomics to investigate meat tenderness. Trends in Analytical Chemistry 52:47–53.

Dando I, Donadelli M, Costanzo C, Dalla Pozza E, D'Alessandro A, Zolla L et al. (2013). Cannabinoids inhibit energetic metabolism and induce AMPK-dependent autophagy in pancreatic cancer cells. Cell Death and Disease 4:e664.

Davies KJ (1995). Oxidative stress: the paradox of aerobic life. Biochemical Society Symposium 61:1-31.

Destefanis G, Barge MT, Brugiapaglia A (1993a). Variabilità delle caratteristiche qualitative nella carne di bovini di razza piemontese con ipertrofia muscolare. Zootecnica e Nutrizione Animale 19:177–183.

Destefanis G, Brugiapaglia A, Barge MT (1993b). The influence of breed type on texture and sensory characteristics of beef meat. Proceedings 39th International Congress of Meat Science and Technology. Calgary, Alberta, Canada, S2P06.WP. 1–6.

Edmonds MS, Lowry KR, Baker DH (1987). Urea cycle metabolism: Effects of supplemental ornithine or citrulline on performance, tissue amino acid concentrations and enzymatic activity in young pigs fed arginine-deficient diets. Journal of Animal Science 65(3):706–716.

Feng Y, He D, Yao Z, Klionsky DJ (2014). The machinery of macroautophagy. Cell Research 24:24-41.

Gong MC, Arbogast S, Guo Z, Mathenia J, Su W, Reid MB (2006). Calcium-independent phospholipase A2 modulates cytosolic oxidant activity and contractile function in murine skeletal muscle cells. Journal of Applied Physiology 100(2):399-405.

Grau R, Hamm R (1953). Determination of the water binding power of muscle. Naturwissenschaften 40:29–30.

Graziewicz MA, Day BJ, Copeland WC (2002). The mitochondrial DNA polymerase as a target of oxidative damage. Nucleic Acids Research 30(13):2817-2824.

Grivennikova VG, Vinogradov AD (2013). Mitochondrial production of reactive oxygen species. Biochemistry (Moscow) 78(13):1490-1511.

Guillemin N, Bonnet M, Jurie C, Picard B (2011). Functional analysis of beef tenderness. Journal of Proteomics 75(2):352–365.

Holmstrom KM, Finkel T (2014). Cellular mechanism and physiological consequences of redox-dependent signaling. Nature Reviews Molecular Cell Biology 15:411-421.

Hoogland C, Mostaguir K, Sanchez JC, Hochstrasser D, Appel RD (2004). SWISS-2DPAGE, ten years later. Proteomics 4(8):2352–2356.

Hudzik E (1990). Comparaison de la determination du fer heminique dans lens viandes crues par la method de Hornseyavec l'absorption de l'extraits aqueux à 410 nm. Sciences des Aliments 10:209–213.

Huff-Lonergan E, Lonergan SM (2005). Mechanisms of water-holding capacity of meat: The role of postmortem biochemical and structural changes. Meat Science 71(1):194–204.

Hwang IH (2004). Application of gel-based proteome analysis techniques to studying post-mortem proteolysis in meat. Asian–Australasian Journal of Animal Science 17(9):1296–1302.

Ibáñez C, Simó C, García-Cañas V, Cifuentes A, Castro-Puyana M (2013). Metabolomics, peptidomics and proteomics applications of capillary electrophoresis-mass spectrometry in Foodomics: a review. Analytica Chimica Acta 802:1–13.

Ji LL (2007). Antioxidant signaling in skeletal muscle: a brief review. Experimental Gerontology 42(7):582-593.

Kanehisa M, Goto S (2000). KEGG: Kyoto encyclopedia of genes and genomes. Nucleic Acids Research 28(1):27–30.

Kelley EE, Khoo NK, Hundley NJ, Malik UZ, Freeman BA, Tarpey MM (2010). Hydrogen peroxide is the major oxidant product of xanthine oxidase. Free Radical Biology and Medicine 48(4):493-498.

Kemp C, Parr T (2012). Advances in apoptotic mediated proteolysis in meat tenderization. Meat Science 92:252–259.

Kim J, Kundu M, Viollet B, Guan KL (2011). AMPK and mTOR regulate autophagy through direct phosphorylation of Ulk1. Nature Cell Biology 13(2):132–141.

Kim JW, Tchernyshyov I, Semenza GL, Dang CV (2006). HIF-1-mediated expression of pyruvate dehydrogenase kinase: A metabolic switch required for cellular adaptation to hypoxia. Cell Metabolism 3(3):177–185.

Koohmaraie M, Geesink GH (2006). Contribution of postmortem muscle biochemistry to the delivery of consistent meat quality with particular focus on the calpain system. Meat Science 74:34-43.

Kraft C, Martens S (2012). Mechanism and regulation of autophagosome formation. Current Opinion in Cell Biology 24(4):496-501.

Laemmli UK (1970). Cleavage of structural proteins during the assembly of the head of bacteriophage T4. Nature 227:680–685.

Lepetit J, Culioli J (1992). Mechanical Properties of Meat. Meat Science 36:203‑237.

Marchi S, Giorgi C, Suski JM, Agnoletto C, Bononi A, Bonora M et al (2012). Mitochondria-ros crosstalk in the control of cell death and aging. Journal of Signal Transduction 2012:17. Article ID 329635.

Marino G, Niso-Santano M, Baehrecke EH, Kroemer G (2014). Self-consumption: the interplay of autophagy and apoptosis. Nature Reviews Molecular Cell Biology 15:81:94.

Marsh BB, Leet NG (1966). Studies in meat tenderness. III. The effects of cold shortening on tenderness. *Journal of Food Science* 31:450-459.

Murphy MP (2009). How mitochondria produce reactive oxygen species. Biochemical Journal 417(1):1-13.

Ouali A, Herrera-Mendez CH, Coulis G, Becila S, Boudjellal A, Aubry L, Sentandreu MA (2006). Revisiting the conversion of muscle into meat and the underlying mechanisms. Meat Science 74(1):44–58.

Peachey BM, Purchas RW, Duizer LM (2002). Relationships between sensory and objective measures of meat tenderness of beef m. longissimus thoracis from bulls and steers. Meat Science 60(3):211–218.

Petracci M, Betti M, Bianchi M, Cavani C (2004). Color variation and characterization of broiler breast meat during processing in Italy. Poultry Science 83(12):2086–2092.

Piedmontese – origins of breed. Breeds of livestock. (2014). Oklahoma State University. Available from: http://www.ansi.okstate.edu/breeds/breeds/cattle/piedmontese/index.htm.

Rasola A, Bernardi P (2011). Mitochondrial permeability transition in Ca^{2+}-dependent apoptosis and necrosis. Cell Calcium 50(3):222-233.

Repnik U, Stoka V, Turk V, Turk B (2012). Lysosomes and lysosomal cathepsins in cell death. Biochimica and Biophysica Acta 1824(1):22-33.

Rolfe DFS, Hulbert AJ, Brand MD (1994). Characteristics of mitochondrial proton leak and control of oxidative phosphorylation in the major oxygen-consuming tissues of the rat. Biochimica et Biophysica Acta 1188:405–416.

Rowe LJ, Maddock KR, Lonergan SM, Huff-Lonergan E (2004). Influence of early postmortem protein oxidation on beef quality. Journal of Animal Science 82(3):785–793.

Scopes RK (1974). Studies with a reconstituted muscle glycolytic system: The rate and extent of glycolysis in stimulated post-mortem conditions. Biochemical Journal 142:79–86.

Shen QW, Means WJ, Underwood KR, Thompson SA, Zhu MJ, McCormick RJ et al. (2006). Early post-mortem AMP-activated protein kinase (AMPK) activation leads to phosphofructokinase-2 and -1 (PFK-2 and PFK-1) phosphorylation and the development of pale, soft, and exudative (PSE) conditions in porcine longissimus muscle. Journal of Agricultural and Food Chemistry 54(15):5583–5589.

Shevchenko A, Wilm M, Vorm O, Mann M (1996). Mass spectrometric sequencing of proteins from silver-stained polyacrylamide gels. Analytical Chemistry 68:850–858.

Sierra V, Oliván M (2013). Role of mitochondria on muscle cell death and meat tenderization. Recent Patents on Endocrinology and Metabolic Immune Drug Discovery 7(2):120–129.

Solaini G, Baracca A, Lenaz G, Sgarbi G (2010). Hypoxia and mitochondrial oxidative metabolism. Biochimica et Biophysica Acta-Bioenergetics 1797(6–7):1171–1177.

Strandine EJ, Koonz CH, Ramsbottom JM (1949). A study of variations in muscles of beef and chicken. Journal of Animal Science 8:483-494.

Van Laack RLJM, Kauffman RG, Greaser ML (2001). Determinants of ultimate pH of meat. In Proceedings of 4th International Congress of Meat Science and Technology (pp. 22–26). Poland: Warsaw.

Warriss PD (2000). Meat science: An introductory text. CAB-International: Wallingford.

Wheeler TL, Shackelford SD, Casas E, Cundiff LV, Koohmaraie M (2001). The effects of Piedmontese inheritance and myostatin genotype on the palatability of longissimus thoracis,

gluteus medius, semimembranosus, and biceps femoris. Journal of Animal Science 79(12):3069–3074.

Yam KL, Papadakis SE (2004). A simple digital imaging methods for measuring and analyzing color of food surfaces. Journal of Food Engineering 61:137‑142.

PART 3

MEAT AGING: THE OMIC INVESTIGATION SUGGESTS THE APOPTOTIC BEHAVIOR OF MEAT CELLS

3.1 INTRODUCTION

Considering the impaired mitochondrial respiration and the concomitant increase in ROS concentrations, the question about the duality apoptosis/ autophagy in the process of muscle to meat conversion finds its 'raison d'etre': do the postmortem muscle cells counteract the oxidative stress activating autophagy, in an attempt to rescue the damaged structures, or do they directly fall into one of the programmed cell death forms? This survey is further complicated by many other factors influencing the development of muscle into meat, such as pH, calcium concentration, sarcomere length and collagen content (D'Alessandro & Zolla, 2013), age, gender, genotype, breed, nutritional status and levels of pre-slaughter stress (due to transportation and slaughter itself (Gregory, 2008; Van de Perre et al., 2010). The complex network originating from these aspects makes it difficult to build up a univocal and unambiguous underlying mechanism valid for any case of muscle to meat conversion. In the previous part of the thesis I have analyzed the Piedmontese meat from an omic standpoint, making use of metabolomics and 1D gel electrophoresis. With the present study, I have deepened the study of prolonged aged meat peculiarities from the omic point of view, using the 2D electrophoresis techniques coupled with mass spectrometry spot identification, supported by metabolomic and phosphoproteomic analyses along a 0-44 days time course experiment on Piedmontese longissimus thoracis muscle. The aim was the search for suggestive clues about the apoptotic or the autophagic behavior of meat cells.

3.2 MATERIALS AND METHODS

Ten Piedmontese cull cows between 4 and 13 years old were raised in farms belonging to Consorzio La Granda (CN, Italy), located in Piedmont, then transported in about 20 min to a near slaughterhouse. The carcasses of the slaughtered animals were stored in a chilling room

at 4 °C, then transported to a meat processing plant on post-slaughter day 1. Longissimus thoracis muscles were removed and stored in a cooler at 1 °C (steady or dynamic), with a relative humidity of 78%. A section of 10 cm was removed from all of the individual longissimus thoracis samples at days 0, 1, 10, 17 and 44 post-slaughter and used for all subsequent analyses. Liquid nitrogen was used to refrigerate each sample and to permit a fine grinding by means of mortar and pestle previously cleaned with acetone.

- *3.2.1. Proteomics*

- *3.2.1a Sample preparation*. Frozen samples of longissimus thoracis from 10 Piedmontese cows (approximately 5 mg per sample) were crushed in a mortar containing liquid nitrogen. After grinding, the samples were incubated at 4 °C for 60 min in an extraction buffer containing 7 M urea, 2 M thiourea, 2% (w/v) CHAPS, 40 mM Tris, 0.1 mM EDTA (pH 8.5), 2% (v/v) protease inhibitor cocktail (Sigma-Aldrich, Basle, Switzerland), 2 mM PMSF and 1 mM DTT. Samples were centrifuged at 17,000 g for 20 min at 4 °C and the supernatants were collected (Talamo et al., 2003). The protein concentration of each group was determined using 2D Quant-kit (GE Healthcare Life Sciences, UK) according to the manufacturer's instructions.

- *3.2.1b 2D-PAGE*. 2DE analyses on muscle samples were performed as previously reported (Talamo et al., 2003). 600 μg of proteins were precipitated from a desired volume of each sample with a cold mix of tri-n-butyl phosphate/acetone/methanol (1:12:1). This solution is able to remove the lipid component. Before focusing, the proteins were reduced with 5 mM tributylphosphine (TBP) and alkylated with 7.7 mM iodoacetamide in a solution of 7 M urea, 2 M thiourea, 4% CHAPS, 40 mM Tris and 0.1 mM EDTA (pH 8.5). To prevent overalkylation, iodoacetamide excess was destroyed by adding equimolar amount of dithioerythritol (DTE). Seventeen centimeters IPG strips (Bio-Rad, CA, USA) pH 3–10 were

rehydrated overnight with 330 µL of rehydratation solution containing 7 M urea, 2 M thiourea, 4% (w/v) CHAPS and 0.5% (w/v) pH 3–10 carrier ampholyte (Bio-lyte; Bio-Rad, CA, USA) and 100 µL of sample were loaded using the cup-loading method. The total product time per voltage applied was 80,000 V for each strip at 20 °C. After IEF, the IPG gel strips were incubated at room temperature for 30 min in 6 M urea, 30% w/v glycerol, 2% w/v SDS, 5 mM Tris–HCl and pH 8.8. The strips were sealed at the top of a 1.5 mm vertical second dimensional gel with 0.5% agarose in 25 mM Tris, 192 mM glycine, 0.1% SDS and pH 8.3. SDS-PAGE was carried out on homogeneous running gels 12% T and 2.6% C. Running conditions were 40 mA/gel until the bromophenol blue reached the bottom of the gel. Protein spots were stained by sensitive Coomassie brilliant blue G-250 stain. Three technical replicates per sample were performed.

- *3.2.1c Image analysis*. 150 stained gels (10 biological replicates × 5 storage points × 3 technical replicates) were digitalized using an ImageScanner and LabScan software 3.01 (Bio-Rad Hercules, CA). The 2-DE image analysis was carried out and spots were detected and quantified using the Progenesis SameSpots software version 2.0 (Nonlinear Dynamics, New Castle, UK). For each protein spot, the average spot quantity value and its variance coefficient in each group were determined. One-way analysis of variance (ANOVA) was carried out at $p < 0.05$ to assess for relative protein changes among day 0 and the other time points. The statistically significant spots with fold ≥ 1.5 were cut and subjected to in-gel trypsin digestion (Shevchenko et al., 1996).

- *3.2.1d LC–ESI–CID–MS/MS*. Samples were analyzed using a split-free nano-flow liquid chromatography system (EASY-nLC II, Proxeon, Odense, Denmark) coupled to a 3D-ion trap (model AmaZon ETD, Bruker Daltonik, Germany) equipped with an online ESI nano-sprayer (the spray capillary was a fused silica capillary, 0.090 mm O.D., 0.020 mm I.D.). For all experiments a sample volume of 15 µL was loaded by the autosampler onto a homemade 2

cm fused silica precolumn (100 μm I.D.; 375 μm O.D.; Reprosil C18-AQ, 5 μm, Dr. Maisch GmbH, Ammerbuch-Entringen, Germany). Sequential elution of peptides was accomplished using a flow rate of 300 nL/min and a linear gradient from Solution A (2% acetonitrile; 0.1% formic acid) to 50% of Solution B (98% acetonitrile; 0.1% formic acid) in 40 min over the precolumn on-line with a homemade 15 cm resolving column (75 μm I.D.; 375 μm O.D.; Reprosil C18-AQ, 3 μm, Dr. Maisch GmbH, Ammerbuch-Entringen, Germany). The acquisition parameters for the mass spectrometer were as follows: dry gas temperature, 220 °C; dry gas, 4.0 L/min; nebulizer gas, 10 psi; electrospray voltage, 4000 V; high-voltage end-plate offset, −200 V; capillary exit, 140 V; trap drive: 63.2; funnel 1 in. 100 V out of 35 V and funnel 2 in. 12 V out of 10 V; ICC target, 200,000 and maximum accumulation time, 50 ms. The sample was measured with the Enhanced Resolution Mode at 8100 m/z per second (which allows monoisotopic resolution up to four charge stages), positive polarity, scan range from m/z 300 to 1500, 5 spectra averaged, and rolling average of 1. The "Smart Decomposition" was set to "auto". Acquired CID spectra were processed in DataAnalysis 4.0, and deconvoluted spectra were further analyzed with BioTools 3.2 software and submitted to Mascot search program (in-house version 2.2, Matrix Science, London, UK). The following parameters were adopted for database searches: NCBInr database (release date 22/09/2012; 20,543,454 sequences; 7,050,788,919 residues); taxonomy = all entries; peptide and fragment mass tolerance of ±0.3Da; enzyme specificity trypsin with 2 missed cleavages considered; fixed modifications: carbamidomethyl (C) and variable modifications: oxidation (M).

- *3.2.2 Immunoblotting*. 20 μg of proteins was dissolved in sample buffer composed by 12% (w/v) sucrose, 4 M urea, 50 mM Tris–HCl, 4% (w/v) SDS, 200 mM DTT and 0.01% (w/v) bromophenol blue and loaded on a 12% acrylamide gel. Gel run at 100–120 V for 2 h. 1D gels were transferred to nitrocellulose filters for immunoblot analysis and probed with anti-phosphoserine/ threonine antibody (1:1500) (612548, BD Transduction Laboratories). Goat

anti-mouse secondary antibody (IgG1-HRP, sc-2060) was from Santa Cruz Biotechnology (CA, USA). ECL-Plus (GE Healthcare, UK) was used as revealing system. The bands recognized by antibody were cut, trypsin digested (Shevchenko et al., 1996) and identified by nano-HPLC–MS/MS.

- *3.2.2a TiO2 enrichment and ETD / neutral loss analysis*. Purification of phosphopeptides was then performed according to Thingholm et al. (2006). The TiO2-enriched samples were analyzed using a split-free nano-flow liquid chromatography (LC) system (EASY-nLC II, Thermo Fisher Scientific) coupled to a 3D-ion trap (model AmaZon ETD, Bruker Daltonics) equipped with an online ESI nano-sprayer (the spray capillary was a fused silica capillary, 90 μm O.D., 20 μm I.D.) working in positive ion mode. To identify phosphorylation sites, two types of peptide fragmentation were carried out in parallel in the mass spectrometer: (i) collision induced dissociation (CID) and (ii) electron transfer dissociation (ETD). When CID was used a MS^2 was automatically performed on the three most intense MS ions, and MS^3 was triggered if one of the top three MS^2 peaks corresponded with neutral loss (NL) of 98.0, 49.0 and 32.7 m/z. A detailed description of the used LC–MS/MS conditions has been previously given (D'Alessandro et al., 2012). Results are summarized in Table 3.

- *3.2.3 Metabolomics*. Metabolomic analysis has been carried on as previously reported, with minor modifications (D'Alessandro et al., 2012). Metabolites were extracted from 50 mg of each sample, by means of 500 μL solution of 50:30:20 of ice-cold methanol:acetonitrile:bidistilled water; samples were vortexed in a thermomixer for 30 min at 4 °C, then centrifuged at 13,500 g for 15 min at 4 °C. The supernatants, containing the extracted metabolites, were used for the analysis, while the bottom residues discarded. Samples were thus loaded onto a rapid resolution HPLC system (LC Packings, DIONEX, Sunnyvale, USA) as to perform chromatographic separation of hydrophilic metabolites. The system featured a binary pump and vacuum degasser, well-plate autosampler with a six-port

micro-switching valve and a thermostated column compartment. A Phenomenex Luna 3 μm HILIC 200A (150 × 2.0 mm), protected by a guard column HILIC 4 × 2.0 mm ID (Phenomenex) was used to perform metabolite separation over a phase B (100% acetonitrile + 10 mM ammonium acetate) to phase A (double distilled 18 mΩ water, +10 mM ammonium acetate) gradient lasting 35 min. In details, we set the following LC parameters: injection volume, 20 μL; column temperature, 25 °C; and flow rate of 0.3 mL/min. The multistep gradient was set as follows: 0–5 min 100% B; 5–15 min, from 100% B to 70% B; 15–20 min, from 70% B to 50% B; 20– 25 min, from 50% B to 0% B; 25–30 min, isocratic at 0% B; 30–30.1 min, return to the initial conditions 100% B; and 30.1–35 min, isocratic column equilibration at 100% B. The eluate from the HPLC system was linked online with a Micro Q-Tof Bruker Daltonics mass spectrometer equipped with an ESI ion source. Instrument calibration was performed externally everyday with a sodium formate solution consisting of 10 mM sodium hydroxide in 50% isopropanol:water and 0.1% formic acid. External mass scale calibration was performed twice a day through direct automated injection of the calibration solution by a 6-port divert-valve. Mass spectrometer runs were exported into mzXML files and analyzed through the software MAVEN (Clasquin et al., 2012) for correct metabolite assignment, on the basis of absolute intact mass (within a 10 ppm window) against the KEGG database (Kanehisa & Goto, 2000), and expected retention times on the basis of metabolite chemical properties. The outcoming time course trends for each metabolite of interest result from the analysis of 30 replicates (3 technical for each of the 10 biological).

3.3 RESULTS AND DISCUSSION.

The proteomic analysis is based on classical 2D gel electrophoresis, able to separate proteins by their isoelectric point and molecular weight (Figure 19). In this second part of my work I

used 2D technique, that owns a better resolving power over the 1D technique as to deepen the study of proteome variations; I carried out quantitative comparisons between the 0-day proteome and the proteomes extracted from the other time course points (1, 10, 17 and 44); the results are summarized in Table 8, in which I have reported the spots appeared to be differential at least in one of the four time point comparisons (with a fold change > 1.5). The differential spots were identified as the known protein by MASCOT database searching; the validation of the identifications was carried out taking into account the number of peptide matching against the candidate protein and the coverage of its amino acidic sequence by these peptides. There are 44 differential spots, but there is not a correspondence with the factual number of differential proteins, which are a total of 26. Indeed, some identified proteins are redundant and are repeated at least in two different spots.

- *3.3.1 Proteolysis.* The proteome changes during the muscle-to-meat conversion process are radical; many studies have been finalized to shed light on these variations (Koohmaraie, 1994; Luciano et al., 2007; Paredi et al., 2012; Murgiano et al., 2010; D'Alessandro et al., 2011), and many others demonstrated the process of muscle proteolysis as the hub of muscle evolution into meat (Ashgar & Yeates, 1978; Huff-Lonergan et al., 2010; Kemp & Parr, 2012); the 2D results are in agreement with previous findings, as stated by variations in differential spots containing structural proteins: spots 458, 459, 466 and 471 are identified as troponin T. The time course trend indicates that an important downregulation of troponin T of Piedmontese longissimus thoracis muscle begins to appear from day 17 onward, to reach its top at day 44 (4.3 fold change for spot 458; 7.2 fold change for spot 459, Table 8); this experimental result rewards the 44 days-aged meat, because, as it has been previously reported (Paredi et al., 2012; Muroya et al., 2007), degradation of troponin T is known to be a descriptive indicator of meat tenderization process. Another component of muscular architecture, actin, clearly describes the ongoing proteolysis during the aging period; later in

FIGURE 19. Examples of 2D-gels of protein extracts from the Piedmontese longissimus thoracis samples analyzed in a time-course experiment (0, 1, 10, 17, 44 days)

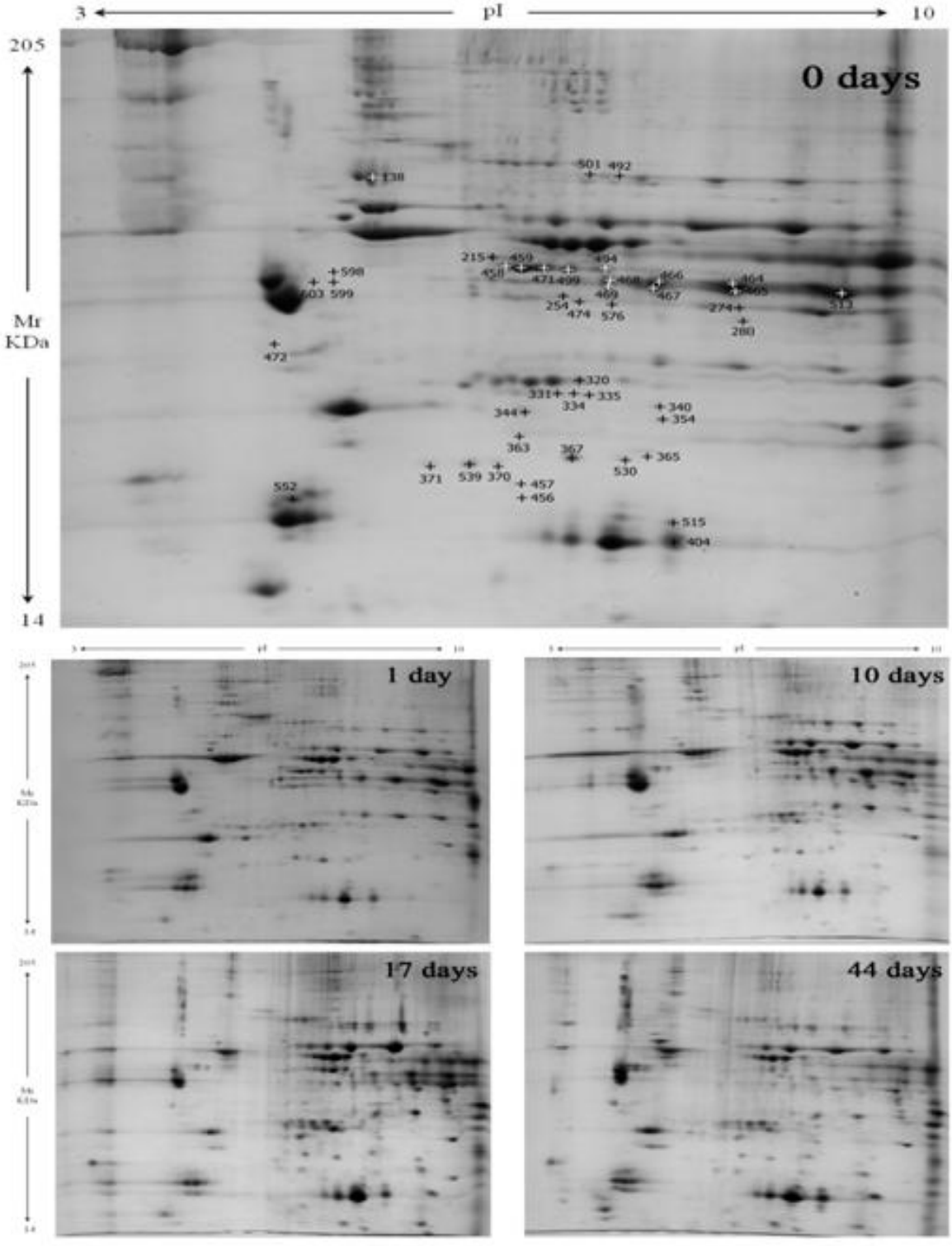

my discussion I will recall the upward trend of a particular actin fragment (31 kDa) linked with apoptosis.

The progressive disruption of muscle architecture is also stated by the time course trend of myosin light chain 2, one of the constituent subunits of myosin: looking at spot 552, we can unequivocally deduce the presence of this protein, due to the similarity of the MW of the spot (about 21 kDa) with the expected MW for myosin light chain 2 (19 kDa); the 1.6 down fold-change appears at day 17. Table 8 shows the presence of myosin light chain 2 also in spots 598, 599 and 603, that could seem quite puzzling referring to the observed MW (about 45 kDa), much higher than the expected (19 kDa); this fact can only be explained by the formation of proteic aggregates due to the presence of ROS, as previously demonstrated in thylakoid membranes (Rinalducci et al., 2005).

Another hint to the proteolytic alterations suffered by muscle cells comes from the downward trend of beta-actin-like protein 2 (MW 66 kDa) (spot 138; table 8, figure 19), a known ubiquitary component of the cytoskeleton and a mediator of internal cell mobility. Finally, the last observation is about the upward trend of spot 457, identified as titin, but representing a fragmented species (as we can deduce reminding the MW of the entire protein, nearly 4 MDa); its increase, reaching the top at 44 days, certifies once more the ongoing proteolysis.

- *3.3.2 Energetic evolution*. Paying attention to the muscle metabolic behavior, we can note from Table 8 that 2D gel comparisons show once again the progressive dysregulation of the principal 'reloading' mechanism of muscle fibers, as stated by the downward trend of creatine kinase M-type (observed MW coincident to the expected, 43 kDa, in spots 494 and 499) and by the upward trend of spots 334 and 335, identified as creatine kinase M-type, but containing only its fragmented species (about 29 kDa). As I have explained, this is one key enzyme in the correct functioning of the so-called creatine–phosphocreatine shuttle: it reconverts

Table 8 – Differential proteins as gleaned from 2DE analyses of *Longissimus thoracis* muscles at post mortem days 0, 1, 10, 17 and 44

no. spot	*MW, Da*	*pI*	*no of peptides identified*	*Mascot score*	*NCBI accession no.*	*Protein ID (Bos Taurus)*	*0 day vs 1 day*	*0 day vs 10 days*	*0 day vs 17 days*	*0 day vs 44 days*
138	42187	5.30	56	483	gi|194676388	actin, beta-like 2 isoform X1	=	2.5 Down	2.1 Down	2.1 Down
215	20301	6.38	8	109	gi|296491201	Glyceraldehyde 3 phosphate dehydrogenase-like	=	=	2.4 Down	2.4 Down
254	38236	6.42	4	83	gi|78365297	glycerol-3-phosphate dehydrogenase [NAD(+)], cytoplasmic	=	=	=	1.9 Down
274	36916	8.12	68	954	gi|27806559	L-lactate dehydrogenase A chain	=	1.5 Up	1.6 Up	1.5 Down
280	35903	8.17	17	367	gi|217590	lactate dehydrogenase-A	=	=	=	1.8 Down
367	20024	6.76	52	595	gi|27805849	alpha-crystallin B chain	=	=	=	1.5 Down
370	17515	5.95	9	124	gi|115496724	heat shock protein beta-6	=	1.7 Down	1.5 Down	2.1 Down
371	17515	5.95	6	86	gi|115496724	heat shock protein beta-6	1.8 Down	1.7 Down	1.8 Down	1.9 Down
458	29800	7.74	60	679	gi|47824864	troponin T, fast skeletal muscle	=	=	2.4 Down	4.3 Down
459	29800	7.74	124	943	gi|47824864	troponin T, fast skeletal muscle	=	=	2.3 Down	7.2 Down
464	39925	8.45	9	256	gi|156120479	fructose-bisphosphate aldolase A	=	=	=	2.2 Down
465	36073	8.50	109	806	gi|77404273	glyceraldehyde-3-phosphate dehydrogenase	=	=	=	2.1 Down
466	29800	7.74	43	585	gi|47824864	troponin T, fast skeletal muscle	=	=	=	1.7 Down
467	36073	8.50	102	768	gi|77404273	glyceraldehyde-3-phosphate dehydrogenase	=	=	=	2.0 Down
468	36073	8.50	67	665	gi|77404273	glyceraldehyde-3-phosphate dehydrogenase	=	=	=	2.6 Down
469	36073	8.50	79	698	gi|77404273	glyceraldehyde-3-phosphate dehydrogenase	=	=	1.5 Down	2.3 Down
471	29800	7.74	90	747	gi|47824864	troponin T, fast skeletal muscle	=	=	=	3.5 Down
472	42451	5.31	3	52	gi|27819614	actin, alpha skeletal muscle	=	=	2.6 Up	3.6 Up
474	38873	6.92	5	111	gi|27807289	Annexin A2	=	1.5 Up	1.5 Up	=
494	43190	6.63	45	812	gi|60097925	creatine kinase M-type	=	=	1.5 Down	2.3 Down
499	43190	6.63	38	837	gi|60097925	creatine kinase M-type	=	=	=	2.0 Down
513	36073	8.50	128	796	gi|77404273	glyceraldehyde-3-phosphate dehydrogenase	=	=	=	1.5 Down
530	20024	6.76	21	330	gi|27805849	alpha-crystallin B chain	=	=	1.8 Down	=
539	17525	5.95	42	237	gi|119224088	Heat shock protein, alpha-crystallin-related, B6	=	=	2.2 Down	2.0 Down
552	19114	4.91	24	432	gi|115497166	myosin regulatory light chain 2, skeletal muscle isoform	=	=	1.6 Down	=
576	35903	8.17	53	875	gi|217590	lactate dehydrogenase-A	=	=	=	1.5 Down
320	26901	6.45	62	1104	gi|61888856	triosephosphate isomerase	=	=	1.5 Up	=
331	26901	6.45	94	1157	gi|61888856	triosephosphate isomerase	=	=	1.8 Up	1.5 Up
334	43190	6.63	100	861	gi|60097925	creatine kinase M-type	=	2.3 Up	3.7 Up	3.1 Up
335	43190	6.63	75	719	gi|60097925	creatine kinase M-type	=	1.8 Up	3.4 Up	2.1 Up

340	23826	6.89	29	555	gi|29135329	glutathione S-transferase P	=	=	1.7 Up	2.0 Up
344	20194	6.84	42	718	gi|62751849	protein DJ-1	=	1.5 Up	1.9 Up	2.1 Up
354	27525	7.59	64	797	gi|528969811	adenylate kinase isoenzyme 1 isoform X1	=	=	=	1.5 Up
363	20024	6.76	45	466	gi|27805849	alpha-crystallin B chain	2.7 Up	3,2 Up	3.0 Up	2.2 Up
365	21106	7.72	24	484	gi|75812940	Phosphatidylethanolamine binding protein 1	=	=	1.6 Up	1.7 Up
404	17067	6.90	81	745	gi|27806939	myoglobin	=	=	1.5 Down	=
456	20024	6.76	36	324	gi|27805849	alpha-crystallin B chain	=	=	1.5 Up	1.9 Up
457	3741526	6.07	11	200	gi|296490722	titin	=	1.7 Up	2.5 Up	3.3 Up
492	58536	7.62	35	680	gi|528961976	pyruvate kinase isozymes M1/M2 isoform X3	=	1.6 Up	1.5 Up	1.9 Up
501	65490	7.98	66	1042	gi|528961972	pyruvate kinase isozymes M1/M2 isoform X1	=	1.8 Up	1.8 Up	2.2 Up
598	19114	4.91	74	801	gi|115497166	myosin regulatory light chain 2, skeletal muscle isoform	1.8 Up	=	2.2 Up	2.6 Up
599	19114	4.91	34	486	gi|28372499	myosin regulatory light chain 2, skeletal muscle isoform	=	2.0 Up	=	3.6 Up
603	19114	4.91	80	816	gi|115497166	myosin regulatory light chain 2, skeletal muscle isoform	=	=	1.8 Down	2.1 Up

myofibrillar ATP from ADP thanks to the inorganic phosphate group provided by the high-energy compound phosphocreatine, which is synthesized by mitochondrial creatine kinase from creatine and the ATP coming from oxidative phosphorylation (Bessman, 1987); the sudden O_2 shortages impair ATP production by electron transport chain, so the lack of great quantities of ATP induces phosphocreatine shuttle impairment, as stated by the decreasing levels of creatine kinase M and by the metabolomic relative quantification of the phosphocreatine levels (progressively decreasing); as I explained, phosphocreatine quantities depend on the availability of ATP, and the metabolomic results for ATP are in agreement with phosphocreatine and creatine kinase M trends (figure 20); this result from the analysis of the second set of Piedmontese bovines resembles and confirms the first one (figure 10). The muscles try to counteract the progressive depletion of energetic molecules relying on glycolysis; in physiological conditions, with abundance of O_2, its endproduct is pyruvate, oxidized through the Krebs cycle; nevertheless, the absence of O_2 hampers the electron transfer from NADH and $FADH_2$ to obtain NAD^+ and FAD useful to the Krebs reactions. So,

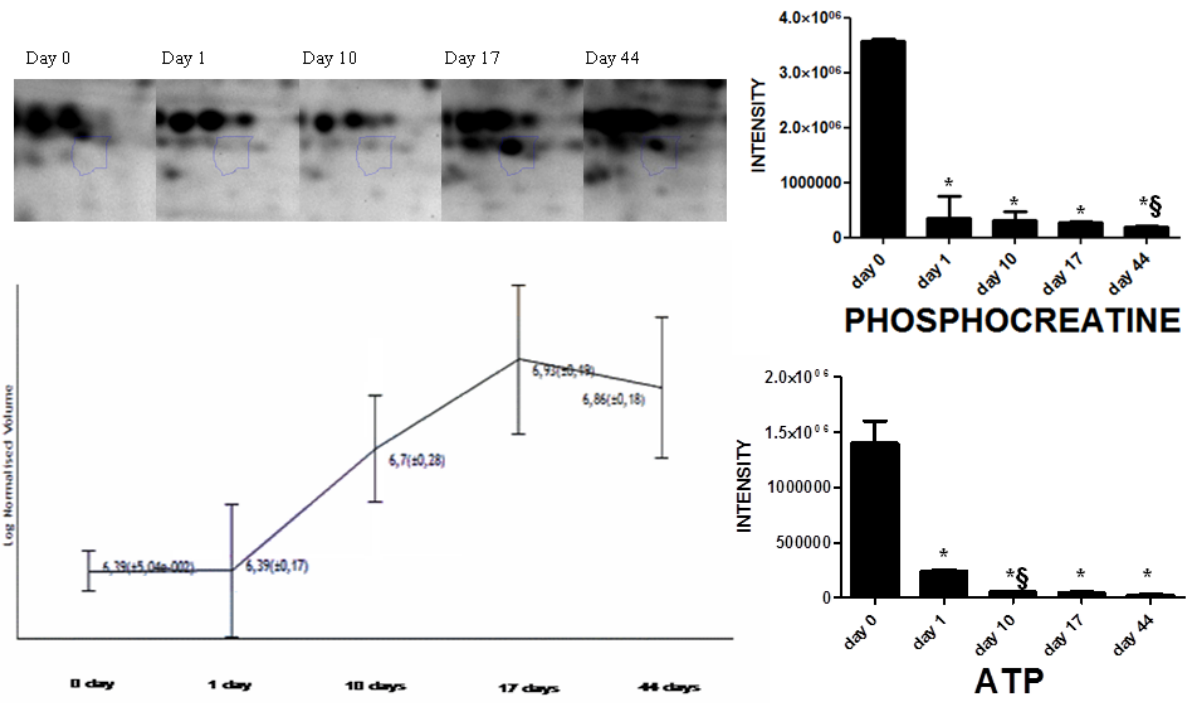

FIGURE 20 – Cr/pCr shuttle impairment for the second set of Piedmontese bovines. Spot 334 on gels and its graphical trend (creatine kinase fragment), with the intensity values (mean±SD) reported for each time point. Metabolomic results for creatine kinase shuttle (considering ATP and phosphocreatine)
*indicates a statistically significant difference ($p < 0.05$) existing between the relative quantification at day N and day 0.
§ indicates a statistically significant difference ($p < 0.05$) existing between the relative quantification at day N and the previous time point.

the slaughtered muscle makes use of the lactic fermentation to exhaust the accumulating pyruvate, reducing it thanks to NADH electrons. The result is a progressive increase in lactate, with a steady state reached between days 17 and 44 (figure 21); the concomitant upregulation of lactate dehydrogenase A chain between days 10 and 17 (spot 274) is explainable as to cope with increasing levels of pyruvate to be reduced to lactate; the following fall at 44 days is in agreement with lactate steady state (figure 21, figure 8, Table 8). In the context of glycolysis, we can note the upregulation of two isoforms of pyruvate kinase from day 10 onward (table 8): this enzyme catalyzes one of the ATP-producing glycolytic reactions, and we can hypothesize that the upregulation

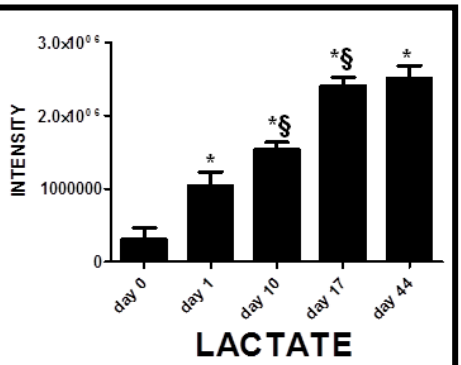

FIGURE 21 – Relative quantification of lactate in the second set of Piedmontese bovines.
*indicates a statistically significant difference ($p < 0.05$) existing between the relative quantification at day N and day 0.
§ indicates a statistically significant difference ($p < 0.05$) existing between the relative quantification at day N and the previous time point.

indicates the cellular attempt to maintain an adequate level of ATP; however, these data are in contrast with the downward trend at 44 days of two other glycolytic enzymes, fructose biphosphate aldolase A and glyceraldehyde phosphate dehydrogenase (table 8), as to indicate the likely consumption of glycolytic intermediates. The 2D time course study of muscle to meat conversion confirms the importance of glycolysis as the central mechanism producing ATP that has been inferred from the first data set (see the 'part II'); nevertheless, as showed in figure 20, its level drops soon in the first day after slaughter, concurrently with the establishment of rigor mortis.

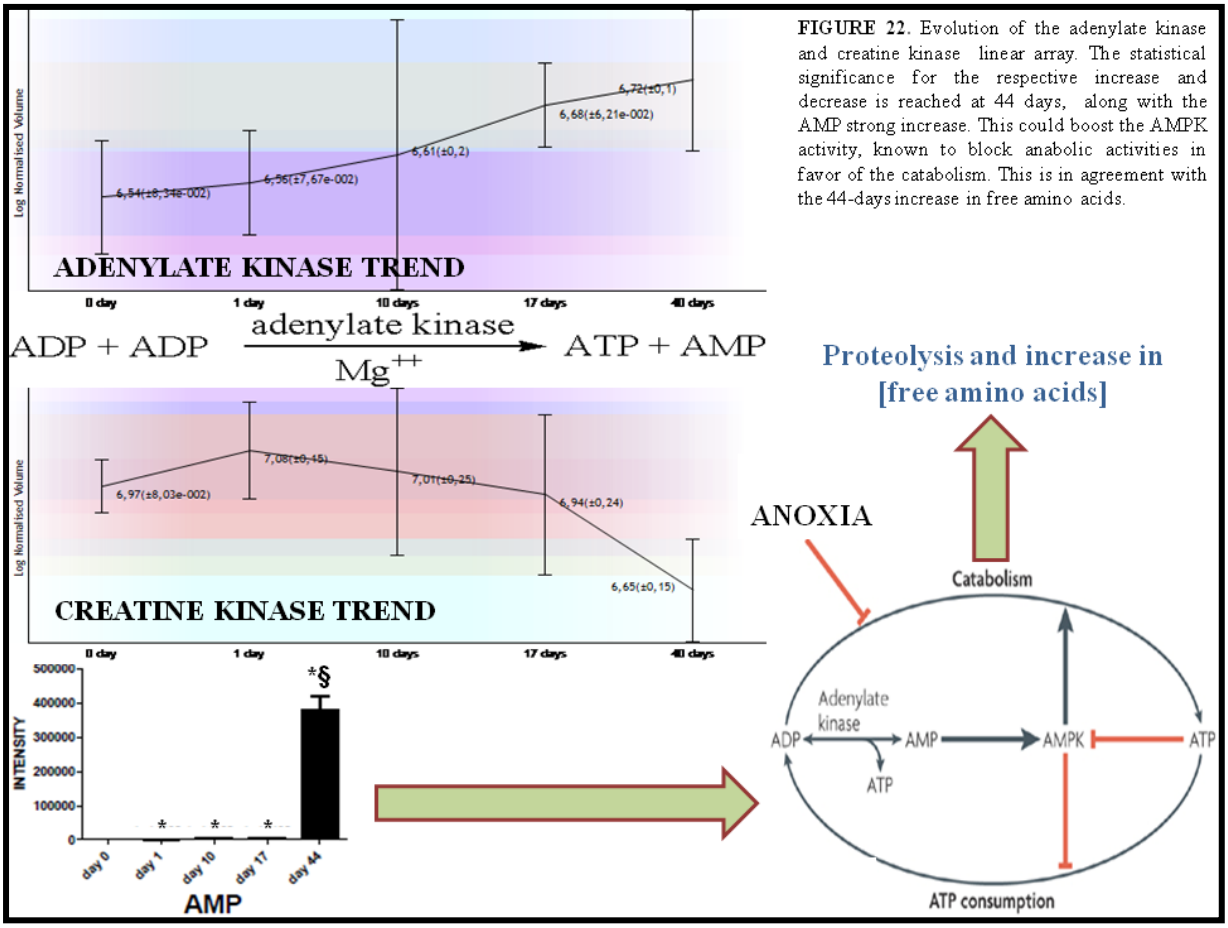

FIGURE 22. Evolution of the adenylate kinase and creatine kinase linear array. The statistical significance for the respective increase and decrease is reached at 44 days, along with the AMP strong increase. This could boost the AMPK activity, known to block anabolic activities in favor of the catabolism. This is in agreement with the 44-days increase in free amino acids.

Another feature delineated by gel analysis is the time course trend of adenylate kinase, which is upregulated at 44 days. This is a key enzyme in muscle energetic homeostasis, and it is known to be spatially organized in linear arrays along with creatine kinase (Wegmann et al., 1992), suggesting an interaction and a sort of mutual 'communication' about the muscular

energetic state, particularly regarding adenine nucleotide flux (Dzeja & Terzic, 2003). The safeguard of cellular energy economy needs the promotion of high-energy phosphoryl transfer through the adenylate kinase system when there is a reduction of creatine kinase activity, especially under hypoxic stress (Janssen et al., 2000). From our results, it seems that adenylate kinase undergoes an upregulation at 44 days, with the simultaneous drop in the levels of creatine kinase; this evidence could be seen as an attempt to obtain ulterior ATP when ATP tokens are exhausted and the ADP/ATP ratio is high. Indeed, adenylate kinase is able to convert two ADP molecules into one AMP and one ATP; the hypothesis is confirmed by the AMP trend, showing a sudden rise at 44 days (figure 22). This could boost the AMP-activated Kinase (AMPK), which is known to inhibit the anabolic pathways in favor of catabolism; the results about the amino acidic accumulation at 44 days efforts this theory.

As to photograph the oxidative state of this second set of Piedmontese meat samples, I have monitored the levels of glutathione and glutathione disulfide (figure 23). The GSH/GSSG ratio is progressively decreasing, confirming the previous results (figure 11) and the overcoming of the oxidative stress on cellular defensive responses; in the 'Part II' of my thesis, I demonstrated the importance of the upregulation of pentose phosphate pathway as to cope with the oxidative stress (by means of the increase in NADPH production, able to restore GSH from GSSG), which is not further sustainable after day 17 (figure 12). The trends of GSH and GSSG resemble those of the first set, with the evident difference for the GSSG levels at day 0 (compare figure 11

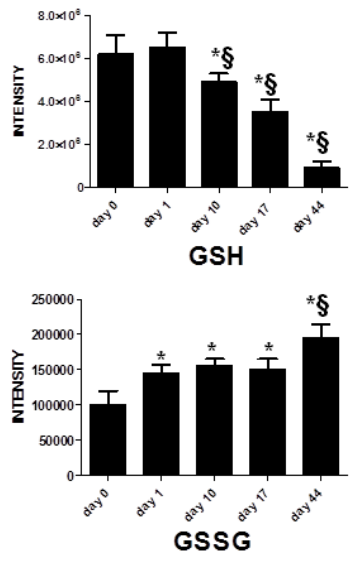

FIGURE 23 – Relative quantification of GSH and GSSG in the second set of Piedmontese bovines.
*indicates a statistically significant difference ($p < 0.05$) existing between the relative quantification at day N and day 0.
§ indicates a statistically significant difference ($p < 0.05$) existing between the relative quantification at day N and the previous time point.

and 23): this is probably dependent on a superior preslaughter stress of the second set of Piedmontese bovines with respect to the first set.

Regarding the analysis of the phosphoproteome, Western results are shown in figure 24, and the corresponding identifications are listed in Table 9; Table 10 shows the phosphorylated peptides and respective phosphorylation sites of each protein as to confirm Western results. A global overview shows a strong degree of phosphorylations between 0 and 1 day after slaughter, indicating a sort of cellular response to the anoxic shock; from day 10 onward, phosphorylations seem to drastically decrease, and it is a logic result in the context of the exhaustion of ATP energetic tokens used as source of phosphate groups. Band C (figure 24) contains phosphorylated phosphoglucomutase (PGM) enzyme. It is one of the three enzymes (glycogen phosphorylase; debranching enzyme; PGM) whose sequential action leads to the release of a glucose- 6-phosphate monomer from glycogen. Literature reports the enhancing effect of phosphorylation on PGM activity (Gururaj et al., 2004), and the Western results follow the expectations: muscle cells subjected to the anoxic conditions become needy of the lacking ATP, no more produced by the oxidative phosphorylation, so they veer to an anaerobic ATP production by increasing the degree of glycolysis, exploiting glycogen reservoirs and extracting glucose-6-phosphate monomers for directing them to glycolytic consumption. Phosphorylation of phosphofructokinase muscle-type (PFK-M) (Table 9, figure 24) is interpretable towards the same direction; this enzyme undergoes a strong phosphorylation between 0 and 1 day, as to indirectly potentiate its task to add a phosphate group to fructose- 6-phosphate to obtain fructose-1,6-biphosphate, now fixed to glycolysis. PFK-M phosphorylation interferes with its regulation by allosteric modulators, such as lactate, able to inhibit its activity (Leite et al., 2007). Therefore, its phosphorylation can be seen as a preventive action against the possible inhibition coming from the increasing lactate concentration; obviously muscle cells lose this preventing ability when ATP concentration is

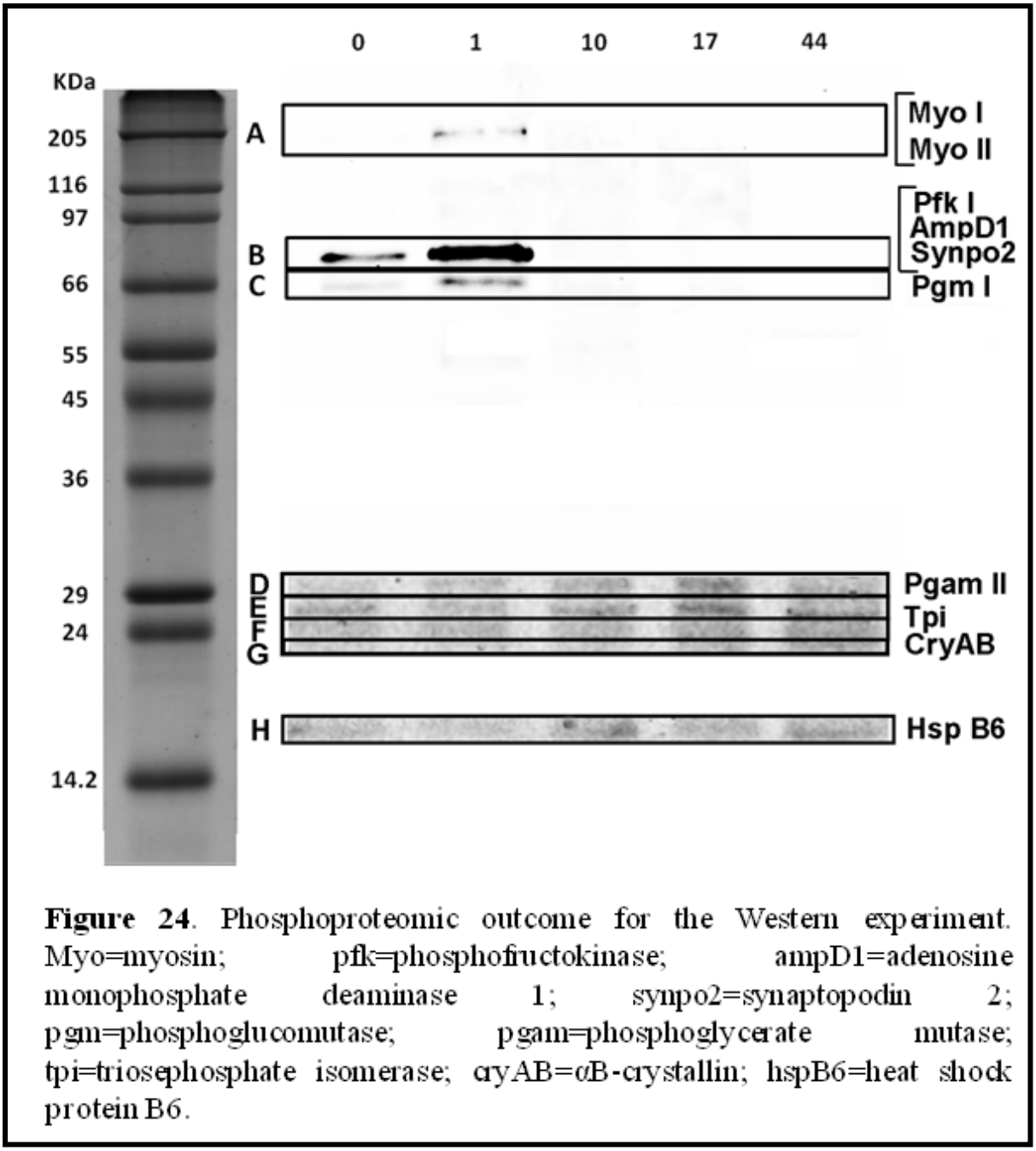

Figure 24. Phosphoproteomic outcome for the Western experiment. Myo=myosin; pfk=phosphofructokinase; ampD1=adenosine monophosphate deaminase 1; sympo2=synaptopodin 2; pgm=phosphoglucomutase; pgam=phosphoglycerate mutase; tpi=triosephosphate isomerase; cryAB=αB-crystallin; hspB6=heat shock protein B6.

strongly reduced, clearly from day 10 onward. AMP-deaminase undergoes a phosphorylative regulatory modification which boosts its enzymatic activity (Tovmasian et al., 1990) at days 0 and 1 (Figure 24). It falls into the context of skeletal muscle energetic maintenance: the ATP consumption increases ADP levels, paving the way to the action of adenylate kinase; the consequently increasing AMP, which would impair muscular energetic flux, is maintained to a low level thanks to the boosted action of AMP deaminase, which converts AMP into IMP and NH3 (as the metabolomic IMP screen confirms, fig 25). From day 10, concomitantly to

the dephosphorylation of AMP deaminase, IMP level begins to fall, to reach the minimum at day 44 (when AMP, indeed, rises exponentially); these time course trends demonstrate the progressive energetic impairment suffered by the skeletal muscle, which inevitably fails to

Spot name	MW (Da)	no of peptides identified	Mascot score	NCBI accession no.	Protein ID (Bos Taurus)
A	224106	228	5406	gi|261245063	myosin-2
	223764	221	5254	gi|41386691	myosin-1
B	86095	92	1891	gi|115497288	6-phosphofructokinase, muscle type
	87202	42	979	gi|154152079	AMP deaminase 1
	135765	31	481	gi|139948281	synaptopodin-2
C	61836	100	1533	gi|116004023	phosphoglucomutase-1
D	28838	8	164	gi|84000195	phosphoglycerate mutase 2
E	28838	27	337	gi|84000195	phosphoglycerate mutase 2
F	26901	7	262	gi|61888856	triosephosphate isomerase
G	20024	45	466	gi|27805849	alpha-crystallin B chain
H	17525	42	237	gi|119224088	Heat shock protein, alpha-crystallin-related, B6

Table 9. Identification of proteins evidenced as phosphorylated by the Western analysis.

maintain its homeostasis in the long term. All these data depict a picture of the battle fought by the muscle cells against the growing oxidative stress throughout the aging period. Obviously, cells have no possibilities to emerge victorious, and sooner or later they have to surrender and to pave the way to one of the programmed cell deaths; by means of 2D electrophoresis and mass spectrometry technologies, we have looked for peculiarities of the aging meat able to shed light on the duality autophagy/apoptosis. I investigated it on three different fields: the proteome, the metabolome and the phosphoproteome. I discuss the results in the next section.

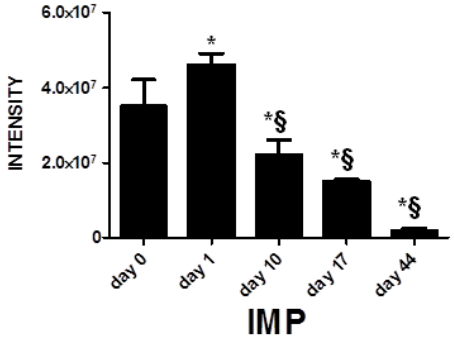

FIGURE 25 – Relative quantification of IMP.
*indicates a statistically significant difference ($p < 0.05$) existing between the relative quantification at day N and day 0.
§ indicates a statistically significant difference ($p < 0.05$) existing between the relative quantification at day N and the previous time point.

- *3.3.3 Omic clues towards apoptosis*. The 'omic' time course analysis shows interesting hints about the duality autophagy/apoptosis, indirectly suggesting a propensity of the slaughtered

Spot	Protein	NCBI accession number	Prec.ion	Charge	Peptide sequence	Mascot score
A	myosin-2	gi|261245063	848.99	4+	AAAEGGS**Sp**SVFSMFDQTQIQEFK	78 (ETD)
	myosin-1	gi|41386691	895.41	2+	VQLLHTQNT**Sp**LINTK	55(NL*, MS^2)
B	synaptopodin-2	gi|139948281	714.80	2+	AH**Sp**PTPSLPAGWK	48 (ETD)
C	Phospho glucomutase	gi|116004023	585.76 585.74 762.66	2+ 2+ 3+	L**Sp**GTGSAGAIR LSG**Tp**GSAGAIR AIGGIILTA**Sp**HNPGGPNGDFGIK	96 (ETD) 95 (ETD) 66 (ETD)
D	Phosphoglycerate mutase 2	gi|84000195	863.33	2+	ERHYGG**Tp**GLNKAET	50(ETD)
E	phosphoglycerate mutase 2	gi|84000195	863.33	2+	ERHYGG**Tp**GLNKAET	56(ETD)
F	triosephosphate isomerase	gi|61888856	642.76 703.80	2+ 2+	SNVSDAVAQ**Sp**AR IIYGGSVTGATCK	76 (ETD) 59 (ETD)
G	alpha-crystallin B chain	gi|27805849	771.81	2+	AP**Sp**WIDTGLSEMR	99 (NL, MS^3)
H	HSPB6	gi|119224088	715.36	2+	RA**Sp**APLPGLSAPGR	44(ETD)

TABLE 10. Mass spectrometric confirmation of phosphorylated proteins identified in 1D-gel.

muscle cells for the apoptotic solution; figure 26 summarizes the results and their connections with apoptosis, and I will refer to it along the following discussion. First of all, I want to consider the trend of two proteins belonging to the family of heat shock proteins (HSPs), HSPB6 and αB-crystallin. The importance of HSP into the muscle-to-meat conversion has been recently recognized and associated to meat tenderization (Ouali et al., 2006; Guillemin et al., 2011), although there is no clear hypothesis about the biological mechanisms underpinning postmortem events. Furthermore, a link between HSP and apoptosis (Beere, 2004; Takayama et al., 2003; Lanneau et al., 2008) is ascertained, evidence that endorses the attention on HSP identifications in this time course experiment. HSPB6 has clear roles in smooth and cardiac muscles, while in the skeletal muscle it is less understood (Dreiza et al., 2010). Gusev and colleagues (2005) described for HSPB6 a protective role against apoptosis in cardiomyocytes, by means of the inhibition of the activation of procaspase 3 to caspase 3. This outcome is the final step of a signaling cascade walking

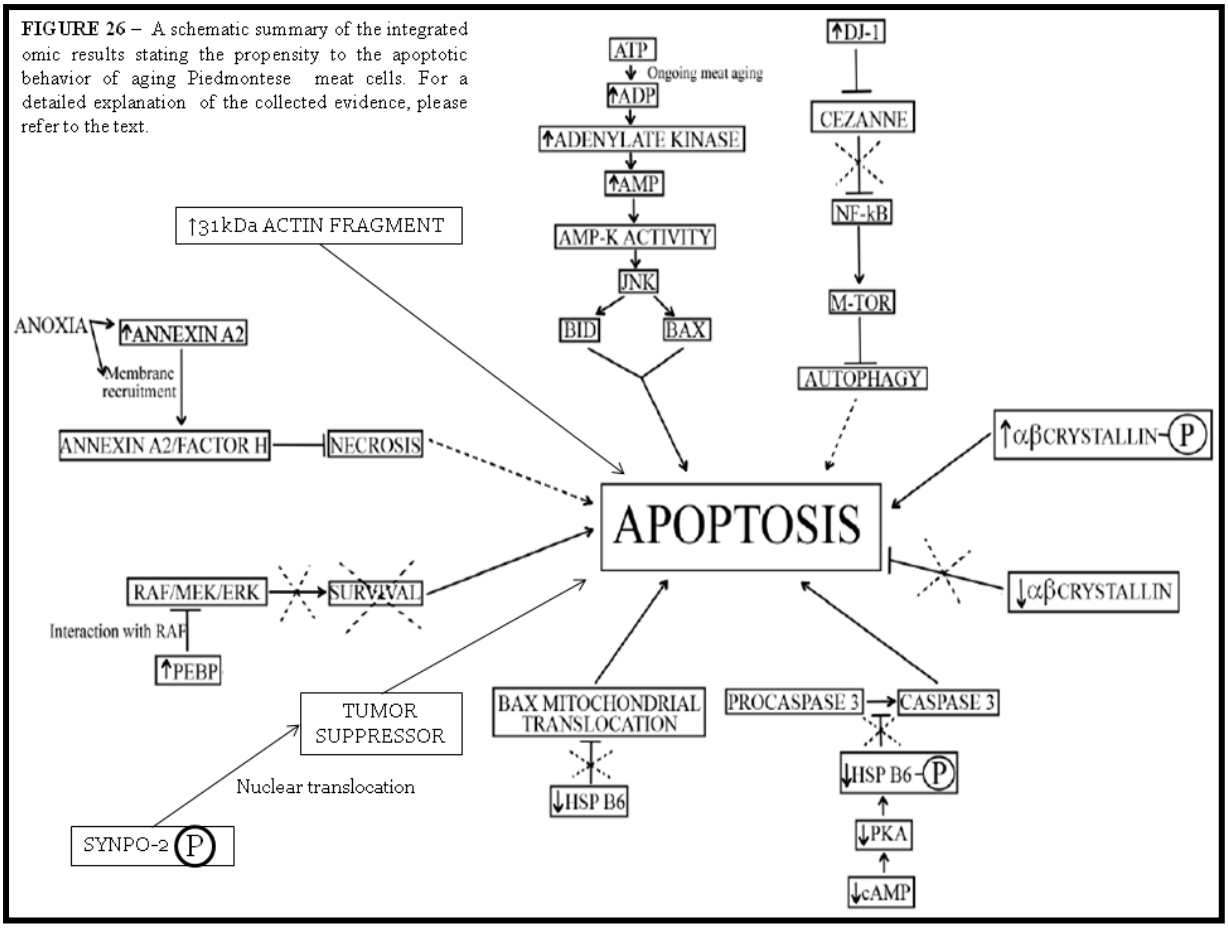

FIGURE 26 – A schematic summary of the integrated omic results stating the propensity to the apoptotic behavior of aging Piedmontese meat cells. For a detailed explanation of the collected evidence, please refer to the text.

through the phosphorylation of HSPB6 by protein kinase A (PKA), which in turn has to be activated by high levels of cAMP; the metabolomic time course investigation of cAMP trend shows a sudden decrease soon from day 1 (figure 27); if we hypothesize a similar mechanism of action for HSPB6 in the skeletal muscle, the sudden cAMP decrease could trigger PKA inactivation to avoid HSPB6 phosphorylation, which at this point is no more able to inhibit caspase 3 activation; indeed, spot 371, probably containing the phosphorylated form of HSPB6, decreases along the time course (table 8), and consistently, phosphoproteomic analysis confirms the presence of the phosphorylated form of HSPB6, as indicated in figure

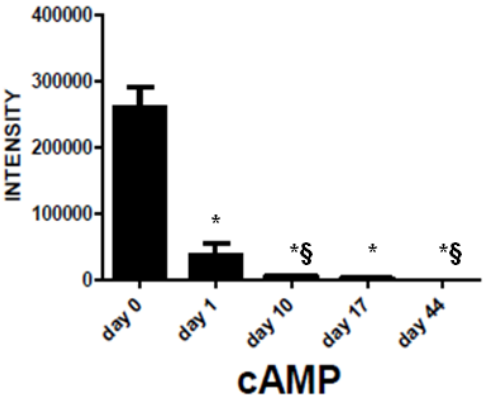

FIGURE 27 – Relative quantification of cAMP.
*indicates a statistically significant difference ($p < 0.05$) existing between the relative quantification at day N and day 0.
§ indicates a statistically significant difference ($p < 0.05$) existing between the relative quantification at day N and the previous time point.

24 and tables 9 and 10. The downward trend of unphosphorylated HSPB6 (the more basic spot, 370; table 8, figure 19) may be read in the same direction, as to foster the apoptotic solution to muscle cells: HSPB6 is able to interact with Bax, a proapoptotic protein, hampering its translocation to the mitochondria where it performs its proapoptotic function (Fan & Kranias, 2011); the decrease in HSPB6 levels discourages this prosurvival interaction (figure 26).

αB-crystallin protein has been identified in four different spots in the 2D time course analysis; spots 367 and 530 show a downward trend from day 17, while 363 and 456 show an upward trend. There are different pIs, and this phenomenon is attributed to posttranslational phosphorylation, able to acidify the pI of αB-crystallin (Golenhofen et al., 1998); I confirmed the presence of the phosphorylated form of αB-crystallin by its detection and identification in Western analysis (table 9, figure 24). Many studies have been conducted on the possible role of this protein in apoptosis: Ray and colleagues (2001) demonstrated that transgenic overexpression of αB-crystallin confers simultaneous protection against cardiomyocyte apoptosis and necrosis during myocardial ischemia and reperfusion; Kamradt and colleagues (2005) found that wild-type αB-crystallin promotes xenograft tumor growth and inhibits TRAIL-induced apoptosis in vivo in a murine model, while a pseudophosphorylated αB-crystallin mutant, impaired in its antiapoptotic function, inhibits xenograft tumor growth; Dou and colleagues (2012) observed that overexpression of αB-crystallin protects a model of retinal pigment epithelial cell from ER-stress induced apoptosis, while the apoptotic answer is increased when these cells are αB-crystallin-deficient. All these evidences lead us to hypothesize an apoptotic boost by the αB-crystallin in our time course, because of the upward trend of the phosphorylated form, soon from day 1 (spots 363, 456), which seems to promote apoptosis, and of the downward trend of the unphosphorylated form (spots 367, 530), which in turn seems able to inhibit apoptosis (figure 26). Notably, the full

proapoptotic potential in terms of αB-crystallin seems to be completely expressed from day 17.

Recalling the aforementioned increase in adenylate kinase at day 44, confirmed by the sudden rise in [AMP], we can hypothesize a link between the adenylate kinase metabolic monitoring system and the apoptotic cascade, as evidenced in figure 26: the ATP consumption fuels [ADP] growing (as described by the metabolomic analysis, figure 28) which in turn, as evident at day 44, turns on the activity of adenylate kinase for the extreme but futile attempt to restore ATP reservoirs; consequently, [AMP] rises, promoting the activities of the 'AMP sensor' enzymes (Dzeja & Terzic, 2003). Among these members, AMP-dependent kinase (AMPK) is able to induce the JNK pathway (figure 26, figure 28), a known apoptotic inducer in a model of MIN6 beta-cell line (Kefas et al., 2003).

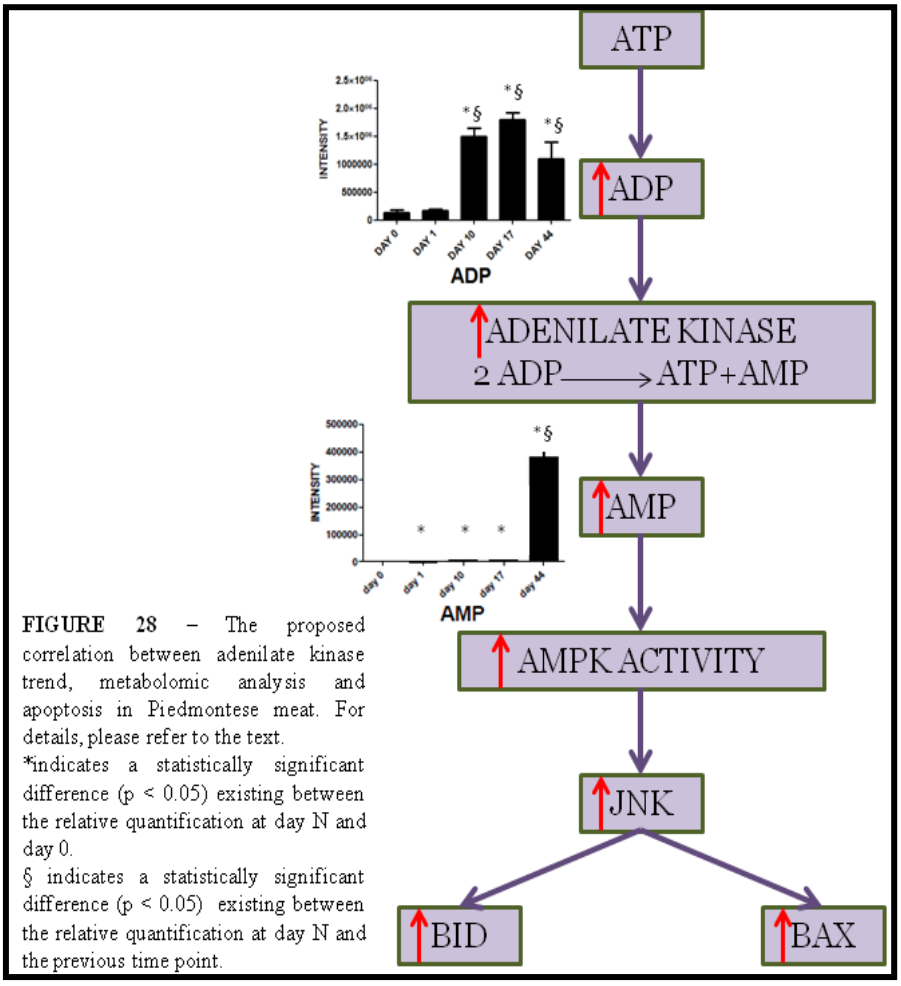

FIGURE 28 – The proposed correlation between adenilate kinase trend, metabolomic analysis and apoptosis in Piedmontese meat. For details, please refer to the text.
*indicates a statistically significant difference ($p < 0.05$) existing between the relative quantification at day N and day 0.
§ indicates a statistically significant difference ($p < 0.05$) existing between the relative quantification at day N and the previous time point.

Particular attention must be paid to spot 474, annexin A2, which shows an upward trend in the central part of the aging period (days 10 and 17; table 8) and a final return to the post-slaughter level. This protein is more or less directly linked to apoptosis, as it has been shown

its exposure on surfaces of apoptotic cells (Leffler et al., 2010), and it falls into the context of [Ca^{2+}] increase in postmortem muscle cytoplasm while the sarcoplasmic reticulum gradually loses this ion (Vignon et al., 1989); the increase in [Ca^{2+}] could be linked to the upregulation of annexin A2, which undergoes plasma membrane recruitment in conditions of anoxic stress (Monastyrskaya et al., 2008). It is interesting to point out a recent discovery by Leffler and colleagues (2010) about the ability of annexin A2 present on apoptotic cells to bind factor H; it is well known that during ischemia (a situation comparable with the anoxic muscles of the slaughtered animals) there are hypoxia, lactic acidosis, cell swelling and depletion in ATP tissutal reservoirs; the increased concentration of ROS contributes to eventual tissue necrosis (Rubin et al., 1996) led by an inappropriate activation of the complement mechanism (Ward, 1996). Factor H is a 155 kDa glycoprotein able to regulate complement protein activity in order to prevent the formation of anaphylatoxins and membrane attack complexes, with the risk of subsequent necrosis; the finding made by Leffler et al. about the factor H-binding ability of annexin A2 implies the deduction of a possible proapoptotic evidence in the upregulation of annexin A2 during the time course, whose binding potential could be exploited to avert the necrotic risk thanks to the recruited factor H functions. So, following the conclusions of Leffler about the exposition of annexin A2 by apoptotic cells, we can speculate a concomitant upregulation of this protein towards the apoptotic road in muscle/meat cells (figure 26).

Another noteworthy identification is the spot 344, containing the protein DJ-1 (progressive upregulation from day 10 onward; Table 8). There is a number of evidence stating that DJ-1 is directly linked to anoxia conditions and that its oxidative stress-related function seems to be specific: a work conducted by Meulener and colleagues (Meulener et al., 2005) on DJ-1 deficient flies treated with ROS-generating compound shows that these animals were susceptible to oxidative damages, but not to alternative forms of stress. Another recent study

(McNally et al., 2011) demonstrates the ability of DJ-1 to positively regulate NF-kB, thanks to the upstream DJ-1 binding to the deubiquitinating enzyme Cezanne that loses the inhibitory effect exerted on NF-kB. When active, under conditions of high ROS concentrations, NF-kB functions as an autophagic repressor by means of mTOR, so we can hypothesize that the stated upregulation of protein DJ-1 in aging meat could fuel NF-kB antiautophagic activity; in the light of DJ-1 indirect antiautophagic effect and of our proteomic results, this speculation contributes to the prevailing of the apoptotic hypothesis on the autophagic one during meat aging (figure 26).

Spot 365 has been identified as phosphatidylethanolamine-binding protein 1 (PEBP, also known as RKIP, Raf-1 Kinase Inhibitor Protein; table 8); we pointed our attention on this differential 2D-GE result because RKIP is linked with the Raf pathway. Raf is the upstream pawn of this evolutionarily conserved pathway comprising the sequential activities of three protein kinases: RAF, MEK, and ERK. This signaling pathway is able to transmit extracellular signals into nuclear instructions, particularly those with cellular survival meaning against apoptosis (Murakami & Morrison, 2001); RKIP is a member of the phosphatidylethanolamine binding proteins shown to disrupt RAF/MEK/ERK signaling pathway (Odabaei et al., 2004), thanks to its physical interaction with RAF. RKIP has thereby a proapoptotic function, and the upregulation demonstrated in this proteomic study is another brick put for the apoptotic hypothesis (figure 26).

I have discussed the increasing rate of the proteolytic events appearing into the aging meat, by the metabolomic point of view in the previous section of the thesis (through the progressive increase in single amino acid concentrations), and by the proteomic point of view; another interesting proteomic evidence to be recalled from the ‘proteolysis’ paragraph (3.3.1) is referred to spot 472, identified as a 31 kDa fragment of actin (figure 19, table 8), a known structural/functional pivotal protein in the muscles, and I decided to resume it in this

paragraph because of its implications regarding apoptosis: indeed, this specific 31 kDa fragment is considered as an apoptotic marker (Laville et al., 2009; Yang et al., 1998). It is

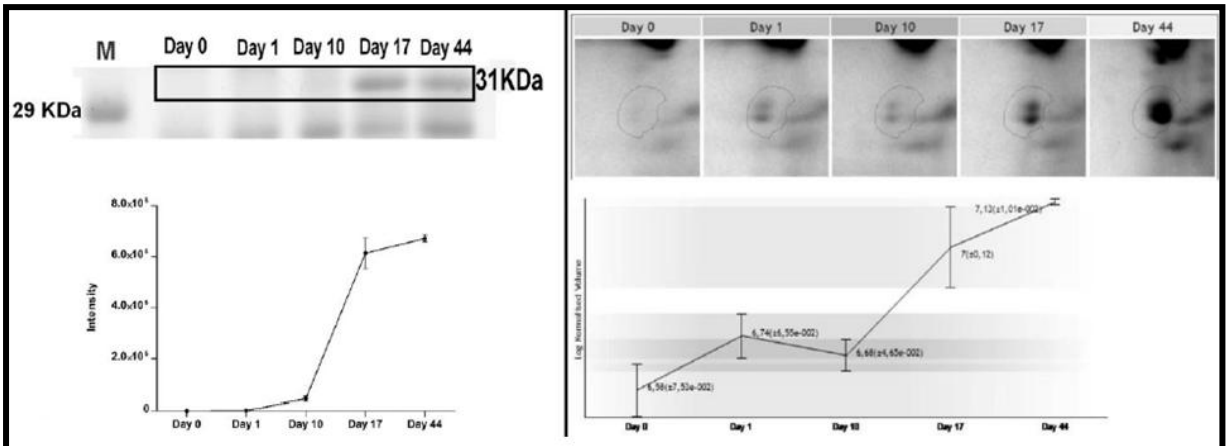

FIGURE 29 – Time-course trend of the 31 kDa actin fragment. On the left, a 1D gel showing the fragment, confirmed by the 2D spot on the right, which is an enlarged view of the 2D spot 472.

clearly appreciable from figure 29 the progressive upward trend of this fragment, attesting the presence of apoptosis and its increase among meat cells throughout the aging period.

The analysis of phosphorylated proteins revealed a time-specific phosphorylation of myosins 2 and 1 at day 1; this is, on average, the period during which rigor mortis begins to dissolve, and myosin phosphorylation could be seen as a factor influencing the activity of the proteolytic systems intervening for muscle architectural destructuration. Myosin 1 and 2 phosphorylation is not a novel or unexpected finding (Huang et al., 2012); recently, Iwasaki and colleagues (2013) have produced compelling evidences about the promotion of a hyperphosphorylated state of myosin 2 in apoptotic cells, due to the inhibition of the myosin 2-dephosphorylating activity of MYPT enzyme. Our result could suggest a sort of apoptotic programming of muscle cells even from the very beginning of rigor mortis dissolution.

Band B (figure 24) hides synaptopodin 2, indicating a phosphorylation starting from day 0 and reaching a high degree at day 1. This protein is normally located at Z-disks, but under stress conditions it is removed from the cytoplasm and transferred to the nucleus (Weins et

al., 2001); synaptopodin 2 nuclear import is possible only when it is phosphorylated (Faul et al., 2007). The phosphorylation state showed by our results suggests the nuclear translocation of synaptopodin 2 caused by the increasing oxidative stress. Reminding the tumor-suppressor role of nuclear-imported synaptopodin 2 demonstrated by Sanchez-Carbayo and colleagues (2003), we could infer the proapoptotic role played by this protein in the progression of meat maturation, adding another evidence favorable to the apoptotic hypothesis (figure 26).

From the metabolomic point of view, we have already mentioned the decreasing trend of the GSH/GSSG ratio throughout the 44 days (figure 11, figure 23). This ratio is a potential key indicator for an ongoing apoptosis (Merad-Boudia et al., 1998; Lu & Armstrong, 2007), even if the precise role of GSH/GSSG balance is not clearly understood, and further complicated

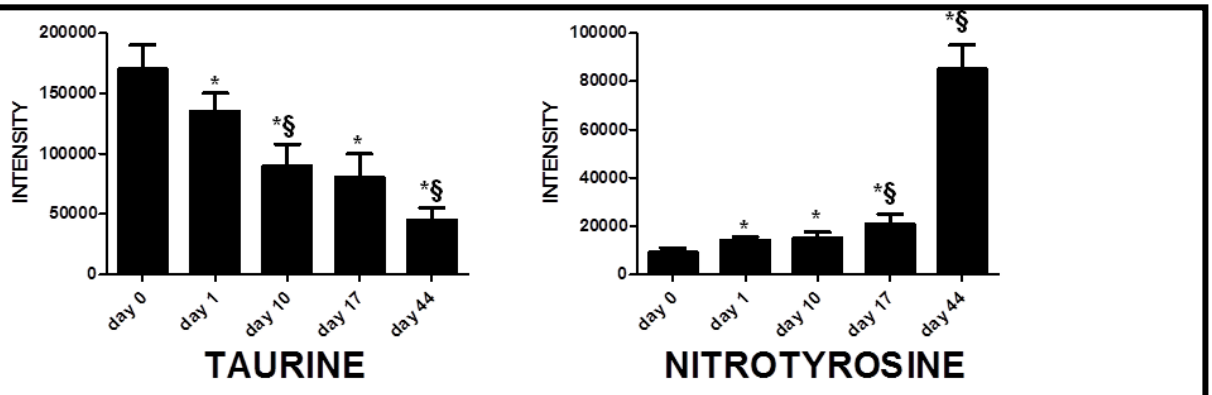

FIGURE 30 – Relative quantification of taurine and nitrotyrosine.
*indicates a statistically significant difference ($p < 0.05$) existing between the relative quantification at day N and day 0.
§ indicates a statistically significant difference ($p < 0.05$) existing between the relative quantification at day N and the previous time point.

by cell-type specificity and nature of proapoptotic stimuli. I have also investigated the time course trend of a particular amino acid, taurine, because of its known abilities to inhibit apoptosis (Takatani et al, 2004); it is thought to have putative antioxidant function against ROS, inhibitory effect on p53 and NF-kB proapoptotic pathway, and a prosurvival stimulating effect on PI3K/Akt pathway (Das et al., 2012); figure 30 shows a downward trend sustaining the apoptotic hypothesis. On the contrary, the trend of nitrotyrosine has a constant slight increase until day 17 and undergoes a strong rise at day 44 (figure 30); I have considered this

particular metabolite because of its role as an apoptotic marker (Jumper et al., 2002; Moulian et al., 2001) and as an indicator of nitrosative stress (that is, the production of RNS, reactive nitrogen species, coming from the accumulation of superoxide radical reacting with nitric oxide [Squadritoa & Pryor, 1998]). Taurine and nitrotyrosine time course trends confirm the apoptotic way for meat evolution, and the increasing degree of the apoptotic events throughout aging.

3.4 CONCLUSIONS

The second part of my work is based on an 'omic' study led to obtain a deeper glance into the biomolecular evolutions suffered by Piedmontese longissimus thoracis muscle cells during the 44 day process of muscle-to-meat conversion. In particular, among the proteomic, phosphoproteomic and metabolomic results I looked for some clues able to shed light on the controversial debate arisen about the destiny of the skeletal muscle cells of slaughtered animals; they are fatally directed to death, and there are three main feasible ways: the exclusion of necrosis, which is not the way walked by maturing palatable meat, paves the way to the famous duality autophagy/apoptosis. My omic evidences suggest apoptosis as the only choice: I have discussed the peculiarities of the ongoing oxidative stress integrating proteome, phosphoproteome and metabolome indications, and then I pointed the attention on the indirect clues able to bring out the predominance of the apoptotic hypothesis on the autophagic one; I didn't find any indication about a hypothetic cellular autophagic response. My suggestion is that apoptosis is the opted behavior, at least in the specific kind of meat considered.

However, I want to underline that this interpretation does not claim to be the incontrovertible solution of the 'contrast' between autophagy and apoptosis in aging meat, due to the extreme variability inherent in different kinds of species, muscles and animal management. When

considering different samples, the biological mechanism could be different and could also involve autophagy or a crosstalk between autophagy and apoptosis. Further studies are needed to verify if a common, underlying mechanism for any kind of muscle-to-meat conversion does exist.

REFERENCES

Asghar A, Yeates NT (1978). The mechanism for the promotion of tenderness in meat during the post mortem process: a review. Critical Reviews in Food Science and Nutrition 10(2):115–145.

Beere HM (2004). "The stress of dying": the role of heat shock proteins in the regulation of apoptosis. Journal of Cell Science 117:2641–2651.

Bessman SP (1987). The creatine phosphate energy shuttle: the molecular asymmetry of a "pool". Analytical Biochemistry 161(2):519–523.

Clasquin MF, Melamud E, Rabinowitz JD (2012). LC–MS data processing with MAVEN: a metabolomic analysis and visualization engine. Current Protocols of Bioinformatics 14: Unit 14.11.

D'Alessandro A, Marrocco C, Zolla V, D'Andrea M, Zolla L (2011). Meat quality of the longissimus lumborum muscle of Casertana and Large White pigs: metabolomics and proteomics intertwined. Journal of Proteomics 75(2):610–627.

D'Alessandro A, Rinalducci S, Marrocco C, Zolla V, Napolitano F, Zolla L (2012). Love me tender: an omic window on the bovine meat tenderness network. Journal of Proteomics 75:4360-4380.

D'Alessandro A, Zolla L (2013). Meat science: from proteomics to integrated omics towards system biology. Journal of Proteomics 78:558–577.

Dou G, Sreekumar PG, Spee C, He S, Ryan SJ, Kannan R et al. (2012). Deficiency of αB crystallin augments ER stress-induced apoptosis by enhancing mitochondrial dysfunction, Free Radical Biology Medicine 53(5):1111–1122.

Dreiza CM, Komalavilas P, Furnish EJ, Flynn CR, Sheller MR, Smoke CC et al. (2010). The small heat shock protein, HSPB6, in muscle function and disease. Cell Stress Chaperones 15:1–11.

Dzeja PP, Terzic A (2003). Phosphotransfer networks and cellular energetics, Journal of Experimental Biology 206:2039–2047.

Fan GC, Kranias EG (2011). Small heat shock protein 20 (HspB6) in cardiac hypertrophy and failure. Journal of Molecular and Cellular Cardiology 51:574–577.

Golenhofen N, Ness W, Koob R, Htun P, Schaper W, Drenckhahn D (1998). Ischemia-induced phosphorylation and translocation of stress protein alpha B-crystallin to Z lines of myocardium. American Journal of Physiology 274:1457–1464.

Gregory NG (2008). Animal welfare at markets and during transport and slaughter. Meat Science 80:2–11.

Guillemin N, Bonnet M, Jurie C, Picard B (2011). Functional analysis of beef tenderness. Journal of Proteomics 75(2):352–365.

Gururaj A, Barnes CJ, Vadlamudi RK, Kumar R (2004). Regulation of phosphoglucomutase 1 phosphorylation and activity by a signaling kinase. Oncogene 23:8118–8127.

Gusev NB, Bukach OV, Marston SB. Structure, properties, and probable physiological role of small heat shock protein with molecular mass 20 kD (Hsp20, HspB6). Biochemistry 70(6):629–637.

Huff-Lonergan E, Zhang W, Lonergan SM (2010). Biochemistry of postmortem muscle: lessons on mechanisms of meat tenderization. Meat Science 86(1):184–195.

Janssen E, Dzeja PP, Oerlemans F, Simonetti AW, Heerschap A, de Haan A et al. (2000). Adenylate kinase 1 gene deletion disrupts muscle energetic economy despite metabolic rearrangement. EMBO Journal 19:6371–6381.

Kamradt MC, Lu M, Werner ME, Kwan T, Chen F, Strohecker A et al. (2005). The small heat shock protein alpha B-crystallin is a novel inhibitor of TRAIL-induced apoptosis that suppresses the activation of caspase-3. Journal of Biological Chemistry 280(12):11059–11066.

Kanehisa M, Goto S (2000). KEGG: Kyoto Encyclopedia of Genes and Genomes. Nucleic Acids Research 28(1):27–30.

Kefas BA, Cai Y, Ling Z, Heimberg H, Hue L, Pipeleers D et al. (2003). AMP-activated protein kinase can induce apoptosis of insulin-producing MIN6 cells through stimulation of c-Jun-N-terminal kinase. Journal of Molecular Endocrinology 30(2):151–161.

Kemp C, Parr T (2012). Advances in apoptotic mediated proteolysis in meat tenderization. Meat Science 92:252–259.

Koohmaraie M (1994). Muscle proteinases and meat aging. Meat Science 36:93–104.

Lanneau D, Brunet M, Frisan E, Solary E, Fontenay M, Garrido C (2008) Heat shock proteins: essential proteins for apoptosis regulation. Journal of Cellular and Molecular Medicine. 12(3):743–761.

Leffler J, Herbert AP, Norström E, Schmidt CQ, Barlow PN, Blom AM et al. (2010). Annexin-II, DNA, and histones serve as factor H ligands on the surface of apoptotic cells. Journal of Biological Chemistry 285(6):3766–3776.

Leite TC, Da Silva D, Coelho RG, Zancan P, Sola-Penna M (2007). Lactate favours the dissociation of skeletal muscle 6-phosphofructo-1-kinase tetramers down-regulating the enzyme and muscle glycolysis. Biochemical Journal 408:123–130.

Luciano FB, Anton AA, Rosa CF (2007). Biochemical aspects of meat tenderness: a brief review. Archivos de Zootecnia 56:1–8.

Monastyrskaya K, Tschumi F, Babiychuk EB, Stroka D, Draeger A (2008). Annexins sense changes in intracellular pH during hypoxia. Biochemical Journal 409:65–75.

Murgiano L, D'Alessandro A, Egidi MG, Crisà A, Prosperini G, Timperio AM et al. (2010). Proteomics and transcriptomics investigation on longissimus muscles in Large White and Casertana pig breeds. Journal of Proteome Research 9(12):6450–6466.

Muroya S, Ohnishi-Kameyama M, Oe M, Nakajima I, Chikuni (2007). Postmortem changes in bovine troponin t isoforms on two-dimensional electrophoretic gel analyzed using mass spectrometry and western blotting: the limited fragmentation into basic polypeptides. Meat Science 75:506–514.

Ouali A, Herrera-Mendez CH, Coulis G, Becila S, Boudjellal A, Aubry L et al. (2006). Revisiting the conversion of muscle into meat and the underlying mechanisms. Meat Science 74:44–58.

Paredi G, Raboni S, Bendixen E, de Almeida AM, Mozzarelli A (2012). “Muscle to meat” molecular events and technological transformations: the proteomics insight. Journal of Proteomics 75(14):4275–4289.

Ray PS, Martin JL, Swanson E, Otani H, Dillmann WH, Das DK (2001). Transgene overexpression of αB-crystallin confers simultaneous protection against cardiomyocyte apoptosis and necrosis during myocardial ischemia and reperfusion. FASEB Journal 15:393–402.

Rinalducci S, Campostrini N, Antonioli P, Righetti PG, Roepstorff P, Zolla L (2005). Formation of truncated proteins and high-molecular-mass aggregates upon soft illumination of photosynthetic proteins. Journal of Proteome Research 4:2327–2337.

Shevchenko A, Wilm M, Vorm O, Mann M (1996). Mass spectrometric sequencing of proteins from silver-stained polyacrylamide gels. Analytical Chemistry 68:850–858.

Takayama S, Reed JC, Homma S (2003). Heat-shock proteins as regulators of apoptosis. Oncogene 22 (56):9041–9047.

Talamo F, D'Ambrosio C, Arena S, Del Vecchio P, Ledda L, Zehender G et al. (2003). Proteins from bovine tissues and biological fluids: defining a reference electrophoresis map for liver, kidney, muscle, plasma and red blood cells. Proteomics 3:440–460.

Thingholm TE, Jorgensen TJ, Jensen ON, Larsen MR (2006). Highly selective enrichment of phosphorylated peptides using titanium dioxide. Nature Protocols 1:1929-1935.

Tovmasian EK, Hairapetian RL, Bykova EV, Severin Jr SE, Haroutunian AV (1990). Phosphorylation of the skeletal muscle AMP-deaminase by protein kinase C. FEBS Letters 259(2):321–323.

Van de Perre V, Permentier L, De Bie S, Verbeke G, Geers R (2010). Effect of unloading, lairage, pig handling, stunning and season on pH of pork. Meat Science 86:931–937.

Vignon X, Beaulaton J, Ouali A (1989). Ultrastructural localization of calcium in postmortem bovine muscle: a cytochemical and X-ray microanalytical study. Histochemical Journal 21:403–411.

Wegmann G, Zanolla E, Eppenberger HM, Wallimann T (1992). In situ compartmentation of creatine kinase in intact sarcomeric muscle: the acto-myosin overlap zone as a molecular sieve. Journal of Muscle Research and Cell Motility 13:420–435.

LIST OF PUBLICATIONS ON THE ARGUMENT:

- Lana A, Longo V, Dalmasso A, D'Alessandro A, Bottero MT, Zolla L. Omics integrating physical techniques: aged Piedmontese meat analysis. Food Chemistry, 2015; 172:731-741.
- Longo V, Lana A, Bottero MT, Zolla L. Apoptosis in muscle-to-meat aging process: the omic witness. Journal of Proteomics, 2015; 125:29-40.
- Lana A, Zolla L. Apoptosis or autophagy, that is the question: two ways for muscle sacrifice towards meat. Trends in Food Science and Technology, 2015; 46(2A):231-241.
- Lana A, Zolla L. Proteolysis in meat tenderization from the point of view of each single protein: a proteomic perspective. Journal of Proteomics, 2016; in-press.